National Library of Canada
Acquisitions and Bibliographic Services Branch
395 Wellington Street
Ottawa, Ontario
K1A 0N4

Bibliothèque nationale du Canada
Direction des acquisitions et des services bibliographiques
395, rue Wellington
Ottawa (Ontario)
K1A 0N4

Your file *Votre référence*

Our file *Notre référence*

NOTICE

The quality of this microform is heavily dependent upon the quality of the original thesis submitted for microfilming. Every effort has been made to ensure the highest quality of reproduction possible.

If pages are missing, contact the university which granted the degree.

Some pages may have indistinct print especially if the original pages were typed with a poor typewriter ribbon or if the university sent us an inferior photocopy.

Reproduction in full or in part of this microform is governed by the Canadian Copyright Act, R.S.C. 1970, c. C-30, and subsequent amendments.

AVIS

La qualité de cette microforme dépend grandement de la qualité de la thèse soumise au microfilmage. Nous avons tout fait pour assurer une qualité supérieure de reproduction.

S'il manque des pages, veuillez communiquer avec l'université qui a conféré le grade.

La qualité d'impression de certaines pages peut laisser à désirer, surtout si les pages originales ont été dactylographiées à l'aide d'un ruban usé ou si l'université nous a fait parvenir une photocopie de qualité inférieure.

La reproduction, même partielle, de cette microforme est soumise à la Loi canadienne sur le droit d'auteur, SRC 1970, c. C-30, et ses amendements subséquents.

Canada

GEOMETRY, KINEMATICS AND COMPUTER SIMULATIONS OF THRUST FAULTING, CENTRAL CANADIAN ROCKY MOUNTAINS, ALBERTA.

by

Daniel Lebel

Department of Earth and Planetary Sciences

McGill University

Montréal, Québec, Canada

April 1993

A thesis submitted to the Faculty of Graduate Studies and Research

in partial fulfillment of the requirements for

the degree of Doctor of Philosophy

© Daniel Lebel, 1993

National Library of Canada
Acquisitions and Bibliographic Services Branch
395 Wellington Street
Ottawa, Ontario
K1A 0N4

Bibliothèque nationale du Canada
Direction des acquisitions et des services bibliographiques
395, rue Wellington
Ottawa (Ontario)
K1A 0N4

Your file Votre référence

Our file Notre référence

The author has granted an irrevocable non-exclusive licence allowing the National Library of Canada to reproduce, loan, distribute or sell copies of his/her thesis by any means and in any form or format, making this thesis available to interested persons.

L'auteur a accordé une licence irrévocable et non exclusive permettant à la Bibliothèque nationale du Canada de reproduire, prêter, distribuer ou vendre des copies de sa thèse de quelque manière et sous quelque forme que ce soit pour mettre des exemplaires de cette thèse à la disposition des personnes intéressées.

The author retains ownership of the copyright in his/her thesis. Neither the thesis nor substantial extracts from it may be printed or otherwise reproduced without his/her permission.

L'auteur conserve la propriété du droit d'auteur qui protège sa thèse. Ni la thèse ni des extraits substantiels de celle-ci ne doivent être imprimés ou autrement reproduits sans son autorisation.

ISBN 0-315-91713-X

Canada

SHORT TITLE:

GEOMETRY, KINEMATICS AND COMPUTER SIMULATIONS OF THRUSTS, CENTRAL ROCKY MOUNTAINS, ALBERTA

TABLE OF CONTENTS

LIST OF TABLES

LIST OF FIGURES

ABSTRACT

In the central Canadian Rocky Mountain thrust-fold belt, three types of first order décollements are outlined within or along the border of the present orogenic wedge: one basal décollement, three intermediate or internal décollements and one upper décollement. Structural relationships suggest that each internal décollement is the result of one of the successive forward shifts of early basal décollements to new positions within the stratigraphic pile.

Two computer programs have been developed to analyze the propagation of multiple thrust faults and their influence on the geometry of a thrust belt. The computer programs generate graphical simulations used to demonstrate a model of thrust propagation and thrust belt development that fits current knowledge about fault propagation and can replace the thrust transfer zone concept.

A structural analysis of mesoscale structures in two thrust sheets indicates that a thrust sheet consist of a series of elongated blocks separated by subtle brittle-ductile shear zones along which differential motion occurred. These shear zones are oriented perpendicular to the mean strike of the thrust faults.

RÉSUMÉ

Dans la chaîne de montagnes des Rocheuses Canadiennes centrales, trois types de surfaces de chevauchement de premier ordre sont reconnus, en bordure ou à l'intérieur du biseau orogénique actuel: un décollement basal, trois décollement internes et un décollement supérieur. Les relations structurales font suggérer que chaque décollement interne est le résultat d'un saut vers l'avant d'un décollement basal précoce, dans le prisme sédimentaire.

Deux programmes informatiques ont été développés pour analyser la propagation de multiples failles de chevauchement et l'influence de ces failles sur la géométrie d'une chaîne orogénique. Ces programmes génèrent des simulations graphiques qui sont utilisées pour démontrer un modèle de propagation de failles de chevauchement et de développement d'une chaîne orogénique qui est conforme aux connaissances actuelles concernant la propagation des failles et qui permet de remplacer le concept des zones de transfert de déplacement des chevauchements.

Une analyse structurale de deux écailles de chevauchement du centre des Front Ranges montre que des structures mesoscopiques, plus particulièrement des zones de cisaillement fragile-ductile, ont permis le transport différentiel de blocs structuraux allongés, et orientés perpendiculairement à la direction des failles de chevauchement, pendant le mouvement et la propagation des mêmes failles.

GENERAL ACKNOWLEDGEMENTS

I acknowledge the continuous and patient support of my thesis supervisor, Professor Eric Mountjoy who suggested this research project and who was instrumental in obtaining support from the Geological Survey of Canada to undertake the completion of the geological maps of the Mountain Park and Cardinal River areas. He introduced me to the intricacies of Western Canada stratigraphy and geological mapping in the Rocky Mountains while completing the Mountain Park map sheet. His discussions were helpful, particularly pointing out many field examples and sharing his knowledge of the structure of the region. His thorough review of the drafts of this thesis greatly improved the formulation of my ideas and the English expression. The early geologic mapping of the Cardinal River area by R.J.W. Douglas in the 1950's provided me with an excellent preliminary map on which to base my field mapping. Professor Andrew Hynes also visited me in the field and contributed numerous and helpful discussions, which resulted in the theoretical model and the computer programs presented in this thesis.

Shell Canada funded the first field season in the Mountain Park area (1985) when I was still a neophyte in Rocky Mountain geology. I especially thank Charlie Bruce, then chief geologist, and Peter Fermor, senior geologist who guided my efforts at building realistic cross-sections of the Foothills and Front Ranges and contributed helpful discussions on the research project.

I am grateful to Walter Nassichuk, Don Cook and Margot McMechan (Institute of Sedimentary and Petroleum Geology, Geological Survey of Canada) for sponsoring the field work and completion of the Mountain Park and Cardinal River geological maps (NTS 83C/14 and 83C/15). A contract in 1986 and 1987 provided funding for field work and a field assistant. Margot McMechan was particularly helpful in reviewing the

geological maps, providing logistical support and preparations for field work. Pierre Hudon served as an excellent assistant during the 1987 field season.

I gratefully acknowledge the award of several scholarships between 1985 and 1988, a FCAR grant (1985-1987), the Reinhardt and Howard scholarships (awarded by the Department of Geological Sciences, McGill University) and the Geology Graduate Scholarship of the Canadian Society of Petroleum Geologists (1986).

I am indebted to Parks Canada (Western Region) for granting me the opportunity to study and collect samples in the Jasper National Park.

I am also grateful to the Ministère de l'Énergie et des Ressources (Québec) for providing work and opportunities to do geological mapping in various regions of the Appalachians during the last five years. These years of experience have influenced the results of the research presented here.

Many others have been helpful during this research and I thank all of them. Professor H.K. Charlesworth of the Department of Geology of the University of Alberta for providing theses by Kilby (1978), Hill (1980), and Johnston (1987). Willem Langenberg from the Alberta Research Council, Tomas Jerzykiewicz from the GSC, Gregg River Mines (particularly Randy Karst) and Gary Johnston from Luscar-Sterco Mines (Coal Valley) are also acknowledged for their help during mapping of the Mesozoic and Cenozoic stratigraphy, particularly the coal beds. Professor Paul Williams (University of New Brunswick) kindly made a photometric analysis of calcite fabric of a sample from the Nikanassin thrust sheet. Ray Price made very helpful comments on an early version of Chapter Three of this thesis.

Finally I thank my wife, Lynn Gagnon, who patiently endured the long period of thesis preparation and also served as an excellent assistant during the 1985 and 1986 field seasons, enduring hazardous episodes on mountain bikes and mountain slopes. Without Lynn's continuing support and the patience of our daughters, Sarah and Laurence, this work would never have been finished.

PREFACE

This research project was initiated in May of 1985 under the supervision of Dr. Eric W. Mountjoy of McGill University. Dr. Mountjoy suggested the project based upon his previous structural studies of the Rocky Mountains of the central Canadian Cordillera (e.g. Mountjoy, 1960a, b; 1962, 1970, 1980). Three field seasons (1985-1987) were spent mapping and studying the structure of the Rocky Mountain thrust-fold belt in the segment situated between the Athabasca and the Brazeau Rivers. This thesis is a synthesis of the author's observations and interpretations of thrust faults based on: 1) regional mapping and the construction of structure cross-sections in the Rocky Mountain thrust belt, 2) theoretical development and computer modeling, and 3) a structural analysis of field observations. In addition, a new geological map at a scale of 1:100,000 of the Athabasca-Brazeau area is presented here, which is a compilation based in part on published and unpublished maps at a scale of 1:50,000 co-authored by the author of this thesis (Douglas and Lebel, 1993; Mountjoy *et al.*, 1992).

Responsibility for the content of this thesis rests with the author, except where indicated in the text. Dr. Mountjoy's name will appear as a junior author on the manuscripts of the papers that will be submitted for scientific publication, having served as supervisor, editor and having assisted in the field during the tenure of this project. In addition, Dr. Mountjoy contributed unpublished regional information and some mapping from airphotos, particularly in the Cadomin and Mountain Park areas.

THESIS FORMAT

The thesis is composed of five chapters. Chapter One is the general introduction to the thesis. Chapter Two, entitled *'Geometry and role of multiple thrust décollements,*

central Canadian Rocky Mountains' summarizes the results of regional mapping and compilation, and the construction of a series of structure cross-sections of the Athabasca-Brazeau area. This indicates the location and kinematics of extensive thrust décollement surfaces during the development of the Canadian Cordilleran Foreland thrust belt. Chapter Three consists of a theoretical approach to thrust belt development in a paper entitled: *'Numerical modeling of thin-skinned thrust systems-Insights on the propagation and overlap of faults, with application to the thrust-fold belt of central Alberta'*. The theoretical approach is based on a simplified model of thrust belt evolution termed the 'overlap-spreading simple shear mechanism'. This mechanism has been tested through two computer programs developed by the author. These programs permit graphic simulations of thrust faulting as seen in map view. The results of these simulations serve in turn to explain several geometries commonly found on the geological map of a thrust belt. An application of one of the computer programs is presented which reconstructs the map patterns of thrust faults in the central Canadian Rocky Mountain thrust-fold belt, using map length of major thrusts, and realistic rates of thrust propagation. Chapter Four, entitled *'Mesofabric record of strain in large thrust sheets of the central Canadian Rocky Mountains, Alberta'* examines the mesoscopic fabric elements of two contiguous thrust sheets. The results demonstrate that non-coaxial, rotational strain fields have been present at the mesoscale, to allow for thrust emplacement, as expected by the overlap mechanism described in the second part of this thesis. The results of the study of the regional structure presented in Chapter Two have been used to explain the structural relationships found by the structural analysis of Chapter Four. The general conclusions of the thesis are derived from the more specific conclusions in chapters Two, Three and Four.

Chapters Two, Three and Four are written as preliminary manuscripts for journal publication, and some repetition is unavoidable. A comprehensive reference list is included at the end of the thesis. Cross-reference to figures and discussions used in the different chapters has been used for sake of conciseness and to link the chapters. All the

figures are grouped at the end of the thesis, separated with reference to chapter Two, Three and Four. Four folded maps are included in the pocket. The computer programs and code are on file in the Department of Earth and Planetary Sciences, McGill University, c/o Professor Eric Mountjoy and can be obtained from the author for a nomimal fee.

PURPOSE, PROBLEMATIC AND ORIGINAL CONTRIBUTIONS TO KNOWLEDGE

The main subject of this thesis is the nature and origin of thrust transfer zones, in particular the Nikanassin-Miette-McConnell transfer zone that occurs in the central Rocky Mountains thrust-and-fold belt near Cadomin, Alberta (Dahlstrom, 1969, 1970). In order to understand the possible mechanisms of displacement transfer between these thrust faults, the analysis of the mesoscale fabric in relation to the macroscale structures was carried out within the adjacent Nikanassin and Fiddle River thrust sheets.

Concurrently, the production of geological maps covering a wider area, at the scale of 1: 50,000 co-authored by the author (Mountjoy, Price and Lebel, 1992; Douglas and Lebel, 1993) has permitted the construction of a series of structure cross-sections to show the relationships between the different thrusts in this transfer zone. Although the area of study appeared ideal for such study because of the existence of the numerous exploration wells yielding information on the deep (1-6 km below surface) geological structure of the area, in the end, the cross-sections did not provide sufficient constraints to understand the details of thrust displacement transfer. Hence, it became clear that the displacement measured on one thrust fault could vary too significantly along strike (depending on the projection that was done with the surface geology), to extrapolate precise theoretical principles of thrust growth. One of the ultimate purposes of these structure sections was to reliably graph the displacement measured at the surface along the main thrust faults. However, more subsurface data are needed and a better answer to this question might be obtained if oil companies were to release seismic profiles. The cross-sections show the presence of important structures and relationships that are not evident on the geological maps and help understand the three-dimensional geometry of the thrust belt. An interesting conclusion from this research is the recognition in the region of early

décollements which are cross-cut by later-formed faults rising from underlying décollements.

The work of Scholtz *et al.* (1986) and Walsh and Watterson (1988) on thrust fault growth was critical in the approach that was taken in the later phase of this research. Since analyzing the structure using conventional techniques did not provide sufficient constraints to resolve the thrust transfer zone mechanism problem, a theoretical and computer modeling study, building on the work of Elliott (1976a) was attempted. The results provide a simplified concept of thrust belt development, made of a composite mechanism. This composite mechanism provides a means of explaining how the non-homogeneous displacement observed along each fault in a series of contiguous thrust faults translates into the relatively uniform shortening observed along most thrust belts of the world. The results of the meso- and macroscale structure analysis, obtained in the early phase of this research, are better understood in the light of the theoretical and computer modeling study. The major contributions of this study are:

1) Three types of décollements can be deduced from the current geometry of the Canadian Cordilleran foreland thrust belt, namely basal, intermediate internal and upper décollements, based on data from the Athabasca-Brazeau region and integrated with regional information. An internal décollement is recognized by a layer-parallel glide horizon that correspond to an extensive flat segment above a ramp that links it to a portion of the basal décollement situated further in the hinterland of the thrust belt. Many fault imbricates emanate from an internal décollement. The internal décollement is underlain by continuation of the basal décollement toward the foreland and overlain in most cases by an upper décollement surface.

2) Overall, the shortening within the Mesozoic sequence in the Foothills is equivalent to that in the Paleozoic sequence. However, the two sequences have discrepancies in relative

shortening when only short segments of the cross-sections are considered. Thus section balancing using relative bed lengths must be done for the entire Foothills to produce valid determinations of shortening amounts.

3) In the Athabasca-Brazeau region, six extensive layer-parallel glide horizons are recognized: the Sassenach-basal Palliser formations, the Fernie Group, the upper portion of the Nikanassin Formation, the Blackstone Formation, the Wapiabi Formation and the lower part of the Brazeau Formation.

4) Successive forward shifts of the basal décollement to new positions within the stratigraphic pile led to the formation of internal décollements (some of which may be cross-cut), folded by the stacking of thrust sheets of younger faults rising from deeper and more northeastward décollements.

5) The upper more forward segment of an early décollement appears to have been used as a roof thrust during the development of deeper-seated duplexes (i.e. the Folding Mountain and Luscar duplexes underlying the Blackstone décollement).

6) The abandonment and forward shift of basal décollements in the external part of the Rocky Mountain belt appears related to the development of the upper décollement and can be explained by the Coulomb orogenic wedge model. The formation of the upper décollement caused increased friction along both the basal and upper décollement surfaces that gradually raised the critical taper angle of the orogenic wedge. Renewed internal deformation within the wedge eventually led to a shift of the basal décollement to reduce friction and allowed for renewed foreland accretion along a new basal décollement until friction again built up sufficiently to cause another cycle of basal décollement abandonment.

7) Two original computer programs (OVERLAP and THREE THRUSTS), that generate graphical simulations, have served to demonstrate a model of thrust propagation and thrust belt development that fits current knowledge about fault propagation.

8) The numerical model, used in the computer simulations, is based on an original mechanism, a composite of two mechanisms: a) the *spreading simple shear mechanism* applies a simple form of layer-parallel shear strain, symmetrical about the center of the leading edge of a thrust fault to its lateral tips, that is subsequent to the lateral and forward propagation and motion of a single thrust fault; b) the *overlap mechanism* is a conceptual model that suggests at what moment an individual fault will propagate when it belongs to a group of thrust faults linked through a common décollement. The mechanism is an analog of a local stress buildup and its eventual relaxation by slip on the single fault that is best situated for this stress relaxation.

9) The computer simulations provide useful information about the behavior of multiple faults:

(a) The number of faults and the positions of their nucleation points (their density), and the rheology and consequent speed of fault propagation govern the uniformity of the shortening along the thrust belt.

(b) The branch lines and hanging wall strain pattern of two intersecting thrust faults can be used to trace back the thrusting sequence of the two thrusts.

(c) The OVERLAP computer simulations show that the shortening of a thrust belt can be distributed more evenly by means of propagation of a large number of small faults than by a few large thrusts.

(d) The THREE THRUSTS computer simulations also demonstrate that the final geometry of a large thrust fault on a geological map leaves few clues about its

origin, whether it was produced by the coalescence of multiple, en échelon, thrust faults or from only a single nucleation point.

10) The study of the geometry and spatial orientation of the mesoscale structures within the Paleozoic lithotectonic unit and along the strike of the Nikanassin and Fiddle River thrust sheets of the Front Ranges shows that :

(a) A solution cleavage (S_1) is observed throughout the Nikanassin and Fiddle River thrust sheets, typically fanning around an axis parallel to the local fold axis.

(b) In some domains, this fanning of the S_1 cleavage and the mean intersection lineation between this cleavage and bedding is not parallel to the fold axis. This is interpreted to result from the rotation of early folds just before some new cleavage planes formed. A second cleavage (S_2) is superimposed upon the early formed S_1 cleavage in some areas.

(c) Both wide and narrow shear zones mainly consisting of spaced, thin and long en échelon veins are observed throughout the thrust sheets, and display a statistical mode of vein set orientations nearly perpendicular to the mean map trend of the thrust fault. These shear zones are subvertical and attest that layer-parallel simple shear was an active deformation mechanism. Volume dilation by the veins within these shear zones is considered to be balanced by the solution of material coming from cleavage planes. Shear zones of opposite dextral and sinistral sense have been observed to intersect each other.

11) The study of the mesostructures suggests a progressive strain history involving:

(a) The formation of early folds, probably related to the propagation of the thrust faults (fault-propagation folds), together with the inception of some early cleavage planes.

(b) The continued lateral and forward propagation of the Nikanassin and Fiddle River thrust faults and the consequent internal deformation within the thrust sheets by layer-parallel simple shear through a series of dextral and sinistral shear zones, sub-parallel to the transport direction.

(c) During the latest phase of deformation, the stacking of underlying thrust sheets above Foothills thrust faults in some areas has caused the rotation of fold axes and other mesoscale structures to a position oblique to the regional stress field. This rotation explains the local transection of folds and early cleavage by later formed cleavage planes.

PAPERS AND ABSTRACTS

Prior to the completion of this thesis, parts of this research have been published as abstracts, or presented orally or as posters. The geological maps of Mountain Park and Cardinal River areas have been published recently and are based on some field mapping by the author (Mountjoy, Price and Lebel, 1992; Douglas and Lebel, 1993). The structure cross-sections published with these maps were constructed by the author and are reproduced herein at a larger scale with slight modifications. The information contained in the above maps, structure cross-sections and abstracts is integrated into the body of the thesis (see following list).

Abstracts

Lebel, D. 1986. Structure cross-section Cadomin area [poster]. Cordilleran Workshop, Queen's University, Kingston, Ontario, January 1986.

Lebel, D. 1987. Geology of the Cardinal River area. Map and cross-sections [poster]. Cordilleran Workshop, McGill University, Montreal, Quebec, January 1987.

Lebel, D. 1988. Structural analysis of a segment of the Central Eastern Front Ranges east of Jasper, Alberta [abs. and oral pres.]. Cordilleran Workshop, University of Alberta, Edmonton, Alberta, January 1988.

Lebel, D. 1989. Structural analysis of a segment of the Front Ranges between Bow and Athabasca Rivers, Alberta [abs. and oral pres.]. Geological Association of Canada-Mineralogical Association of Canada, Program with abstracts, Annual Meeting, Montréal 1989.

Lebel, D. and Mountjoy, E.W. 1993. Structure of a segment of the eastern Front Ranges and Foothills between Athabasca and Brazeau Rivers, Alberta [abs. and poster]. Cordilleran Workshop, Queen's University, Kingston, Ontario. February 1993.

Lebel, D. and Mountjoy, E.W. 1993. Numerical modeling of thin-skinned thrust systems-Insights on the propagation of faults and the thrust transfer zone problem [abs., poster and oral pres.]. Cordilleran Workshop, Queen's University, Kingston, Ontario. February 1993.

Lebel, D. and Mountjoy, E.W. 1993. Structure of a segment of the eastern Front Ranges and Foothills between Athabasca and Brazeau Rivers, Alberta [abs. and poster]. Geological Association of Canada/ Mineralogical Association of Canada Annual Meeting, Edmonton, May 1993.

Lebel, D. and Mountjoy, E.W. 1993. Numerical modeling of thin-skinned thrust systems-Insights on the propagation of faults and the thrust transfer zone problem [abs. and oral pres.]. Geological Association of Canada/ Mineralogical Association of Canada Annual Meeting, Edmonton, May 1993.

NOTES ON THE GEOLOGICAL MAP OF THE ATHABASCA-BRAZEAU AREA (SCALE 1:100,000)

The 1:100,000 geological map (Fig. 2.3) is a compilation with minor additions that includes parts or the whole of five 1:50,000 NTS (National Topographic System) sheets (see insert on Fig. 2.3): Miette (83F/4, Mountjoy, 1960b), Cadomin (83F/3, MacKay, 1929b; Douglas, unpublished; Lebel, unpublished; Langenberg and Fietz, 1990), Medicine Lake (83C/13, Mountjoy and Price, 1976), Mountain Park (83C/14, Mountjoy *et al.*, 1992) and Cardinal River (83C/15, Douglas and Lebel, 1993). The map follows the tectonic strike between latitude 52°45' and 53°15', near the Athabasca River to the northwest. The extreme northeast portion of the Cardinal River area lies within the Alberta Plains.

A large segment of the eastern part of Jasper National Park is included in the area studied. The eastern boundary of the park crosses the geological map diagonally from Pocahontas (in the Athabasca River valley). Highways 16 and 40 and branch roads from them provide access to most of the study area. Apart from these roads, many seismic trails and rough roads cut or constructed for oil exploration provide access by motorbikes to otherwise remote areas. The more difficult areas of access lie within Jasper National Park where vehicles are prohibited and traversing has to be done on foot, or by horse, or helicopter.

PREVIOUS WORK

Allan and Rutherford (1924) made the first reconnaissance geological map of the area. The Cadomin, Mountain Park and Cardinal River areas were mapped in more detail (1:63,000 scale) by MacKay (1929a, b, 1940a, b, 1943), who outlined the principal

geological divisions and carefully followed the coal beds. Hake *et al.* (1935, 1942) and Sanderson (1939) described the stratigraphy and the structure of the Brazeau area and outlined the folded thrust faults of the Cardinal River area. Other maps include the regional geological map (1:1,000,000 scale) of NTS sheet 83 (Price *et al.*, 1977) and the 1:2,000,000 scale map by Wheeler *et al.* (1991). The regional stratigraphic framework has been thoroughly reviewed, described and redefined in part by Mountjoy (1960a) in the Miette and adjacent areas (Mountjoy, 1962). This work provided a stratigraphic base for mapping the Mountain Park, Cadomin and Cardinal River areas, in addition to numerous other detailed stratigraphic studies carried out since.

The rocks of the study area range from the Cambrian to the Tertiary (see insert for stratigraphic relationships on Fig. 2.3). The Paleozoic rocks are dominated by platformal carbonates that are dividable into: Middle and Upper Cambrian, Upper Devonian, and Carboniferous. The Mesozoic-Cenozoic sequence consists of clastic sediments that were deposited in the foreland basin in front of the rising Cordilleran thrust belt (Price and Mountjoy, 1970, Underschultz and Erdmer, 1991), and dividable into four unconformity bounded sequences: Triassic, Jurassic to Lower Cretaceous (?), Lower Cretaceous, and Upper Cretaceous to Tertiary.

Cambrian strata were described by Mountjoy (1960a), Pugh (1971), Aitken *et al.* (1972), Mountjoy and Aitken (1978) and Aitken (1989). The overlying Devonian Fairholme reef complex and adjacent strata have been the subject of numerous studies (Mountjoy, 1965, 1980a, 1989; Mackenzie, 1965a,b, 1967, 1969; Cook, 1972; Klapper and Lane, 1988; Weissenberger and McIlreath, 1989; Shields and Geldsetzer 1992) due to excellent exposures and the strong interest in these strata as petroleum reservoirs. The Devonian Palliser Formation has been described by Mountjoy (1960a), and the Carboniferous Rundle Group and Banff Formation measured and described by Mountjoy (1960a) and Macqueen (1966, 1967). The Triassic Spray River Group was described by Best (1958) and Gibson (1968), and the Jurassic Fernie Group by Frebold (1957) and

Frebold *et al.* (1959). The Nikanassin Formation has been studied by Kryzca (1959) and Gibson (1978), while the overlying Lower Cretaceous Cadomin Formation and Luscar Group are described and discussed by McLean (1977), Schultheis and Mountjoy (1978), Kilby (1978) and Hill (1980) and revised by McLean (1982) and by Langenberg and McMechan (1985). A complete description of the overlying Alberta Group in the Cardinal River area can be found in Stott (1963). The Upper Cretaceous and Tertiary Saunders Group (Brazeau, Coalspur and Paskapoo Formations), which forms the uppermost part of the preserved stratigraphic sequence, has been described thoroughly by Jerzykiewicz and McLean (1979) and revised by Jerzykiewicz (1985). An overview of the Cretaceous sequences can be found in Stott (1984).

No recent regional geological report covers the study area, but there are reports on neighboring areas that provide pertinent stratigraphic and structural information (Douglas, 1956a, b, 1958; Irish, 1965). The Alberta Research Council recently published a report and geological map of the Cadomin East map-area (Langenberg and Fietz, 1990).

Studies of the structural geology of the area include the early work by Hake *et al.* (1935, 1942) and Sanderson (1939), with additional interpretations by Scott (1951) on the complex stack of folded faults that overlie the Brazeau thrust fault, often referred to as the 'Brazeau structure'. Part of this structure was discussed by Douglas (1956a, 1958b). Dahlstrom (1970), Jones (1971, 1982), Price and Mountjoy (1970) and Price (1981) have presented regional and structural studies covering the Athabasca-Brazeau area. The deformation affecting coal-bearing strata in the Lower Cretaceous sequence of the Cadomin and Mountain Park has been discussed by Kilby (1978), Hill (1980) and Charlesworth and Kilby (1980). Close to, or in the study area, the triangle zone has been studied regionally by Jones (1982) and in detail by Charlesworth and Gagnon (1985) and Charlesworth et al. (1987). Mountjoy (1960a, 1960b, 1992) has described the structures affecting the Paleozoic strata in the Miette and adjacent areas. O'Brien (1960), Mountjoy

(1962, 1980b), Ziegler (1969) and Jones (1982) have presented structure sections along or near the Athabasca Valley.

CHAPTER ONE

GENERAL INTRODUCTION

This thesis is written in manuscript-style. It is composed of three papers: chapters Two, Three and Four. Each chapter contains an abstract, an introduction, a main body concerning previous work, methods, results and discussion of the results, and finally a conclusion. The objectives of each chapter are briefly outlined below.

OBJECTIVES

1. Outline the structural geology of the central Rocky Mountain thrust-fold belt in three dimensions and decipher the relationships between the various macroscopic thrust faults and folds. This study also attempts to: a) calculate the total shortening accommodated by these structures across the Foothills thrust belt, and b) outline a regional kinematic model of development for the eastern Front Ranges and Foothills thrust belt.

2. Use computer simulations to: a) develop a numerical model that imitates the propagation of individual thrust faults emanating from a décollement, and the effect of this propagation on hanging wall strata, b) discuss the validity of this model in comparison to the evolution of geologic structures, c) predict the effects and the timing of thrust propagation within a thrust belt with multiple active thrust faults, c) attempt a computer simulation of the central Rocky Mountain thrust belt, and d) discuss the model in relation to the concept of thrust displacement transfer zones.

3) Analyze the internal strain at the mesoscopic and macroscopic scale within two large thrust sheets of the Front Ranges of the Athabasca-Brazeau area and explain this strain in relation to adjacent structures within a model of progressive deformation.

CHAPTER TWO

GEOMETRY AND ROLE OF MULTIPLE THRUST DÉCOLLEMENTS, CENTRAL CANADIAN ROCKY MOUNTAINS

ABSTRACT

Regional mapping, the study of data from deep petroleum exploration wells and the construction of a series of cross-sections through the Athabasca-Brazeau portion of the central Canadian Rocky Mountain thrust-fold belt outline three types of first order décollements within or along the border of the present orogenic wedge: one basal décollement, three intermediate or internal décollements and one upper décollement. The basal décollement changes geometry both laterally and toward the foreland and has two ramps, one from the base of the stratigraphic pile to a slippage zone in the Devonian and another from this flat to another flat in the Upper Cretaceous. Internal décollements are recognized by layer-parallel glide horizons that correspond to extensive flat segments above ramps linking them to the part of the basal décollement situated behind in the more hinterland area of the orogenic wedge. Like in the case of the basal décollement, many fault imbricates emanate from the basal and internal décollements. Internal décollements are underlain by the foreland extension of the basal décollement and overlain in some cases by an upper décollement surface. In the study area, six extensive layer-parallel glide horizons are recognized. Successive forward shifts of the basal décollement to new positions within the stratigraphic pile led to the formation of internal décollements, most of which were cross-cut by younger faults rising from deeper and more northeastward décollements. It is suggested that the formation of the upper décollement caused and thrust sheet emplacement increased friction along both the basal and upper décollement

surfaces that gradually raised the critical taper angle of the orogenic wedge. Renewed internal deformation within the wedge eventually led to a shift of the basal décollement to reduce friction and allowed for renewed foreland accretion along a new basal décollement until another cycle of basal décollement abandonment occurred. The presence of several internal décollements in the study area also signifies that conventional section balancing using relative bed lengths must be done for the entire Foothills to produce valid cross-sections.

INTRODUCTION

The Cordilleran foreland thrust-and-fold belt in the central Canadian Rocky Mountains belt is a classical example of thin-skinned tectonics where the thrust belt is imbricated above a basal décollement situated at or near the base of the sedimentary package that was deposited on Precambrian crystalline basement rocks (Price and Mountjoy, 1970, Price, 1981). At the surface, thrust faults are observed to follow particular stratigraphic horizons (Douglas, 1950; Mountjoy, 1960a) but these horizons are not always associated with an imbricated thrust system (Bower and Elliott, 1982) , like décollements. Through the interpretation of subsurface structural features outlined with seismic data and deep drill holes, it has also been observed (Bally *et al.* 1966, Dahlstrom, 1970) that a middle or internal décollement occurs in Jurassic strata, which separates the upper and lower part of this sedimentary package. An upper décollement is situated along the edge of the Foothills and is associated with backthrusts of the triangle zone (Jones, 1982). These décollements have been delineated on detailed structure cross-sections of the southern Canadian Cordillera, where the middle décollement is more predominant than the the upper décollement (Price and Fermor, 1985). In the northern part of the Rocky Mountains the upper décollement is represented by an extensive layer-parallel, west-verging backthrust which overlaps most of the Foothills and hides underlying east-verging thrust faults (Thompson, 1981, McMechan, 1985). Each of these décollements

played a major role in the evolution of the thrust belt, but still little is known about: 1) the exact location of these décollement horizons, and 2) their kinematic significance. This paper: 1) outlines the presence of several stratigraphic horizons that served as décollements, and 2) discusses the consequences of thrust propagation on the geometry and kinematic history of these décollements.

Three types of décollements are recognized (Fig. 2.1), termed basal, internal and upper décollements, and named according to the relevant stratigraphic horizons followed by each. Typical examples are presented where a particular décollement links several imbricate thrust faults. These sets of thrust faults are referred to as thrust networks. This paper builds on the earlier research of Mountjoy (1960a) in the Miette and adjacent areas.

Field observations, mapping and the structure cross-sections presented here have been used to decipher the three-dimensional character of the deformation and to delineate the various stratigraphic horizons that served as décollements during the evolution of the thrust belt.

GEOLOGICAL FRAMEWORK

The Athabasca-Brazeau area, studied herein, is situated in the eastern Front Ranges and Foothiils of the Central Canadian Rocky Mountains, 50 km east of Jasper, Alberta (Figs. 2.2 and 2.4). Resistant Paleozoic rocks crop out west of the Nikanassin Range and mark the physiographic limit between the Front Ranges and the dominantly Mesozoic-Cenozoic Foothills.

The Front Ranges and Foothills of this area are characterized by thrust faults extending for several tens of kilometres, up to 400 km in the case of major faults like the McConnell thrust. A few major thrust faults account for most of the shortening (Mountjoy, 1960a). These faults generally dip gently southwest and have transported rocks towards the northeast, forming a system of imbricate thrusts that scraped rocks

from above the Precambrian crystalline basement, along a basal décollement during the Laramide orogeny (see Price, 1981 for a review).

In the Athabasca-Brazeau area, thrust faults are generally oriented northwest-southeast (Fig. 2.4), which differs from the more northerly NNW-SSE trend observed near the Bow River in southern Alberta. This progressive change in orientation between the North Saskatchewan and the Brazeau Rivers, close to the central part of the Alberta syncline, forms a major reentrant or arc along the thrust belt (Fig. 2.2). The bedding dips and structural style change substantially from the internal part to the external part of the Rocky Mountain Belt, across the Main Ranges-Front Ranges boundary. Southwest of the studied area, in the Main Ranges and Western Front Ranges, moderately dipping and homoclinal thrust sheets contain thick Paleozoic and Neoproterozoic sequences. The Neoproterozoic, Lower Cambrian and a thick sequence of Ordovician-Silurian rocks thin and disappear northeastward, while Middle and Upper Cambrian strata thin substantially towards the Interior Platform. Along the northeastern edge of the Front Ranges, the McConnell thrust fault juxtaposes Paleozoic rocks over the upper part of the Mesozoic sequence. This thrust is the dominant structure west of Calgary, but northwestward it dies out in the Miette area (Fig. 2.3, 2.4; Mountjoy, 1960a, b). The disappearance of this fault is balanced by the appearance of a number of thrust faults (Miette, Nikanassin, Folding Mountain thrusts) that transport Paleozoic strata to the surface further northeast in the thrust belt, in the vicinity of the Athabasca River. In the Foothills to the northeast, Cretaceous and Tertiary strata outcrop over a wide area (Fig. 2.4), and are deformed into a complex set of imbricated folded faults (Hake *et al.*, 1942; Scott, 1951; Douglas, 1956, 1958; Douglas and Lebel, 1993). To the southeast, close to the North Saskatchewan River, the Foothills contain only a few thrust faults, which do not have numerous imbricates.

From southwest to northeast, major northeast-verging thrust faults crossing the area comprise the Balcarres, Medicine Tent, Makwa, McConnell, Miette, Bighorn, Fiddle River, Nikanassin, Grave Flats, Brazeau, and Ancoma thrusts (Fig. 2.3), in addition to numerous second-order thrust faults branching from them. The Lovett thrust (or Pedley thrust of Charlesworth and Gagnon, 1985) constitutes the edge of the thrust belt and is southwest-verging (backthrust of the triangle zone).

DÉCOLLEMENT SURFACES

A décollement (or detachment) is a zone of mechanical weakness and slippage above or below which deformation has occurred (Dahlstrom, 1970). The term décollement is also commonly used to describe a geometric feature, the last or an abandoned basal bounding surface ('basal décollement') of an orogenic wedge that permitted advancement and internal deformation of the said wedge (Davis *et al.*, 1983; Brown *et al.*, 1992; Dechesne and Mountjoy, 1992, Hatcher and Hooper, 1992). Commonly, a series of faults have propagated along and from such a zone to form an imbricated thrust system, or network (Bally *et al.*, 1966; Boyer and Elliott, 1982; Suppe, 1985). In thin-skinned tectonics of the Canadian Rocky Mountains, the stacking of thrust sheets is generally recognized to be the consequence of the advancement of a deforming wedge (Fig. 2.1) above a basal décollement (Bally *et al.*, 1966; Dahlstrom, 1970; Price and Mountjoy, 1970; Ollerenshaw, 1978; Price, 1981; Price and Fermor, 1985). In this paper, the term décollement refers to a geometric structure, an extensive sole thrust from which numerous thrusts rise (basal décollement) or a roof thrust where thrusts merge upwards (upper décollement). It is in general parallel to a particular stratigraphic level, but ramps may be present along it, to link it to the base of the stratigraphic pile (Fig. 2.1).

In the study area, the upper décollement (Jones, 1982) comprises a prominent zone in Upper Cretaceous strata in which layer-parallel backthrust faults, associated with the triangle zone, are situated along most of the northeastern edge of the Cordilleran

foreland thrust belt (Price, 1986). It is linked in the subsurface with the basal décollement via east-verging blind thrusts (Fig. 2.1, Jones, 1982, Price, 1986).

The term *'internal décollement'* is designated for extensive layer-parallel glide horizons, out of which numerous thrust faults rise and that occur within the deformed sedimentary wedge in contrast to the basal and upper décollements that bound the wedge (together with the topographic surface, Fig. 2.1). Internal décollements may be present at multiple stratigraphic horizons and may represent the remnants of abandoned basal or upper décollements, or the location of roof thrusts (Boyer and Elliott, 1982). Because internal décollements are mostly hidden in the subsurface, their exact location is difficult to assess. In the southern Canadian Rocky Mountains, the Fernie décollement is usually recognized by large discrepancies in total displacement (the Mesozoic sequence is more shortened than the Paleozoic strata within segments of the Foothills; Bally *et al.*, 1966; Price and Fermor, 1985) or a change in structural style above and below it, or cross-cutting fault relationships (Bally *et al.*, 1966; Boyer, 1992; Cooper, 1992). Understanding the exact role of internal décollements in the evolution of thrust-fold belts is important because they are extensive, although subtle structural features.

EFFECTIVE AND ABANDONED BASAL DÉCOLLEMENTS

The base of the deformed orogenic wedge is termed herein the *effective basal décollement*, because it is the last décollement surface that was active when deformation of the foreland thrust belt ceased. For most of the Front Ranges and Main Ranges, this basal décollement is thought to be situated near the contact between the sedimentary cover and the top of the Precambrian crystalline basement. The dip of the basement is very shallow, changing only from about 1 to 1.5° under the Foothills and Front Ranges to about 4° beneath the Main Ranges (Price and Mountjoy, 1970; Cook, 1988). It is generally recognized (Bally *et al.*, 1966; Brown *et al.*, 1992; Simony *et al.*, 1980) that this basement remained rigid and uninvolved in the thrusting east of the southern Rocky

Mountain Trench (Fig. 2.2). Westward, in the Shuswap Complex of the Omineca crystalline Belt, and north of Mica Dam in the Rocky Mountain Trench, basement complexes are present at the surface and are thought to represent slivers of the North American craton involved in the east-directed thrusting during the late phase of the development of the Rocky Mountains Foreland thrust belt (Read and Brown, 1981; Okulitch, 1984; McDonough and Simony, 1988; Brown *et al.*, 1991, Brown *et al.*, 1992). Tectonic erosion of low-grade metamorphic cover strata in the Eocene by crustal-scale extension and uplift exposed these basement complexes within dome-shaped windows (Fig. 2.2). One of these windows is encircled by a crustal-scale décollement, the Monashee Décollement that is thought to represent an early easterly verging and westerly rooted basal décollement that acted mechanically as a ductile compressional shear zone along which cover rocks of the Selkirk allochthon were transported eastward until the Late Paleocene (Carr, 1989). Because it is folded and exposed at the surface, the Monashee Décollement is interpreted to have been abandoned after a shift of the basal décollement to a deeper crustal level, to explain the stacking of crystalline thrust sheets into an antiformal duplex underneath the Monashee Décollement (Brown *et al.*, 1986; Brown *et al.*, 1991). Similar décollement abandonment and downward shifting have been interpreted by Dechesne and Mountjoy (1992) in the western Main Ranges for the Fraser River antiform, east of the southern Rocky Mountain Trench. In this case, thrust sheets have also been stacked into an antiformal duplex, where each slice has a highly sheared zone at the bottom, with strain decreasing in intensity upwards.

Although there is evidence that the basal décollement shifted downward to deeper crustal levels through time to involve crystalline thrust sheets in the hinterland of the Canadian Cordilleran thrust belt, only few authors discussed such downward shift in the stratigraphic pile of the foreland of the Cordilleran thrust belt (Bally et al., 1966; Boyer and Elliott, 1982).

In the Front Range portion of the southwestern part of the Athabasca-Brazeau area, the Colin, Rocky River, Balcarres, Medicine Tent and McConnell, Miette, Fiddle River thrust sheets consistently contain Middle Cambrian rocks at their bases (as noted by Mountjoy, 1960a). A deep well near Mountain Park also encountered Cambrian rocks at the base of the Nikanassin thrust (Fig. 2.6, section C-C'). These strata come from near the base of the sedimentary cover, thus the basal décollement that is floor of the present orogenic wedge beneath the Front Ranges must follow a zone near the top of the crystalline basement east to the footwall cutoff where the Nikanassin thrust originates (Fig. 2.6, section A-A').

While the basal décollement detached the sedimentary cover from the Precambrian crystalline basement for most of the area that used to be situated beneath the Main Ranges and Front Ranges, it does not beneath the Foothills. In the Foothills, the basal décollement in the Athabasca-Brazeau area evolved through two ramps which successively brought it up to different stratigraphic levels.

The first ramp cuts stratigraphy at a low angle and occurs southwest and under the surface trace of the McConnell fault. Section A-A' (Fig. 2.6) shows the geometry of the thrust belt between the McConnell thrust and the Lovett thrust, where an upward shift of the basal décollement is observed through the stratigraphic package. Near the middle of the section, structural constraints from a deep well (Shell Lovett, 15-21-44-19 W5) show that the Frasnian Fairholme Group is not involved in the thrusting east of this well, while Cambrian strata are brought high within the orogenic prism (near sea-level on section A-A') by the Nikanassin and Fiddle River thrusts. Thus the hanging wall cutoffs of these thrust sheets demonstrate the presence of a ramp between the Cambrian and the Palliser Formation further westward downdip along the basal décollement. Section balancing using additional well control indicates that the ramp should be situated at a depth of 5.5 km below sea-level about 25 km southwest of the McConnell thrust surface trace (Section A-A', Fig. 2.6). This ramp cuts at low angles (about 2°) through all the Cambrian and

Frasnian section over a distance of more than 30 km. This is an estimated position and angle using cut-offs in the hanginging wall of thrust fault originating from this ramp and the estimated dip of the basement of 4° west of the McConnell thrust surface trace, a dip commonly used in regional cross-sections of the Rocky Mountains (Price and Mountjoy, 1970, Price and Fermor, 1985) and in agreement with the current knowledge of the depth to basement further west under the Main Ranges based on seismic data (Cook, 1988).

Northeast of the first ramp, the décollement occurs near or within the Frasnian-Famennian boundary unit, the Sassenach Formation or base of the overlying Palliser Formation, for a distance of more than 50 km, beneath most of the Foothills to within just a few kilometres of the triangle zone. From this point, the basal décollement forms a second but steeper ramp that merges with the upper décollement in the Upper Cretaceous Brazeau Formation. The Famennian Palliser Formation has been encountered within several thrust sheets beneath the Foothills in other deep wells of the Athabasca-Brazeau area (e.g. Gulf *et al.* 3-24-45-21W5, B.A. *et al.* 5-7-48-22W5), but no Frasnian strata are involved in thrusting east of the Nikanassin thrust. The Sassenach Formation was utilized because it is a thin weak layer situated between the rigid Fairholme and Palliser carbonate units in this area.

In contrast, west of Calgary where the stratigraphic sequence is similar to that of the Athabasca-Brazeau region, most of the Foothills are underlain by a basal décollement that follows a layer-parallel zone within the uppermost Devonian (Exshaw Fm.) and basal Mississippian (Banff Fm.) rocks (Price and Fermor, 1985). The basal décollement cuts upward from the top of the crystalline basement to this higher thrust flat through a ramp situated about 15 km west of the McConnell thrust surface trace and 5 km below sea level. This flat is followed eastward to the triangle zone where a steep ramp links it to the Upper Cretaceous strata of the upper décollement. It is thus interesting to note that, along these two cross-sections of the Foothills, the effective basal décollement occurs at a lower

stratigraphic position in the Athabasca-Brazeau region but both display a similar ramp-flat geometry.

INTERNAL DÉCOLLEMENTS

The décollement at or near the Mesosoic-Paleozoic boundary portrayed on numerous cross-sections of the Foothills of Alberta (Bally *et al.*, 1966; Dahlstrom, 1969, 1970; Price and Fermor, 1985; Douglas and Lebel, 1993) represents an internal décollement. In the study area, Mountjoy (1960a) recognized at the present erosion surface, stratigraphic horizons which occur extensively next to and parallel to thrust fault surfaces (Table 2.1). Only some of these horizons are recognized as extensive décollement horizons in the subsurface. In the Foothills of the Athabasca-Brazeau area, evidence is presented for at least three different stratigraphic horizons representing internal décollements. These are: 1) Fernie Group, 2) Nikanassin Formation, and 3) Blackstone Formation (see Fig 2.3 for stratigraphic positions).

In the southern Foothills, the Jurassic Fernie Group has been interpreted the outward portion of an early basal décollement affecting only the Mesozoic sequence which is rooted through a ramp to the basal décollement at the bottom of the sedimentary pile, far to the southwest (Fig. 2.5; Bally *et al.*, 1966). It has also been suggested that the higher portion of this décollement was abandoned and cross-cut by underlying thrust faults rising from the basal décollement. Cross-cutting fault relationships should be expected to be observed in the field (Bally *et al.*, 1966, Fig. 6) but to our knowledge, no examples have been reported in the literature up to now. In most cases the late faults displacing Paleozoic rocks at depth appear to have followed earlier faults in their higher segments through the Mesozoic strata (Bally *et al.*, 1966, Price and Fermor, 1985).

Thrust	Observed at present surface	Projected at moderate depth from geometry of folds and thrust sheets
Eastern Foothills		
Brazeau	Upper Cretaceous	Blackstone Formation
Western Foothills		
Folding Mountain	Folding Mountain anticline	Devonian Cairn or lower
Boule	Luscar, Upper Rundle	Middle Cambrian?
Perdrix	Lower Luscar	Mount Hawk-Perdrix
Ashlar	Mount Hawk-Perdrix	Middle Cambrian
Mystery Lake	Nikanassin, Upper Rundle, Banff or lower	Upper Rundle Group
Drinnan	Upper Rundle, Banff or lower	Palliser Formation or lower
Nikanassin	Lower Luscar, Nikanassin, Palliser formations	Perdrix Formation or lower
(associated Fiddle River fault)	Cambrian Snake Indian Fm and base of Eldon Formation	Cambrian Snake Indian Formation
Front Ranges		
Miette, McConnell	Cambrian Snake Indian Fm. and base of Eldon Formation	Cambrian Snake Indian Formation

Table 2.1: Stratigraphic horizons which occur extensively next to and parallel to thrust fault surfaces in the Miette area (adapted from Mountjoy, 1960 (a), Table 1, p.187)

In the Athabasca-Brazeau region, most deep-rooted faults appear also to have followed the path of earlier faults in the Mesozoic and so there are few cases of cross-cutting fault relationships at the present surface. Poor exposure in the Foothills of the Mesozoic shaly horizons also limits the observation of such relationships. However, cumulative evidence from three-dimensional reconstructions of the structural geometry of the Foothills by means of surface mapping, cross-sections and the projection of deep wells indicate that early basal décollements have been abandoned and were later cross-cut or folded by later faults. These faults originated in the underlying and subsequent basal décollement, and cross-cut what is now an internal décollement.

The Fernie internal décollement

A group of thrust faults termed the Mountain Park thrust network, situated near Mountain Park, between the Nikanassin and McConnell thrusts and that overlap the Miette thrust (Fig. 2.3, 2.4), has been studied in detail by Kilby (1978, also Kilby and Charlesworth, 1980; Charlesworth and Kilby, 1981), who demonstrated that significant slip has occurred along each fault. On the basis of downplunge projections of coal exploration drillholes and surface geology, the cumulative displacement of these faults has been estimated to be on the order of 8 km (Charlesworth and Kilby, 1981). It consists of a set of thrusts, folded together about a series of sub-parallel axes with shallow plunges towards the southeast, more or less parallel with the regional plunge of the Cardinal syncline (Fig. 2.3, 2.4). These imbricates are also internally deformed by folds and minor faults that stacked coal beds within fold hinges (Kilby, 1978). As noted by these authors, the Prospect and Drummond Creek thrust faults do not cut downsection substantially southwest- and northwestward and are sub-parallel to the strata (Fig. 2.3). There is no evidence that these faults might be rooted directly to the basal décollement because, when followed along strike, none of them cross-cut any strata situated lower than the Fernie Group, except for the Miette thrust (Fig. 2.3). One explanation for this situation might be

that these faults are simple 'out-of-syncline' thrusts related to the tightening of the Cardinal syncline during the latest motion of the McConnell thrust situated immediately above it to the southwest (Section E-E', Fig. 2.6). However, all the faults of the Mountain Park thrust network merge together in the Fernie Group and have a substantial cumulative displacement, suggesting that they are rooted in an early, internal Fernie décollement.

The geometry of the Miette thrust suggests that it has cut through the Fernie décollement in the area situated near Mountain Park. The Miette thrust fault extends along strike for close to 80 km, from the Cardinal River in the southeast, to northwest of the Athabasca River. In the Miette area, its throw is important as it brings Cambrian strata to the surface over Lower Cretaceous rocks. Southeastward, from the southeast corner of the Miette map sheet, the stratigraphic displacement of the Miette thrust decreases substantially until it only duplicates Jurassic strata in the Mountain Park area. This dramatic decrease in stratigraphic offset can be explained by the presence of a footwall ramp at depth as outlined on structure section I-I' (Fig. 2.6). In the center of the study area, the McConnell and Miette thrusts merge a few kilometres below sea-level (section I-I', Fig. 2.6) and the Miette and Nikanassin thrusts are part of a fault network linked through a décollement situated near sea-level, about 5 km above the crystalline basement. This geometry places strong constraints on the manner in which other cross-sections to the southeast can be constructed and interpreted. Although the southeastern segment of the Miette thrust fault appears to be part of the Mountain Park thrust network, the northward extension of the Miette thrust attest to the fact that it is not part of the same thrust network because it involves Paleozoic strata (Fig. 2.6, section F-F'). Following the formation of the Mountain Park thrust network and the Fernie internal décollement, the Miette fault appears to have propagated laterally southeastward into the Mountain Park area. Thus, the Mountain Park thrust network appears to be linked to an early décollement that permitted the development of thrust faults only within strata situated above the Fernie

Group. An interpreted and simplified kinematic model explains the geometry and evolution of these structures (Fig. 2.7).

The Fernie internal décollement is difficult to observe in the field because the Fernie Group is poorly exposed. It is inferred to follow a level or a zone within the Fernie Group and more careful stratigraphic work should be able to show where stratigraphic duplication occurs within the Fernie Group using its seven or more distinct formations. Because of its dominantly shaly lithology, the Fernie Group is a favored thrust glide horizon in most of the Rocky Mountains (Douglas, 1950, Bally *et al.*, 1966, Dahlstrom, 1970, Mountjoy, 1960b, Price and Fermor, 1985).

The Nikanassin internal décollement

In the northeast part of the Athabasca-Brazeau area, there is good evidence that the Nikanassin Formation has also been utilized as a décollement. Many thrust faults are found to be parallel with strata within the Nikanassin Formation for large distances within the Athabasca-Brazeau area (Fig 2.3). On structure section A-A' (Fig. 2.6) shortening above the Nikanassin Formation is slightly higher (47.2% shortening measured from restored bed lengths of the Cadomin Formation) than that in the older strata (44.1%, from restored base of Fernie Group). This indicates that the section is not balanced or that some slip along an intermediate décollement took place so that more shortening occurred in the higher stratigraphic level. Although solid geometric constraints from numerous deep wells and surface geology support the interpretation of differing shortening values, the section is not balanced is also plausible, since section construction within such a complex area is difficult and subject to errors. However, the relative shortening values found above and below the Nikanassin Formation are in agreement with cross-sections and a palinspastic restoration of the southern Foothills (Price and Fermor, 1985) that demonstrate that there is no large difference in total shortening across the entire Foothills, from the Paleozoic to the Mesozoic.

In contrast, when considered by segments, section A-A' (Fig. 2.6) shows higher relative discrepancies in shortening measured above and below the Nikanassin Formation, which cannot be explained by erroneous section balancing. For example, the displacement found at the surface on the Nikanassin thrust and on the other fault splays to the northeast (including the Bighorn thrust) cannot be balanced with the large displacement of Paleozoic rocks along the Nikanassin-Bighorn sole thrust (≈13 km). This discrepancy, found in several segments of this cross-section, can be resolved by inferring the presence of a décollement along the Nikanassin Formation across most of the Foothills of this area.

The Nikanassin, Fiddle River, Miette and Bighorn thrusts emanate from a common sole thrust situated between Cambrian rocks (hanging wall) and the Nikanassin Formation (footwall) (Fig. 2.6, section H-H', G-G'). This sole thrust forms part of the Nikanassin décollement which is situated between 1.5 and 5 km above the effective basal décollement since it generally dips at a low angle southeast in the area situated between the Nikanassin and McConnell thrust, following the plunge of the Cardinal syncline (Fig. 2.3, 2.4, structure sections I-I' to A-A', Fig. 2.6). This higher décollement has to be rooted via a ramp within the effective basal décollement west of the McConnell thrust trace, to permit transport of Cambrian and younger strata.

Several observations point towards the interpretation that the Nikanassin décollement has followed a horizon within the upper part of the Nikanassin Formation over a large part of the Foothills of the study area.

1. In the Miette area, near Sphinx Mountain, Mountjoy (1960a) outlined a complex set of fault splays, rising from the Nikanassin thrust at the surface that are folded by footwall structures. He also showed that the Nikanassin thrust follows a glide zone in the Nikanassin Formation, for nearly 4.5 km. Furthermore, for a large segment along strike, the Nikanassin thrust is floored by this unit, which indicates that the thrust has followed a glide zone in this formation.

2. Data from deep wells (i.e. Imp. *et al.* 3-17-44-20W5, CPOG Thistle 6-21-44-20W5) and surface mapping indicates numerous imbrications within the Nikanassin-Luscar stratigraphic interval in the footwall of the Nikanassin thrust along section A-A' (i.e. in the area between Nikanassin and Grave Flats thrust faults) and adjacent areas and does not show any such repetition by thrust imbrications within Fernie Group or older strata.

3. In the cross-section segment situated between the McConnell thrust and the Nikanassin thrust (segment 1, section A-A', Fig. 2.6), the cumulative shortening estimated from bed lengths of the Lower Cretaceous and overlying rocks (e.g. Cadomin Formation) is about two times shorter than that at the base of the the Fernie Group and underlying rocks. The difference in shortening, on the order of 6.4 km, is mainly due to the small displacements of faults at the surface within Cretaceous strata relative to the large motion of Paleozoic strata at depth above the Nikanassin-Bighorn sole thrust. The missing shortening is found northeast of the Nikanassin thrust, along thrusts emanating from the Nikanassin décollement. About 4 km of the missing shortening is found within cross-section segment 2 between the Nikanassin and Grave Flats thrust (section A-A', Fig. 2.6). The remaining missing shortening within the Mesozoic sequence is found further northeast within segment 3. The subsurface control precludes a direct link between the Nikanassin décollement and the faults observed at the surface northeast of the Grave Flats within segment 3, because several faults rooted in the basal décollement intersect the Nikanassin Formation and younger rocks. The cumulative shortening measured within segment 3 is about 6.6 km greater within Cretaceous strata than within Triassic and underlying Paleozoic rocks, mainly due to the large cumulative displacement of the array of thrust faults merging with the Brazeau thrust fault (the 'Brazeau structure'). In segment 4, further northeast, the relative shortening of the Paleozoic and Mesozoic match closely (about 8.0 km of shortening). Thus the relative shortening observed within segment 3 for rocks above the Nikanassin Formation is higher by 4.2 km relative to the missing

shortening from segment 1 and 2, which corresponds to the overall difference in shortening (≈3%) measured between the Cadomin Formation and the base of the Fernie Group over all section A-A'.

Thus, the relative discrepancies in shortening measured above and below the Nikanassin Formation within the various segments of structure section A-A' add up to a balanced cross-section. This geometry is interpreted to be the consequence of early motion along the Nikanassin internal décollement that extended northeastward. In the later phases of the evolution of the thrust belt, the Nikanassin décollement was abandoned through a shift of the basal décollement to the Devonian stratigraphic level, lower within the sedimentary pile that led to the fault intersections interpreted on section A-A' (Fig. 2.6, segments 1, 2, 3, e.g. near the botton of the CPOG Thistle 6-21-44-20W5 well).

The Blackstone internal décollement

An intensely deformed zone in the Upper Cretaceous Blackstone Formation in the Cadomin area, characterized by northeast-verging folds and thrusts was termed the 'Blackstone detachment zone' by Hill (1980) and interpreted to represent a widespread glide horizon separating the distinct structural blocks situated above and below it. Well exposed at the Luscar coal mines in the same area, the Lower Cretaceous strata below this horizon (termed Blackstone décollement here), are considerably deformed and characterized by tight folds and numerous mesoscale faults, whereas the overlying strata observed downplunge to the southeast in the Cadomin syncline are relatively undeformed. A klippe of Mesozoic rocks, northeast of the Luscar thrust near the McLeod River comprises faults with observed cut-offs that suggest they are remnants of folded northeast-directed thrusts (Hill, 1980). The present geometry suggests that these thrusts were probably rooted along the Blackstone décollement. Section I-I' highlights the present geometry of this décollement as reconstructed from local and regional mapping. The Blackstone décollement appears as the roof thrust to a complex set of imbricated

thrusts at the surface and in the subsurface. The extent of the layer-parallel glide zone within the Blackstone Formation is estimated to be a minimum of 5 km long (perpendicular to strike of the belt), but likely was more than 10 km long, because it is folded and plunges underneath the Brazeau syncline (Fig. 2.6, Section I-I'). From surface mapping, the Blackstone décollement does not appear to be cut by thrusts rising out of the underlying basal décollement such as the Folding Mountain and Brazeau thrusts. The structure underlying the Blackstone décollement of the Luscar area, between the Drinnan and Brazeau thrusts is represented by two duplex structures, stacked on top of each other (lower and upper duplex) and interconnected through intermediate faults (section I-I', Fig. 2.6).

The upper duplex comprises the faults and tight folds situated between the Blackstone décollement (hanging wall of this duplex) and the Luscar sole thrust gliding along the lower part of the Luscar Group (footwall of the duplex). This duplex appears to continue towards the southeast, underneath the Cadomin syncline. North of section I-I', the Luscar thrust merges with the Mystery Lake thrust which transports Paleozoic rocks. This upper duplex is only about 4 km wide at the surface, between the Drinnan thrust (southwest) and the Luscar thrust where it tapers off along section I-I'. The base of this upper duplex is situated in the Nikanassin Formation and thus is interpreted as an early structure related to the Nikanassin décollement involving only Mesozoic strata.

The lower Folding Mountain duplex involves Paleozoic and Mesozoic rocks and is situated directly under and folds the upper duplex or Blackstone décollement in the segment that underlies the Brazeau syncline. The Folding Mountain, Mystery Lake, Perdrix, Boule, Luscar and contiguous thrusts (Fig. 2.3, 2.4) form a network of branching faults rising from the basal décollement that transports Paleozoic rocks. These imbricate faults are exposed in a structural culmination in the Miette area where they are oriented at a high angle to the strike of the Folding Mountain thrust (Mountjoy, 1960b). Near Luscar, the Shell Fina Luscar 5-27-47-24 well (section I-I', Fig. 2.6, Fig. 2.3)

indicates that Paleozoic strata are present near the surface, underlain by the Folding Mountain thrust. The downplunge projection from the surface of the Perdrix and Mystery Lake thrusts into section I-I' outlines a duplex of Paleozoic rocks at depth, with the Blackstone décollement as the roof thrust and the Luscar, Mystery Lake and Folding Mountain thrusts as successive floor thrusts. The cumulative displacement of the Folding Mountain duplex is close to 8 km at the Paleozoic level. Because the displacement measured from unit cutoffs above the Blackstone Formation in the area between the Brazeau syncline and the Luscar thrust is smaller (less that 1 km, constrained by the Shell Fina Luscar well and surface mapping), most of the displacement of the Folding Mountain thrust has to emerge at the surface northeast of the Brazeau syncline. The geology of the area underlying the Folding Mountain thrust in section I-I' is uncertain, but thrust faults observed in the Ammin Amoco Trapper 7-18-48-23W5 well suggest that a set of blind thrusts branches with the Folding Mountain thrust.

Link between the Blackstone décollement, the Folding Mountain duplex and the upper décollement

Subsurface and surface data require that most of the displacement (>15 km) found below the Blackstone décollement and additional displacements from other underlying blind thrusts be found somewhere at the surface northeast of the Brazeau syncline. Evidence is presented indicating that this displacement is linked to the upper décollement and transferred to backthrusts of the triangle zone, northeast of the Brazeau thrust.

The difference in displacement between Upper Cretaceous strata and underlying units occurs along much of the Foothills of the study area and was previously recognized by petroleum geologists (Jones, 1982). Interpretations of the Folding Mountain thrust network have changed with the evolution of ideas on thrust geometry (Fig. 2.8). Along the Athabasca River valley, interpretations vary as to the amount of displacement of the Folding Mountain thrust at the Mesozoic level. High displacements favored a simple

structure (Webb, 1955; Mountjoy, 1960a) while low values and a folded thrust interpretation were suggested by Jones (1971). Later, when a new well (Brule 6-6) was drilled during gas exploration, it showed a considerable amount of displacement for the Paleozoic rocks by the Folding Mountain thrust (≈ 5 km) but little displacement of the overlying Upper Cretaceous strata. Folding the Folding Mountain thrust satisfies these structural constraints by allowing it to eventually merge with a prominent southwest-verging upper décollement or triangle zone (Fig. 2.8, Ziegler, 1969; Jones, 1982). The presence of such a triangle zone had been recognized earlier (Mountjoy, 1960a, b) near the Seabolt anticline (Fig. 2.3), and another one also occurs at the northeast edge of the thrust belt (Lovett backthrust fault) in the Athabasca-Brazeau area (Price *et al.*, 1977, Charlesworth *et al.*, 1987). The interpretation illustrated on section I-I' (Fig. 2.6) shows that the early formed Blackstone décollement acted as a roof thrust during the formation of the Folding Mountain and Luscar duplexes, since no important southwest-dipping and northeast-verging faults occur at the present surface between the Luscar thrust and the Lovett backthrust (the Brazeau fault has relatively small displacement in this area). In addition a number of blind thrusts have been encountered in wells situated within this segment of the Cadomin map-area (e.g. Canoxy *et al.* 6-9-48-22 W5, B.A. *et al.* Kaydee 5-7-48-22W5, B.A. *et al.* Kaydey 14-12-48-23W5, Ammin Amoco Trapper 7-18-48-23W5, Ammin Antler 7-31-48-23W5). The interpretation shown follows those of Ziegler (1969) and Jones (1982) with most of the missing displacement occurring at the present surface within the Upper Cretaceous strata along northeast-dipping and southwest-verging thrust faults (Fig 2.8 (c)). This implies that there is a system of 'blind' thrusts in the subsurface that eventually merge with the southwest-verging faults that are linked to the upper décollement. Thus the role of the Blackstone internal décollement within this system of blind thrusts has been two-fold, first it acted as a décollement where a series of northeast-verging thrusts developed underneath the upper décollement, and secondly as a roof thrust to the Luscar and Folding Mountain duplexes.

Recently published seismic data (Skuce *et al.*, 1992) from near Edson more than 30 km northeast of the Lovett thrust, also show an intercutaneous wedge between the Wapiabi Formation (roof thrust or upper décollement) and the Blackstone Formation (basal décollement) with cumulative shortening of close to 2 km between these stratigraphic levels. This indicates that the Blackstone Formation was still used as an active décollement at the end of foreland deformation.

THE UPPER DÉCOLLEMENT

As noted in the previous section, in the Cadomin area most of the displacement on the Folding Mountain and Luscar duplexes, and other northeast-verging blind thrusts situated below, has to occur on faults that emerge at the surface northeast of the Brazeau thrust fault and be linked to the upper décollement of Jones (1982). In contrast, in the Cardinal River area, as explained in the section pertaining to the Nikanassin internal décollement, (Fig. 2.3, segment 1 to 3 of section A-A', Fig. 2.6, Douglas and Lebel, 1993), much of the displacement within the structures encountered along strike in the thrust belt occurs at the surface within the stack of folded thrust faults associated with the Brazeau thrust. However, northeast-verging blind thrusts have also been encountered in deep wells, in the triangle zone (Gulf *et al.* 16-19-46-18W5 and B.A.Triad *et al.* 12-30-46-18W5, segment 4 of section A-A', Fig. 2.6) and merge with the southwest-verging Lovett backthrust. From these wells and surface geology projected on section A-A', the location of the upper décollement appears to occur within the middle of the Brazeau Formation. This is also in agreement with the presence of Brazeau strata at the present surface within northeast directed thrust slices associated with the Brazeau thrust (Fig. 2.3, section A-A', Fig. 2.6) and observations from the structure of the triangle zone in the Foothills map-area, just north of the Cardinal River area (Charlesworth *et al.*, 1987).

In the Miette area, Mountjoy (1960a, b) observed southwest-verging, northeast-dipping thrust faults gliding within the Upper Cretaceous Wapiabi Formation (e. g. next

to the Seabolt anticline). Jones (1982, p.65) also suggested that the upper décollement lies in the Wapiabi Formation. The Wapiabi appears as a reasonable location for a décollement because of its shaly character which is susceptible to faulting. The change in stratigraphic level of the upper décollement from the lower Brazeau Formation between the Cardinal River and Miette areas appears to reflect the presence of a lateral ramp within the surface of the upper décollement between the two areas.

Throughout the central and southern Rocky Mountain thrust belt, the upper décollement occupies various stratigraphic levels but generally lies within Upper Cretaceous strata (Price, 1986; Price and Fermor, 1985, Jones *et al.*, 1992). From detailed work around the Coal Valley mine in Foothills map area, at the northeast edge of the foreland thrust belt, Charlesworth *et al.* (1987) also suggested that the location of the upper décollement within the triangle zone has changed geometry and stratigraphic level, within Upper Cretaceous and Tertiary strata. Spratt *et al.* (1993) have also presented evidence for a similar geometric transition within the same stratigraphic interval between the Jumping Pound and Turner Valley areas of the southern Foothills.

In the Cardinal River area, northeast-verging and southwest-dipping faults that cut through the Brazeau and Paskapoo Formations, are present at the surface northeast of the Brazeau thrust. These faults indicate that part of the upper décollement was carried by younger, deeper thrusts during the late stages of deformation. This event led to the preservation of triangle zones under northeast-verging thrusts, such as the one observed just north of the Cardinal Hills (Fig. 2.3; segment 4, section A-A', Fig. 2.6).

Jones (1982) suggested that a southwest-verging upper décollement may have been active throughout the entire evolution of this segment of the Rocky Mountains. This idea is further supported by the recognition of a number of blind thrusts underneath the Blackstone décollement. An upper décollement with a similar geometry of numerous northeast-verging blind thrusts has also been recognized in the Foothills of the northern Canadian Rocky Mountains (Thompson, 1979, 1981, McMechan, 1985). However, the

geometry outlined here and by Jones (1982) for the Athabasca-Brazeau area, where several northeast-dipping, southwest-verging thrust are observed, makes it also even more plausible that the more advanced portions above the orogenic wedge (towards the hinterland) of the upper décollement panel were successively abandoned through a progressive process of imbrication toward the northeast of this upper décollement panel.

DISCUSSION

Shift and abandonment of décollements

The presence of at least three extensive internal décollements at the Fernie, Nikanassin and Blackstone stratigraphic levels (≥10 km in length across the belt) between the present basal and upper décollements of the Foothills of the Athabasca-Brazeau area is symptomatic of a complicated kinematic history of emplacement of the foreland thrust belt.

In the Cardinal River and Mountain Park areas, it appears that the basal décollement has shifted downward through the stratigraphic pile at least twice (Figs. 2.7, 2.9). First it shifted down and forward from its position within Fernie Group to a new position starting just above the Precambrian crystalline basement and rising up through a ramp to a new flat in the Nikanassin Formation (Figs. 2.7 (c), 2.9 (a, b)). Secondly it shifted again from the Nikanassin Formation to the base of the stratigraphic section and rose through a ramp to the present effective basal décollement in the Sassenach-basal Palliser formation (Fig. 2.9 (c), section A-A', Fig. 2.6). This is demonstrated by the presence of faults that cross-cut or cause folding of: 1) the Fernie internal décollement (e.g. Miette thrust, structure cross-section F-F', Fig. 2.6) from above the Nikanassin décollement, and 2) the Nikanassin internal décollement (e.g. Grave Flats thrust, structure cross-section A-A', Fig. 2.6) from above the Sassenach-basal Palliser basal décollement.

To the northwest, in the Cadomin and Miette areas, an additional décollement is found, the Blackstone décollement, that is not substantially cross-cut, but is folded over

fault ramps situated above the Nikanassin and Sassenach décollements. From these relationships, three interpretations of the Blackstone internal décollement are possible. It represents: 1) an upper flat segment connected to the ancestral Fernie décollement; 2) an upper flat segment of the ancestral Nikanassin décollement, or 3) a separate ancestral décollement that was abandoned. It is difficult to assess the exact origin of this décollement from the available data. However, most thrusts in the Brazeau structure of the Cardinal River area follow long flats in the Blackstone Formation. Since these faults have been interpreted to be linked to motion on the Nikanassin décollement, it is reasonable to interpret the Blackstone décollement as a roof thrust to the duplex developed above the Nikanassin décollement (Fig. 2.9 (b)).

Model of décollement propagation, activity and abandonment

Most of the recent models of thrust belt development recognize that orogenic foreland belts behave as a mechanical entity. The critically tapered Coulomb wedge model presented by Davis *et al.* (1983), Dahlen (1984) and Dahlen *et al.* (1984) on the basis of the early proposal of Chapple (1978) and modified and developed further (Davis and Engelder, 1985; Zhao *et al.* 1986; Dahlen, 1990) has found wide acceptance because it provides a coherent explanation for the geometry and sequential propagation of thrust faults in modern accretionary prisms and in foreland thrust belts. The model proposes that thrusts propagate sequentially towards the foreland, until an overall critical taper is reached. The whole wedge is subsequently transported along a basal décollement and accretion of material occurs along the toe of the wedge that remains at critical taper. This critical taper angle is defined by the surface slope of the wedge topography (α) and the dip of the basal décollement (β) (Fig 2.10 (a)). The shape of the wedge varies with the strength of the deforming material and the frictional strength of the basal décollement. The overall taper angle might decrease and allow for further deformation within the wedge in response to various factors. Increasing the basal friction increases the critical taper,

whereas increasing the internal strength of the wedge material decreases the critical taper. Other factors that affect the critical taper are pore fluid pressure, erosion (Beaumont *et al.*, 1992), accretion of material at the base of the wedge and isostatic response to wedge buildup.

Two categories of accreted material were separated by Platt (1986), frontally accreted and underplated, distinguished by their effect on the behavior of the wedge. Frontal accretion occurs in front and underneath the toe of the wedge, further extending the basal décollement. This causes a lowering of the taper angle in the toe area, that will become sub-critical. Under sub-critical conditions, the wedge is expected to deform internally (Chapple, 1978) and thrust faults should be reactivated or formed behind the leading edge of the wedge. Underplating occurs in the rear part of the wedge. Platt (1986) suggested that underplating of rocks will cause the wedge to thicken so that the taper angle will increase in such a way that extension will occur within the wedge.

The actual shape of the basal décollement is flat and low-dipping under most of the Main Ranges and Front Ranges, but under the Foothills (near or at the toe of the Canadian Cordilleran orogenic wedge), it displays a staircase geometry, with two ramps slightly more inclined than the rest of the décollement. Because the basal décollement occurs along the top of the Precambrian basement beneath most of the Main Ranges and Front Ranges, with renewed motion during a new episode of thrusting, underplating at the rear of the orogenic wedge would have to involve the basement. A crustal basement duplex would likely form like the one underlying the Monashee Décollement, together with the consequent thickening in the rear of the orogenic wedge. In the Foothills of the thrust belt, the accretion of thrust sheets first occurred along a basal décollement that ramped from the base of the stratigraphic cover to a long flat along the Jurassic Fernie Group, in the middle of the stratigraphic pile (Fig. 2.9 (a)). Later, in the Foothills, foreland accretion has involved at least two episodes of forward relocation of the basal décollement in the stratigraphic pile to a new position situated underneath and ahead of its early

position (Fig. 2.9 (a-c)), first to another step involving a long flat in the Nikanassin Formation and secondly to its present geometry with a long flat within the Sassenach Formation.

Dechesne and Mountjoy (1992, Table 1) have discussed possible controls for the abandonment of basal décollements, some of which apply to the examples observed in the Foothills, namely 1) erosion of topography and molasse deposition, 2) changes in the mechanical properties of the basal décollement. Molasse deposition due to the erosion of the advancing orogenic wedge is known to have occurred during most of the development of the foreland thrust belt (Bally *et al.*, 1966; Price and Mountjoy, 1970). More than 4 kilometres of sediments have accumulated in the foreland basin from Middle Jurassic to Paleocene, when compression is thought to have ceased (Underschultz and Erdmer, 1991). More sediments accumulated in the Late Cretaceous to Paleocene. Although most of the foreland basin was deposited in front of the orogenic wedge, the forward propagation of the leading edge of the thrust belt led to deformation of the western part of the foreland basin (Fig. 2.10 (a)).

Intuitively, a model is proposed where the development of the upper décollement might be related to the accumulation ($\geq$ 2 km thick) of sediments during the Late Cretaceous and Paleocene (Fig. 2.10 (b, c, d)). Backthrusting of those layers of sediments onto the wedge will accentuate pore pressure within the wedge and increase the critical taper angle. The wedge will in turn thicken and reach critical taper, with further advance along the basal décollement, causing further backthrusting along the upper décollement. The consequence of the development of an intercutaneous wedge (Charlesworth and Gagnon, 1985) is that for each kilometre of propagation of the basal décollement, an equivalent kilometre of advancement of material above the upper décollement will occur towards the hinterland of the wedge. Because the basal décollement connects with the upper décollement, the overall length of the décollement surface bordering the wedge will increase, friction along this composite surface will also

increase and the critical taper angle will rise again. In consequence, additional internal deformation will occur allowing the wedge to reach a higher taper angle and to cause further motion along the basal décollement. The gradual increase of the taper angle is likely to yield an equivalent isostatic response, and hence to increase β. Increasing basal friction through further elongation of this intercutaneous décollement together with the increase of β is likely to cause décollement abandonment at the base of the wedge because the basal friction is likely to be lower on a shorter rather than a longer surface (Fig. 2.10 (c)). In addition, the abandonment of the basal décollement to an underlying position in the stratigraphy would lower the β angle of the basal décollement and thus lower the taper angle of the wedge to a critical value that allows for renewed tectonic accretion to the wedge.

Active thrust faults in recent thrust belts are known to propagate very slowly through rock bodies and by sudden steps, or slip events marked by earthquakes (Berberian, 1982; Nabalek, 1985; Bombolakis, 1992). It is thus reasonable to consider that the forward and downward shift of a basal décollement through the stratigraphic pile progresses in a similar manner. During this episodic process, a single fault will nucleate in the footwall of the basal décollement and gradually propagate laterally and towards the foreland, similarly to the current models of thrust fault propagation (Ellis and Dunlap, 1988; Geiser, 1988; Walsh and Watterson, 1988). However, there is an apparent contradiction between this model of critical-taper wedge and the thrust model proposed above for the Athabasca Foothills, requiring that the abandonment of the basal décollement be concomitant with the abandonment of the upper décollement to relieve friction along the wedge. Early faults branching off from the older basal décollement to form the new basal décollement are likely to merge upwards with the older basal décollement and eventually cause motion along the frontal upper décollement. However, faults such as the Miette thrust or the Grave Flats thrust cut through the wedge and the earlier formed basal décollement, and rise up to the topographic surface or the upper

décollement (Fig. 2.10 (d)). The gradual formation of a series of imbricate faults along the new décollement in this manner causes accretion of material from underneath the older décollement and the eventual use of the older or a new upper décollement, without motion along the older basal décollement (Fig. 2.10 (d)). Also intuitively, slight changes within the delicate balance between critical and subcritical taper during the different stages of the development of faults emanating from the new basal décollement, might cause these faults to merge with the older basal décollement (then internal décollement). This would renewed motion on this older fault plane.

Other faults propagating off the old basal décollement from other locations along strike are likely to occur and would eventually coalesce together and contribute gradually to the formation of a newer basal décollement. Since each fault need not follow the same path to splay from the old basal décollement, it is likely that several different stratigraphic levels would be used and that different basal décollement geometries might be observed in the thrust belt as a whole. Two or more décollements might become active at different stratigraphic levels along a thrust belt during a particular time span. This is similar to the synchronous model of thrusting of Boyer (1992) for the southern Canadian Rocky Mountains, where a higher (here internal) décollement continues to develop during the same period that imbricates form from above the basal décollement. The various décollements may continue to develop even if faults rise from the deeper décollement and cross-cut the shallower décollement surface (s). Thus, during the evolution of a mountain belt, the relationships and displacement of various décollements may be complex. The interpretation of the role of a particular internal décollement can be difficult to assess, unless a detailed three-dimensional framework of the thrust belt is reconstructed and palinspastic restorations made from which relative displacements can be determined.

CONCLUSIONS

Three types of décollements can be deduced from the current geometry of the Canadian Cordilleran foreland thrust belt, namely basal, intermediate internal and upper décollements, based on data from the Athabasca-Brazeau region and integrated with regional information.

1) An internal décollement is recognized by a layer-parallel glide horizon that correspond to an extensive flat segment above a ramp that links it to a portion of the basal décollement situated further in the hinterland of the thrust belt. Many fault imbricates emanate from an internal décollement. The internal décollement is underlain by the continuation of the basal décollement towards the foreland and overlain in most cases by an upper décollement surface.

2) The basal décollement of the Front Ranges and Foothills changes both laterally and towards the foreland. It has two ramps, one that cuts up section from the base of the stratigraphic pile to a slippage zone in the Devonian, and another that cuts up section from the Devonian to another flat in the Upper Cretaceous.

3) Overall, the shortening within the Mesozoic sequence of the Foothills is equivalent to that in the Paleozoic sequence. However, there are discrepancies in relative shortening within the Mesozoic and Paleozoic sequences when only short segments of the cross-sections are considered. Thus section balancing using relative bed lengths must be done for the entire Foothills to construct valid cross-sections.

4) In the Athabasca-Brazeau area six extensive layer-parallel glide horizons are recognized: the Sassenach-basal Palliser formations, the Fernie Group, the upper portion of the Nikanassin Formation, the Blackstone Formation, the Wapiabi Formation and lower part of the Brazeau Formation.

5) Successive forward shifts of the basal décollement to new positions within the stratigraphic pile led to the formation of internal décollements, some of which may be cross-cut, folded by the stacking of thrust sheets of younger faults rising from deeper and more northeastward décollements.

6) The upper more forward segment of an early décollement appears to have been utilized as a roof thrust during the development of deeper seated duplexes (i.e. the Folding Mountain and Luscar duplexes underlying the Blackstone décollement).

7) The abandonment and forward shift of basal décollements in the external part of the Rocky Mountain belt appears related to the development of the upper décollement and can be explained by the Coulomb orogenic wedge model. It is interpreted that the formation of the upper décollement caused increased friction along the composite basal-upper décollement surface that gradually raised the critical taper angle of the orogenic wedge. Renewed internal deformation within the wedge eventually led to a shift of the basal décollement downwards to a new basal décollement to reduce friction. This allowed for renewed foreland accretion until friction again built up sufficiently to cause another cycle of basal décollement abandonment.

CHAPTER THREE

NUMERICAL MODELING OF THIN-SKINNED THRUST SYSTEMS- INSIGHTS ON THE PROPAGATION AND OVERLAP OF FAULTS, WITH APPLICATION TO THE THRUST-FOLD BELT OF CENTRAL ALBERTA

ABSTRACT

Two computer programs have been developed to analyze the propagation of multiple thrust faults and their influence on the geometry of a thrust belt. The computer programs use algorithms based on currently known equations of fault propagation, to generate graphical simulations. The simulations are used to demonstrate a model of thrust propagation and thrust belt development that fits current knowledge about fault propagation. This numerical model is based on two mechanisms: 1) The spreading simple shear mechanism applies a simple form of layer-parallel shear strain symmetrical about the center of the leading edge of a thrust fault to its lateral tips, that is subsequent to the lateral and forward propagation and motion of a single thrust fault. 2) The overlap mechanism is a conceptual model that suggests when each fault might propagate when a group of thrust faults is linked through a common décollement. The mechanism imitates a local stress buildup and the eventual relaxation which takes place by slip on the fault best-situated for this purpose.

The computer simulations provide useful information about the generation and behavior of multiple faults. 1) The number of faults, the positions of their nucleation points, and hence their density, the rheology and consequent speed of fault propagation govern the uniformity of the shortening along the thrust belt. 2) The branch lines and

hanging wall strain pattern of two intersecting thrust faults can be used to trace the thrusting sequence of two thrusts. 3) Computer simulations show that the shortening of a thrust belt can be distributed more evenly by means of propagation of a large number of small faults than by a few large thrusts. 4) Computer simulations also demonstrate that the final geometry of a large thrust fault on a geological map leaves little clues about its origin, whether it was produced by the coalescence of a series of en échelon thrust faults or from only a single fault. The overlap mechanism is a more viable alternative to the thrust transfer zone concept because it conforms to current knowledge about thrust fault propagation.

A computer simulation shows that a simple kinematic model based on map length and position of known thrust faults can imitate the curved fault map patterns of a segment of the thrust-fold belt of central Alberta.

INTRODUCTION

In the last two decades, the extensive mapping of thrust belts has greatly advanced the description and comprehension of thrust fault geometries. The deformation mechanisms leading to the horizontal shortening and vertical thickening of a thrust belt are divisable into three categories: low-angle overthrust faulting, folding, and layer-parallel shortening. The interference and overlap of the structural features created by these mechanisms render it difficult to construct a kinematic model of the deformation leading to a particular set of structures. Hence, much remains to be done to understand the kinematics and deformation mechanisms that cause translation of large rock masses within thrust-and-fold systems.

The thrust fault mechanism has been extensively studied, particularly the linkage between individual thrusts in a thrust belt system, in attempts to explain why the shortening measured along a particular thrust belt remains relatively constant while individual faults have finite width and varying displacements. Thrust transfer zones have

been proposed as a common deformation mechanism for thrust-fold belts, particularly for examples from the Canadian Rocky Mountains (Douglas, 1958; Dahlstrom, 1969). A thrust transfer zone is defined as the zone of overlap between two thrusts. These thrust faults are linked via a common underlying basal décollement. The observed succession of a series of thrusts with intervening overlap zones along the strike of a thrust belt led to the proposal that such thrust faults are correlative and delineate one or several linked thrust sets within the Rocky Mountain thrust belt (Dahlstrom, 1969, Fig. 14). The transfer zone principle has since been used to explain the geometry of natural examples observed in thrust belts (Price and Mountjoy, 1970; Brown and Spang, 1978; House and Gray, 1982; Boyer and Elliott, 1982; Langenberg, 1985; Tysdal, 1986, Sanderson and Spratt, 1992). It is used to explain why shortening apparently remains more or less constant along large stretches of thrust-fold belts, while faults have finite map lengths and show a progressive lateral decrease in their displacement.

However, the study of the final geometry of two neighboring faults or of a large segment of a thrust belt does not give much insight about the history of fault propagation, the timing of motion of the various faults relative to one another, and the sequence of thrust belt development. Several studies highlight the importance of the slow and progressive nature of the propagation of thrust faults (Elliott, 1976a,b, Scholtz *et al.*, 1986, Walsh and Watterson, 1988). The evolving nature of faults is of critical importance to understand the linkage existing between adjacent faults during the formation of a thrust belt. Furthermore, the sequential model of thrust faulting (i.e. hinterland-to-foreland fault development) is being challenged by theoretical models (Davis *et al.* 1983) and field studies (Boyer, 1992). These models suggest a more complex history of faulting, where faults situated in the hinterland may be reactivated, while other faults situated near the toe of a deforming thrust wedge are being formed. In our opinion transfer zones, as usually described, are a simplification of the more complex mechanisms that led to a particular thrust geometry. Because thrust faults propagate spatially through time, the en échelon

overlapping of two neighboring thrusts should be considered as the consequence of fault propagation rather than the reflection of an uncertain mechanism (e.g. the 'compensatory mechanism' of Dahlstrom (1970)) of transfer of thrust displacements between two or more faults.

This paper attempts to clarify how thrusts propagate and what effect the varying amount of displacement along single thrust faults has on the geometry of a thrust-fold belt. A simplified geometrical model of thrust propagation for the cases of a single or three branching thrust faults, showing the effects of thrust propagation on the geometry of a thrust belt is presented. The model is developed and generated by two computer programs, THREE THRUSTS and OVERLAP, and illustrated with simulations of thrust faults generated by these programs.

MODELS OF THRUST FAULT DEVELOPMENT

Three critical questions need to be addressed by models intended to portray the evolution of a series of thrust faults in a thrust belt: 1) the manner by which a single fault will evolve (fault propagation), 2) the deformation that will be caused by a single fault (displacement patterns in the hanging wall), and 3) the critical factors controlling a given rupture on a fault, in other words, why one fault will slip rather than another. By making some simplifying assumptions about the deformation, it is possible to model some aspects of the final deformation of thrust belts. Where the nucleation and slip events of the faults are controlled, the first two questions are addressed, using the THREE THRUSTS computer program. The OVERLAP computer program addresses the third question and is presented later.

Thrust fault propagation and displacement patterns

Various models have been proposed to explain the kinematic evolution and/or the mechanics of a thrust sheet (Bielenstein, 1969, Gretener, 1972), but only recently has

thrust fault propagation become the subject of debate. Older experimental models of thrust fault geometrical evolution used preexisting fault planes (Rich, 1934). This is because these features were assumed to develop almost instantly at the beginning of fault motion. Douglas (1958) proposed that thrust faults of the Rocky Mountain belt propagated gradually both laterally and towards the craton. Elliott (1976a) proposed that a thrust fault propagates radially from a point source, spreading sideways usually more rapidly than forward. The 'Bow and Arrow Rule' was derived from this relationship, and states that the maximum displacement of a thrust fault is a vector perpendicular to the center of the chord joining the thrust terminations in plane view. Elliott (1976a) also presented data that suggested that the value of this maximum displacement of a thrust fault was directly proportional to its map length. This hypothesis is now known to be a generalization of a more complex situation where all thrusts do not obey the rule, particularly because of variations in rock rheology (Ellis and Dunlap, 1988, Walsh and Watterson, 1988, Cowie and Scholz, 1992a, 1992b, Gillespie *et al.*, 1992). Elliott (1976a) also observed that thrust terminations were generally marked by folds which he interpreted to represent a zone of plastic strain or a 'ductile bead'. He noted that these terminal folds are strongly non-cylindrical and propagate just ahead of the sideways propagating thrust (i.e. that the folds are fault propagation folds (Jamison, 1987; Mountjoy, 1992). Thus, the current view is that thrusts develop relatively slowly and continuously, propagating through a rock body during an extended period of time (Elliott, 1976a,b; Scholtz *et al.*, 1986; Walsh and Watterson, 1988, Bombolakis, 1992). This concept needs to be incorporated into a mechanism of thrust development that would explain the varying displacement gradients observed along neighboring and overlapping faults.

Gardner and Spang (1973) used experiments on clay cake models to obtain a better understanding of the stress and strain relationships in areas of neighboring and overlapping thrust faults. Using predetermined fault locations and extensions, they modeled cases such as simple fault-fold transitions, multiple faulting and tear faulting.

Their models showed rather simple relationships because they did not allow faults much lateral growth. Their model results showed fanning effects in the hanging wall of a thrust from the middle of the fault (maximum displacement location) to its tip as the displacement along the fault decreased. A schematic portrayal of the divergent flow lines of such a fanning effect is shown on Fig. 3.1 (b). This kind of displacement pattern would lead to extension along the leading edge of thrust sheets. From field observations, Coward and Potts (1983) showed a displacement gradient similar to that illustrated in Fig. 3.1 (c) for a major thrust fault from the Moine thrust zone, where large shear zones or tear faults were found along the lateral sides of the thrust sheet. This case is clearly unusual in comparison to thrust-fold belts such as the Canadian Rocky Mountains where tear faults are relatively minor but are locally important. Figure 3.1 (a) shows a case of parallel displacement vectors of decreasing values from the center of the fault to its tips. This is a type of heterogeneous simple shear (Ramsay and Huber, 1983) that can be accommodated by a series of small faults or veins such as those described by Price (1967) and Lebel (Chapter Four of this thesis). Hence, several patterns of displacement flow lines can be visualized during the development of a simple thrust sheet, patterns which may be recognized through the study of the internal hanging wall deformation (i.e. brittle or ductile deformation elements: mesoscopic or macroscopic faults, veins, shear zones, folds, see Chapter Four of this thesis). However, the results of such studies may be difficult to interpret due to possible superimposed strain.

One important aspect which is neglected by all the models illustrated in Fig. 3.1 is the effect of thrust propagation on the kinematic pattern of a thrust sheet. Recently, Liu and Dixon (1991) and Dixon and Liu (1992) were able to simulate thrust fault propagation using a centrifuge analogue model. Their results clearly show that significant layer parallel shear strain due to lateral fault propagation must be involved in the final state of a thrust belt. Laboratory and field data from micro- to macroscopic faults, show that displacement measured along the length of faults often shows a zigzag segmentation of gradients of

decrease, but with an average gradient that tends toward a straight line (Cowie and Scholz, 1992, Fig. 7, Walsh and Watterson, 1988, Dixon and Liu, 1992, Fig. 16), rather than an elliptical curve of displacement suggested by theories of elastic fracturing.

Thus, it is reasonable to set up a numerical model of thrust growth that is based on a linear decrease of the displacement of the fault from its center to its lateral tip. Another assumption of the model used herein is that the individual particles of material above the thrust fault are all transported parallel to the slip direction of the fault, as portrayed in Fig. 3.1 (a). Because of the various possible departures of natural strain patterns from this model, this simplified model cannot be applied to all cases of thrust sheet emplacement, but rather should be used as a basis for comparison. As shown below, this model leads to a better comprehension of the effects of lateral thrust propagation.

The spreading simple shear mechanism

Both numerical models presented here use the same deformation mechanism that is termed '*spreading simple shear*' in this paper. Although the end product generated by the models might be relatively uniform shortening along the thrust belt, the driving mechanism is a series of translations of varying values, an adaptation of the simple shear mechanism presented in Fig. 3.1 (a) (Fig. 3.2). The spreading simple shear mechanism differs from ordinary simple shear since the width of the shear zone gradually increases as the thrust fault spreads laterally.

The deformation mechanism is based on simplifications from observations of natural strain patterns observed in thrust sheets (Bielenstein, 1969; Coward and Potts, 1983; Coward and Kim, 1981; Elliott, 1976b; Ellis and Dunlap, 1988), and on the results of analog thrust modeling (Dixon and Liu, 1992). It uses the equations of Walsh and Watterson (1988) to translate the conceptual model into a workable mechanism. These equations express the relationship between the width of a fault (W), its maximum displacement (D, Fig. 3.1a) and its rate of propagation (represented by a single variable,

k, representative of the rock rheology). Thus, these equations permit to derive a thrust fault propagation algorithm. Each fault nucleates from a predetermined point and evolves in a series of steps corresponding to slip events. The suggestion of Elliott (1976a) that a linear relationship exists between maximum displacement and fault width for any thrust fault was contested by Scholtz *et al.* (1986) and Walsh and Watterson (1988) on the basis of measurements of displacement made on faults observed in rocks of varying rheologies. Rather, displacement appears to increase arithmetically relative to the fault width, with each successive slip event (Walsh and Watterson, 1988) explaining the changing ratio of width to maximum displacement of natural faults. Cowie and Scholz (1992) have recently contested the significance of the fault data presented by Walsh and Watterson (1988). Rather, their data favor the hypothesis of a self-similar model of thrust growth (i.e. each displacement event reproduces the same width to maximum displacement ratio for a particular thrust). Additional data from Gillespie, Walsh and Watterson (1992) rule out the self-similar growth model but indicate that the exact value of the variable *n* in their growth algorithm (Gillespie *et al.*, 1992, see below) is uncertain. However, this uncertainty is not sufficiently large to modify significantly the geometric simulations of thrust growth presented here. Thus, $n = 2$ is used (as in Walsh and Watterson, 1988) because it yields a simple arithmetical algorithm of growth.

In the model presented here, the thrust sheet, driven by a given thrust fault, deforms through the spreading simple shear mechanism that permits both forward and lateral thrust propagation (Fig. 3.2). While the center of the fault propagates forward and increases the displacement of the thrust sheet, the lateral tips of the fault propagate laterally. Immediately following the first event of lateral propagation of the thrust tips, the relative segments of the sheet left and right of the nucleation point (point x_0, y_0-Fig. 3.2a) are displaced by a series of vectors decreasing in value with a mirror-plane of symmetry from the center to both thrust tips. After each new increment of fault slip, the value of the total displacement relative to the footwall measured along the thrust trace is assumed to

decrease linearly from the center of the fault (or initiation point) to the lateral tips (Fig. 3.2 (b)).

Walsh and Watterson (1988) proposed an arithmetic growth model in which the relationship between the width (W) and the total displacement (D) on a single thrust fault is dependent upon rock rheology and is not linear but rather arithmetic (log-log), when the total number of discrete increments of displacement (slip events) is large,

$$W^n = D \cdot P \qquad \text{((1), Walsh and Watterson, 1988)}$$

and where P is a constant dependent upon rock rheology and n =2 (see above for discussion). A seismic slip event u is the parameter usually used by earthquake seismologists to portray each increment of displacement on a fault.

On a fault growing according to the arithmetic growth model, with last increment of displacement u_N (amount of slip in a slip event) and with N slip events, if successive events u_1 , u_2 , u_3 , ... u_N have a common difference, a, and the first term is zero

$$u_N = a \cdot (N - 1) \qquad \text{((A1), Walsh and Watterson, 1988)}$$

when N is small. The maximum and total displacement (D) measured in the center of the fault is the summation of all the increments of displacements and is equivalent to:

$$D = N/2 \cdot (N\text{-}1) \cdot a \qquad \text{((A2), Walsh and Watterson, 1988)}$$

Half of the distance (W) between the lateral thrust tips is labeled the fault radius (R), and after a new increment of displacement:

$$R = k \cdot u_{N} \qquad \text{((A5), Walsh and Watterson, 1988)}$$

where k is a rheological constant. k is related to P through:

$$P = k^2 \cdot 8a \qquad \text{((A7), Walsh and Watterson, 1988)}$$

In this model, a and k are fixed by the user so that the incremental values of D (D') and R can be found easily:

$$D' = D + u_N \qquad (1)$$

The model is set in a xy reference frame, with the axis of shortening in the x direction. The position of the new thrust trace (Fig. 3.2 (b)) after each slip increment can be determined easily relative to the footwall position of the nucleation point of the fault, x_0y_0, by tracking the position of central point of maximum displacement and the lateral fault tips before a new increment of displacement (x_1y_0, x_0y_1, x_0y_2). Hence after a new slip increment, the central point of maximum displacement x_2 will be at

$$x_2 = x_1 + u_N \text{ and } y_0, \qquad (2)$$

and the lateral tips will be at

$$y_1' = y_0 - (k \cdot u_N) \text{ and } x_0 \qquad (3)$$

$$y_2' = y_0 + (k \cdot u_N) \text{ and } x_0 \qquad (4)$$

Since the deformation mechanism is a form of heterogeneous simple shear, displacement vectors are parallel to the x axis but of unequal length. By determining $\emptyset_1$

and $\emptyset_2$ (Fig. 3.2 (b)), the displacement vector for each shear plane along the the thrust width is found through

$$u_N [y] = x'' - x' \qquad (5)$$

where left of y_0

$$x' = \tan \emptyset_1 \cdot (y-y_1) \qquad (6)$$

$$x'' = \tan \emptyset_2 \cdot (y-y_1') \qquad (7)$$

and right of y_0

$$x' = \tan \emptyset_1 \cdot (y_2-y) \qquad (8)$$

$$x'' = \tan \emptyset_2 \cdot (y_2'-y) \qquad (9)$$

Naturally, the value of x' is set to 0 before each new slip increment, left of y_1 and right of y_2.

ANALOG MODELS OF THRUST FAULTING

Although much attention has been devoted to thrust belts, little study has been done to determine the geometrical implications of thrust propagation in three-dimensions. Analog sandbox and centrifuge models have been used to simulate various kinds of geological phenomena in three-dimensions (Hubbert, 1937; Ramberg, 1981, Liu and Dixon, 1991, Huiqi *et al.*, 1992)). Some recent technical improvements allow better observations of progressive deformation (e.g.: X-Ray tomography, Coletta *et al.*, 1991). However, because of the smaller scale of these experiments and the material that is used, their results do not answer all the questions related to thrust belt development. As recognized by Hubbert (1937), scale models using plaster, clay and now silicone putty or honey should be carefully compared to actual rocks because of the discrepancy in strengths of materials and the imposed acceleration of deformation compared to the natural case. Consequently, these models do not permit a quantitative correlation of the imposed

deformation rate with naturally occurring geological phenomena, or cannot easily simulate the effects of a change in value of rheological variables on the shape of a fault or its rate of propagation in a rock sequence. So far few experiments have been attempted to study the effects of lateral fault propagation on neighboring faults, although interference effects have been predicted by some (Coward and Kim, 1981; Ellis and Dunlap, 1988).

In much the same way as analog models, computerized modeling of thrust systems or single faults has received considerable attention in the last decade (Jones and Linsser-THRUSTBELT; Kligfield, Geiser and Geiser-GEOSEC-10; Klapstein-FLTBND; Wilkerson and Usdansky-FAULT; Usdansky and Groshong-THRUSTRAMP). These programs have been designed with certain boundary conditions to observe the evolution of a set of predetermined structures and the consequent geometric relationships (fault stack, ramp-related folds, fault-propagation folds, etc.). These models have mostly been devoted to the study of thrust belts as seen in cross-section, because of an interest to replicate structures observed on seismic profiles acquired through petroleum exploration (e.g. Jones *et al.*, 1992). The same approach has been a useful way to check the validity of balanced cross-sections. However, numerical models also have their limitations when it comes to modeling complex situations such as three-dimensional strain calculations related to the propagation of multiple coeval faults.

The approach presented here uses an intermediate technique where the computer is used to perform iterative operations to simulate a thrust belt being shortened; to do so two different programs have been developed to model two different aspects of the thrust belt kinematics:

1-THREE THRUSTS simulates the deformation that one would observe in a thrust belt (or a sandbox) with infinitesimally thin thrust sheets propagating individually without being constrained by physical barriers.

2-OVERLAP simulates a thrust belt using a deformation mechanism that permits an evenly distributed shortening while numerous faults are allowed to nucleate and propagate.

Both programs use algorithms of fault growth based on the equations developed by Walsh and Watterson (1988). They use the graphical output of the computer (a matrix of pixels (square dots), or bitmap) as a means of keeping track of the deformation, imposing incremental strain and detecting special situations. Bitmaps have been used in the past to simulate deformation of single objects or multiple objects within an homogeneous two-dimensional field (de Paor- STRAIN SAMPLER, McEachran, STRAIN GRAPHICS). The technique presented here differs in that the graphical objects (faults) direct the deformation via a series of predetermined growth algorithms. The graphical output is also checked so that the simulation obeys a set of empirical rules, which generates a graphic output that can be compared to geologic phenomena. Since these rules generate scale-dependent simulations, the simulation can represent faults of lateral extent at any scale ranging from several tens of metres to several hundreds of kilometres.

THREE THRUSTS program

The program THREE THRUSTS runs on an Apple Macintosh microcomputer. The screen serves as the device on which the evolution of the numerical model is followed. The screen view is an analog to what an observer would see if looking at the surface of a sandbox or centrifuge model like the ones used by Gardner and Spang (1973) and Dixon and Liu (1992) to simulate the evolution of a single or a series of thrust sheets. The difference with the sandbox models resides in several boundary conditions. The incremental outputs portray, with simplifications, an accelerated simulation of what an observer would see if looking from the air at a thrust belt with up to three coeval thrust

faults. The thrust faults can be situated anywhere within xy space and can be generated at any scale. The consequent simulation is scale-dependent.

Boundary conditions

In addition to the assumptions set up within the spreading simple shear mechanism of thrust faulting as explained above, several simplifications have been introduced in the THREE THRUSTS computer model in order to generate simulations that can be easily understood and compared. These experiments may lead eventually to more complex models. The thrust sheets generated by the THREE THRUSTS model are assumed to be infinitesimally thin, so that no folds are generated either by ramping or over a décollement, and that the effects of thrusting can be isolated. No compensatory mechanism is used to keep a uniform value of shortening along the thrust belt. In the model, having one thrust situated nearer the foreland than another one is taken into account so that the thrust positioned nearest the foreland deforms the hinterland ones when there is an overlapping of the faults (Fig. 3.3). The piggyback carriage of the hinterland thrusts by the foreland thrust imposes layer-parallel shear strains. Overriding of a foreland thrust by hinterland thrusts also needs to be properly simulated, since no assumptions are made about the sequence of thrusting and the individual thrusts are assumed to propagate synchronously. Hence, to get a three-dimensional simulation, a 'hinterland' thrust is allowed to mask a 'foreland' thrust as the former overrides a part of the latter (Fig. 3.6). The imaginary material boundary surfaces of the model are defined in a manner similar to a sandbox model, with a lower plate, two opposite walls (the top and bottom of the screen, with the top wall converging towards the bottom), and the sides of the screen being modeled as free surfaces, as well as the surface between the observer and the screen.

Contrary to a real sandbox-centrifuge model, the mobile rear boundary is not modeled as a fixed rectilinear panel but as a surface that follows the movements permitted

by the propagation of the thrust faults. Because we are using a model of a thrust belt where no mechanism of shortening other than thrust faulting is allowed (i.e. no folding or layer-parallel shortening), and because only a few active faults are present, the shortening along the belt is not evenly distributed until substantial overlapping of the faults occurs. This mobile rear boundary is used to observe the effect of thrust propagation on predetermined structures. Another simple rule does not allow a foreland thrust to cut through an overlying, hinterland thrust but only to merge. This eliminates the possibility of abnormal or out-of-sequence faults, cross-cutting earlier thrusts.

Description of the computer simulations

The execution of the program can be started and interrupted at any time. A series of lines with a spacing defined by the operator are drawn on the screen as strain markers. An option permits one to paste in any bitmap image as an alternative marker, or starting pattern (e.g. an image generated from a previous simulation with locked thrusts). The user can choose between one and three thrusts that can be active during the execution of the simulation. The default parameters that define the fault propagation rate can be changed, that is the value of k and a (defined by Walsh and Watterson, 1988).

If three thrusts faults are set, the program first finds the location of the nucleation points as selected by the user and then proceeds to rank them relative to their position from the bottom of the screen (foreland). The lowermost one is T1, (nearest the foreland or of first rank), the one closest to the rear boundary is T3 (Fig. 3.3). The program will not allow two thrust nucleation points to be placed on the same row of pixels. THREE THRUSTS then proceeds to calculate and draw on the screen each slip increment, for each fault, one fault at a time. Since the three thrusts are developing synchronously each one slipping by minute increments, the order in which each fault moves is not significant. Arbitrarily, the program starts with the first increment of deformation on T1, doing T2, T3 in turn and then back to T1, repeating this cycle until the user stops it. An alternate

mode (manual mode) permits one to choose a preferred fault to be activated by simply clicking on it. The program keeps track of each increment of faulting independently for each fault (e.g. in a three thrust scenario, the user might chose to activate T3 a number of times before the first slip on T1, then make any choices with any of the three faults).

The first and subsequent increments of displacement on each fault are calculated, together with new locations, using their maximum displacement center point and lateral thrust tips. The model is scaled so that the rate of propagation of a fault is related to its width according to the equations of Walsh and Watterson (1988), which describe natural faults of various scales and rocks of various rheologies. The model outlined here is mainly useful for faults of kilometre-scale lateral width, but various situations can be modeled since any scale can be used for the simulations. The default value of the model is 100 metres per pixel (1 pixel = 1/72 inch). Hence in this case, each increment of displacement of 100 metres or more is calculated at the center of the fault, the column of pixels behind this point is displaced by an equivalent number of pixels. The incremental displacement is then distributed with a linear decrease in value on each column of pixels found left and right from the center of the thrust to the new thrust tip where the incremental displacement is nil according to the spreading simple shear mechanism (Fig. 3.2).

The location of each pixel composing the leading edge of each fault, relative to the reference grid, is kept in a positioning matrix (x-y coordinates) so that the strain effect on a hinterland thrust being transposed piggyback by a frontal thrust is always tracked. A hinterland thrust which has changed its position relative to the reference grid can thus be deformed subsequently at its correct new location. Because each foreland thrust applies incremental transport of varying value along strike onto overlapping hinterland thrusts, the location of the affected hinterland thrust has to be followed independently from the screen output, within the positioning matrix. The shape of a hinterland thrust trace will change with the overlap and piggyback transport by a foreland thrust and will not

conform to a simple bi-rectilinear V like the one shown for a single fault (Fig. 3.2). The positioning matrix is thus used by the program so that the same vectorial addition to each pixel column behind the thrust trace is performed as if both fault segments were rectilinear, thus neglecting the effect of shape change on the kinematics (Fig. 3.4). The coordinates of the positioning matrix also allow the program to keep track of the axis of lateral spreading of each thrust tip (Fig. 3.2a).

Special cases

Special situations are handled using test routines in order to prevent the model from producing graphical aberrations that would not be comparable to geologic phenomena. When such special circumstances occur, the program follows corresponding empirical rules. These empirical rules are derived from current knowledge of thrust fault behavior in thrust-fold belts and have been determined while programming, as answers to problematic situations that happened as the code was being tested. Two special cases are discussed below.

Special case 1: T3 thrust tip propagating ahead of T2 thrust tip

Because of the cumulative layer-parallel shear strain developed behind a propagating foreland thrust fault (T1), the rear-most fault (or nearest the hinterland, T3) within the strain zone will be deformed and may eventually grow to a position where one of its tips will be ahead of a tip of T2 (Fig. 3.5 (c)). To spot this situation, the program always verifies if the new thrust tip of T3 occupies such a position relative to T2. If so, the program takes note and executes the subsequent deformations so that T3 carries T2 piggyback (i.e. T2 will hide parts of T3 if it moves over it).

Special case 2: Intersecting thrust traces

During its evolution, a thrust fault may propagate into (or merge with) another fault. In this case, THREE THRUSTS detects the situation and checks if the propagating fault is in the hanging wall or footwall of the other one. If the propagating fault is situated in the footwall, the image created on the screen will be a simulation of piggyback thrusting and merging with the overlying fault, so the thrust trace will not cross-cut the hanging wall fault (in cross-section this situation would appear as a duplex, Dahlstrom, 1970; Boyer and Elliott, 1982). The program takes note of the situation for all future moves of both faults (T1 carries T2, Fig. 3.6 (a)). Another special case may arise if the propagating thrust (T2) has been sufficiently strained by T1 to occur ahead of the lateral tips of T1 (Fig. 3.6 (b1) (b2)). In this case, the propagating fault T2 cannot cut through the intersecting fault T1 because it is constrained within the T1 thrust sheet and thus must tear off the part of T1 situated to the right of the branch point, point X (Fig. 3.6 (b2) see below for further discussion). T2 then follows the former axis of lateral thrust propagation of T1 (compare the growth of T2 from Fig. 3.6 (b2) to Fig. 3.6 (b3)).

Thrust simulations

Several interesting phenomena, important for understanding thrust belt evolution, can be observed using the THREE THRUSTS program. Simplifications are inherent to the computer model and observed features within the simulations can be correlated with natural examples.

1-Strain reversal due to piggyback thrusting

Hanging wall strain during thrust propagation is an important kinematic mechanism. During the development of a thrust belt, a rock body may go through a series of deformations related to the propagation and advance of lower thrust faults transporting it in a piggyback manner. Some of the more important strain will be caused by layer-

parallel shear strain within the thrust sheet, termed 'piggyback longitudinal shear strain'. For example, in Fig. 3.7 (a), the right side of the T2 thrust sheet undergoes sinistral simple shear during an episode of thrust propagation and advancement, but this simple shear strain is reversed by the dextral simple shear introduced by the propagation of the left side of T1 (Fig. 3.7 (b) and (c)), a thrust fault closer to the foreland that overlaps part of T2.

Situations involving several thrust faults propagating within a common time span would create complex kinematics and incremental strain histories in individual thrust sheets. Clearly, hinterland thrust sheets should have undergone a long-lasting and more complex strain history of layer-parallel shear than the foreland ones.

2-Kinematic interpretation of thrust branch points

The line of intersection of two fault planes is termed a branch line; the point of intersection of the branch line on the topographic surface or the point of intersection of two thrust traces on a geological map is termed a branch point (Boyer and Elliott, 1982; Hossack, 1983; McClay, 1992). Branch lines can originate in different manners in nature, which has important implications for computer simulations inasmuch that thrust branch points are in fact the more difficult aspect of thrust propagation to model numerically. The meaning of thrust branch points in nature or as projected on geological maps can be uncertain and several interpretations can be given, depending on what we know about the relative position of each fault (Boyer and Elliott, 1982; Diegel, 1986).

In simulations of two neighboring nucleation points, situated close to the same y axis, a variety of different types of branch points and thrust sheet behaviors are observed depending on relative initial positions along the x axis and the sequence of thrusting. For two thrust T1 and T2 nucleation points, three sequences of thrusting can be simulated: 1) T2 formed before T1 (Fig. 3.6 (a)), 2) T1 formed first (Fig. 3.6 (b)), and 3) the two faults propagated synchronously (Fig. 3.6 (c)).

In case 1 (Fig. 3.6 (a)), where T2 propagates first, the center part of T2 advances ahead of the lateral propagation axis of T1 and stops. The lateral propagation of T1 then leads to a branch point where the right part of T1 continues to propagate under T2 to form a duplex. T1 and T2 will then tend to become parallel, as T1 continues to propagate (Fig. 3.6 (a3)). The branch point will not move laterally during further propagation of T1 under T2.

Case 2 (Fig. 3.6 (b)), where T1 propagates first, leads to imbrication of T1 by T2. T1 overlaps the nucleation point of T2, and T2 is carried ahead of the right lateral tip of T1 (Fig. 3.6 (b1)). Then, motion on T2 will lead to an initial branch point along the right leading edge of T1 (Point X, Fig. 3.6 (b2)). Since T2 and T1 are at a high angle to each other and emanate from the same décollement, T2 will gradually advance over T1 and carry material that used to be part of T1, right of the initial branch point between T2 and T1 (Fig. 3.6 (b2)). The initial location of the material that was part of T1 and transported as a part of the leading edge of T2 at the end of the simulation is shaded in Fig. 3.6 (b3).

In case 3 (Fig. 3.6c), thrusts T1 and T2 propagate synchronously, with alternative slip events. In the simulation, the branch line moves gradually backwards relative to T2 and the branch point moves towards the center of T1 as the deformation progresses. Such displacement of the branch line may be represented in the field by wide shear zones between natural faults close to the branch point.

Thus, computer simulations predict different branch line geometries and hanging wall shear strain for varying sequences of thrusting.

3-Kinematic model of a large segment of a thrust belt

The three-dimensional and complex nature of thrust belts makes it difficult to formulate a detailed kinematic model similar to the configurations of thrusts observed in a thrust belt. In the same manner, a numerical simulation of thrust faulting involving hanging wall deformation becomes increasingly difficult to handle as the number of faults

involved increases. However, this computer model permits the generation of a sequential model of classic foreland directed deformation with up to three simultaneous faults in each sequence of deformation. Tracking deformation with the use of screen markers is much simpler than trying to plot and follow the complex trigonometrical calculations that are needed to describe the effects of deformation of one thrust fault by another.

A sequential model of thrust belt evolution is made on the computer screen by successively pasting in the result of incremental deformations along individual faults. Thus the model can be used to simulate the evolution of a particular segment of a thrust belt and from this obtain an incremental kinematic model of the deformation. A computer simulation that approximates the kinematic model of the Front Ranges and Foothills of the Canadian Rocky Mountains between the Athabasca and the North Saskatchewan rivers (Fig. 3.8) is shown on Fig. 3.9. The construction of the model is straightforward and leads to a surprisingly close approximation of the present pattern of thrust faults in this area (compare Figs. 3.8 and 3.9 (e)).

The generation of a large thrust fault (width >50 km) using realistic a and k values needs a substantial number of slip events (N>1,000), thus it was chosen in this case to work with a sequential model where only one fault was active at a time. This considerably reduces the time required to achieve the simulation. One feature of the THREE THRUSTS computer program is that from a pre-set final thrust width of a particular thrust fault, it calculates the results of all the numerous slip events before any deformation is shown on the screen. Therefore, using the width of a fault as measured from a map and realistic rheological variables, a particular thrust fault can be generated rapidly. When a fault has attained its desired width, it is then easy to increment the deformation of the area by copying and pasting the bitmap result within a new simulation. The next simulation starts simply by placing a new fault of a newly desired width in a new location further toward the foreland of the pasted bitmap from the previous simulation (placing it behind

the previously drawn faults will lead to out-of-sequence fault patterns, since the program cannot recognize faults within pasted bitmaps).

To construct the series of simulations shown on Fig. 3.9, values of a and k were kept constant for all faults and were set according to values suggested by Walsh and Watterson (1988) for rock sequences of similar rheology to the Canadian Rocky Mountain Front Ranges and Foothills (which consist mainly of clastic and carbonate sedimentary rocks). The projection was set to 1:1,000,000, thus trying to image effects of large thrust faults. At this scale, with the set a and k values, short faults (W<33 km) do not have any effect on the simulation, because their maximum displacement is smaller that 353 metres (1 pixel) and do not reach the critical value of 1 pixel for minimum translation within the bitmap. The small faults shown in the simulation have only been set as markers to follow the deformation (e.g. some of the numerous faults located near Mountain Park-Figs. 3.8, 3.9 (b)). The width of each modeled fault was first measured on geological maps of the area (Mountjoy, 1960a, Price *et al.* 1977, Mountjoy *et al.*, 1992, Douglas and Lebel, 1993), then the progression of the deformation involving the formation of each new fault was modeled. Only one fault was active at a time. The faults were activated so that the first faults occurred in the hinterland and the last ones in the foreland following a classical foreland-directed progression of deformation. The top two lines on Fig. 3.9 (a) and subsequent drawings are used as reference lines showing the total shortening accomplished along each new fault.

The end-product (Fig. 3.9 (e)) does not represent a realistic image of the deformation but exemplifies a quantitative simulation. The displaced reference line in the top part of Fig. 3.9 (e) is comparable to the McConnell thrust (MC). It shows, as do other faults in the foreland (like the Nikanassin (NK), and other thrusts behind) a sigmoidal shape related to the sinistral shear resulting from the consecutive development of the numerous faults representing the Brazeau structure (Sanderson, 1939; Hake *et al.*, 1942; MacKay, 1940; Douglas, 1958b, Douglas and Lebel, 1993). Most faults exhibit this

sigmoidal shape on the geological map (Fig. 3.8). Thus, the simulation provides a kinematically plausible explanation for the final general shape of the different faults. A few faults like the Grave Flat thrust have a shape and orientation considerably different from the one generated by the simulation in the above model. However, if the fault is out-of sequence, as suspected by the construction of a balanced cross-section of that area (Douglas and Lebel, 1993; see Chapter Two, this thesis), it would explain the lack of correlation with the computer simulation.

Another benefit of the above approach is to test whether the rheological variables used in the simulation have realistic values. A comparison of the end-product with the geological map shows that the mapped degree of the curvature of the various faults described above is generally higher than what has been generated by the model. This can be explained in several ways: 1) several faults have not been included in the simulation because they were not large enough to model, 2) folding was not taken into account, 3) the slip parameters are not valid, suggesting that different values should be used to permit more displacement to be attained for a certain width of a fault, 4) the thicknesses of the thrust sheets are not considered, 5) the simulation represents faults which are not subject to erosion. Together, these points explain the discrepancy in fault curvature. Another discrepancy is the total shortening in the simulation compared to that measured from the Cretaceous Cadomin Formation, within the Foothills thrust belt. It is estimated to be about 35 km on a cross-section close to the Brazeau river, as measured between the McConnell thrust fault trace and the triangle zone Lovett backthrust fault (Douglas and Lebel, 1993, see Chapter Two of this thesis). The above value is 3 times larger than the shortening measured on our simulation for the same area. Because points 1, 2, 4, and 5 cannot account for this discrepancy, it is thus clear that the slip values of these faults are not correct and should be changed for more appropriate values. A rough estimate is to increase the slip value a by a factor of 3 (to .006 m), that will give roughly a value of D

three times larger for an identical large thrust (e.g. W=80 km, see equations A5 and 1, Walsh and Watterson, 1988).

4-Multiple-fault origin of major thrusts

Ellis and Dunlap (1988) suggested that a major thrust can be made up of a series of coplanar smaller faults, which merge at certain points to form a larger fault, and suggested that some fault bends can be interpreted to be merging points. However, Dixon and Liu (1992) have pointed out that the sinuosity of thrust traces as observed in their centrifuge model is not directly related to the displacement gradient measured along the strike of the fault. In general, they observed a linear decrease in the displacement of a thrust fault from its leading edge center to its tips, but also local variations showing that departures from this simple relationship occurs (Dixon and Liu, 1992, Fig. 16b) which they interpreted to reflect the presence of coplanar faults merging together to form a larger through-going thrust.

Figure 3.10 (a to c) provides a computer simulation of how three en échelon thrust faults from a common décollement (Fig. 3.10 (a)) can lead to a simple displacement gradient at the back of the thrust belt (Fig. 3.10 (c)) similar to that of a different simulation for only a single thrust fault (Fig. 3.10 (d)). There is no clear difference in the final configuration of the thrust trace and shortening gradient for both simulations. The case presented in Fig. 3.10 (a) to (c) uses a synchronous thrust sequence like that illustrated on Fig. 3.6 (c). The right lateral tips of T2 and T3 stopped just short of the leading edge of thrust T1 at the end of the deformation, so that no fault propagated laterally to the right leading edge of the footwall thrust like in the case illustrated on Fig. 3.6 (b). Because the three thrusts are stacked one on top of each other, they give the impression that they are a single fault, with only some small imbrications branching away from the main thrust. Such fault trace geometry is common on geological maps and there are few ways to distinguish between a single and a multiple fault origin of the hanging

wall strain (e.g. several shear zone sets in the hanging wall, subparallel to the displacement vectors and with opposing or cross-cutting relationships). Thus, when reconstructing a large thrust belt using the final width of thrust faults as shown above (Fig. 3.9), it must be kept in mind that some of the larger thrust faults might in fact be an assemblage of several or even a multitude of smaller faults.

The overlap mechanism

A simplified model of thrust belt development, the 'overlap mechanism' can be used to explain the relatively uniform shortening that occurs in different segments of thrust-fold belts. As shown in the preceding sections, the lateral propagation of each individual thrust fault along a thrust belt gradually leads to the overlap of some of the faults. The piggyback layer parallel shear that is induced by individual thrusts faults on other thrusts is the first part of the composite mechanism leading to a relatively uniform shortening in a thrust belt. The second part of this composite mechanism is the 'overlap mechanism'. It explains how thrusts in a thrust belt can be viewed as an evolving system, where a network of propagating thrust faults exists at all times, but only the faults situated in the best position to accommodate shortening will slip and thus propagate even further laterally.

Studies of present-day active thrust faults in New Zealand and California show that they propagate by means of local strain buildup, due to the inhomogenous shortening along the thrust belt, and the eventual strain release through fault slip (Schwartz and Coopersmith, 1984; Berryman and Beanland, 1991). Hence, in an area with a series of faults that overlap each other in map view, the fault which is situated in the most critical position will slip and propagate further laterally and towards the foreland. If there is no fault placed in this critically strained area, a new fault will nucleate. This switching of slip between one fault and another in a series of overlapping thrust faults is herein termed the

overlap mechanism. A simplified computer model, the OVERLAP program, demonstrates the applicability of this concept and mechanism.

OVERLAP program

The OVERLAP computer program was written as an attempt to show how a series of thrusts propagate laterally and overlap each other, allowing one to observe the structural evolution and continuous uniform shortening of a thrust belt. It was conceived as a complement to the THREE THRUSTS computer program which does not illustrate the overlap mechanism. Several simplifications have been made to formulate a working model.

Boundary conditions and description of the overlap mechanism

OVERLAP, in contrast to THREE THRUSTS, allows up to 50 thrust faults to nucleate and propagate within a thrust belt spanning 400 pixels in width and 50 pixels in length (Fig. 3.11). However, the visual aspect of the model is similar to THREE THRUSTS and the algorithms used to control thrust propagation (values of D and W) are the same as in the THREE THRUSTS program, so that the user can change the slip and rheological factors a and k. OVERLAP does not permit the deformation of the hanging wall of each fault because of the increasing complexity of handling fault intersection and longitudinal deformation as deformation proceeds (as demonstrated by THREE THRUSTS). Instead, OVERLAP uses a histogram in the middle part of the computer screen, that shows the amount of shortening at the rear of the thrust belt, evaluated in pixels (Fig. 3.11). The viewer can observe at all times the shortening resulting from the motion of the different faults after each slip event. The maximum value of 50 faults may appear high but it was chosen to see if the parameters set by the user tend to generate a large number of faults, or if only a few are necessary to achieve the desired shortening along the thrust belt.

In the computer model, the overlap mechanism is conceived as follows. The different values of shortening found along each pixel column and represented on the histogram are used to search for the minimum value which will be the most favoured pixel column for future thrust movement. If a series of contiguous minimum values are found, the program chooses the one situated midway between the next higher values of shortening. When the minimum value of shortening is found, the program looks for a thrust which overlaps the related pixel column. If there is one, the fault is allowed to move an additional slip event and propagate laterally to an extent governed by the equations of Walsh and Watterson (1988). The shortening value of each pixel column is incremented by adding the values calculated using the spreading simple-shear mechanism (identical to the one used by the THREE THRUSTS program). The computer program then loops and proceeds to find a new minimum value of shortening. If no fault is found overlapping the minimum shortening pixel column, the program then proceeds to create a new nucleation point on the minimum pixel column and allows its first slip increment. The location of this nucleation point along the pixel column is chosen randomly.

If the number of thrusts reaches the arbitrary value of 50, the OVERLAP program will no longer generate new nucleation points but rather looks for the closest thrust fault in the event that none overlap the minimum pixel column. In order to limit the number of new faults and to allow for the simulation of a certain stress buildup before a new fault will nucleate, new thrusts are only generated if the minimum value of shortening is lower than half the average shortening of the entire thrust belt. The program stops when the arbitrary value of 50 pixels (5 km) of average shortening is reached over the 5 km wide thrust belt, or 50 % shortening.

Experimental results

The overlap mechanism described above provides a good model for transforming the strain applied by a backstop within an imaginary sandbox into relatively uniform

shortening in an algorithmically growing thrust belt. All the test runs performed with this model showed a relatively uniformly distributed shortening (with local minor variations). The highest variations in shortening (between 40% to 60% relative to an average shortening of 50%) were observed in thrust belt simulations using high propagation rates.

Several tests were run to determine the importance of the rheological and slip factors on the final number of faults. These experiments showed a number of interesting features:

1-The number of faults needed for 50 % shortening depends upon the rapidity at which these faults propagate laterally. If the faults are slow to propagate as in hard rock (e.g. a=0.002, k=10,000), the number of thrusts needed will be high, rapidly reaching the maximum allowed number of faults, whereas only 15 faults can accommodate the same shortening uniformly if propagating at an unrealistically fast pace (less than 60 slip events for a=220, k=10).

2-Abnormal results are produced particularly in the initial stages. When using slip and rheological values comparable to natural cases (a=0.002, k=13,870), the faults are very slow to propagate and the computer program rapidly initiates the largest number of possible faults, but not uniformly, the faults being concentrated in the left part of the screen because the program scans for minimum values of shortening from left to right.

3-The locations of the nucleation points of faults along the thrust belt are important because the area with the highest concentration of faults tends to show shorter individual fault lengths (Fig. 3.11). This means that fault propagation is less favored in areas which have a high density of faults.

To prevent abnormal thrust concentrations such as those described in point 2, and to allow uniform shortening within the thrust belt simulation, the computer program permits 50 random nucleation or weakness points to be generated initially.

DISCUSSION

The transfer zone mechanism (Dahlstrom, 1969, 1970) vs the overlap mechanism

The thrust transfer zone mechanism of Dahlstrom (1969, 1970) has been used to explain the phenomenon that although displacement on individual faults varies significantly along strike, the net displacement across the whole thrust belt remains the same when measured from one cross-section to another. To explain this uniform shortening within thrust-fold belts, he suggested that along the extreme lateral parts of individual thrusts, zones of exchange of displacement (transfer zones) occur with en échelon, overlapping thrusts. Dahlstrom (1970) explained that the basal décollement was the mechanism linking the thrusts, and this remains valid. However, it is implicit from this concept that thrusts were believed to show a decrease in their displacement mostly in the portions overlapping other thrusts. In addition, paired en échelon faults within transfer zones are assumed to have grown simultaneously (Dahlstrom, 1970, p.358).

In light of current knowledge about thrust fault propagation, the thrust transfer zone model is problematic, because it is difficult to explain how two faults that are now contiguous and en échelon, and are assumed to have had a long history of lateral thrust propagation, could have transferred their displacements when the nucleation points of the faults were several hundreds of kilometres apart. For example, the current positions of the Miette and McConnell thrust faults (Fig. 3.8) suggest that they were linked by a transfer zone (Dahlstrom, 1969, Fig. 14). The probable nucleation points of these thrusts are situated in the center between the lateral tips of the respective faults (Miette, near the Athabasca River, McConnell near the Red Deer River) approximately three hundred kilometres apart. Thus, the overlap of the two faults should be envisioned as the consequence of a gradual lateral extension, with the two faults overlapping in the latter

stages of their development, if each fault is also assumed to evolve from a single fault or point.

From our modeling, it is dubious that the thrust belt would have developed without other overlapping faults being generated to take up compression in the area between the early McConnell and Miette faults. Other overlapping faults situated immediately behind or ahead in the thrust belt can be regarded as contemporaneous with the McConnell and Miette thrusts over the long period of lateral thrust fault propagation. For shortening to be evenly distributed along the thrust belt, it is clear from the OVERLAP computer simulations that many thrusts should be active during the evolution of the belt, some of the more hinterland thrusts being reactivated while foreland thrusts are being formed. Current knowledge about thrust fault activation also show that all parts of each thrust are not necessarely active during each slip increment as in the model presented here. Future work should consider the cause of these variations and attempt to construct a better model of thrust propagation considering this aspect.

It is unclear from current field evidence if a large thrust like the McConnell thrust could have evolved from a single fault. A multiple-fault origin, such as the one portrayed on Fig. 3.10, might be a better model of the evolution of the McConnell thrust and other large thrusts, because the displacement on numerous early faults in the thrust belt should be more evenly distributed than along only a few faults of large displacement. The results of the OVERLAP and THREE THRUSTS computer simulations presented above, as well as experiments on analog models such as those of Liu and Dixon (1992), favor such a model of thrust fault development.

During the development of a thrust belt, the displacement is not transferred or exchanged between pairs of faults, rather it is the individual fault that is initiated and propagated through fault slippage when a sufficient stress occurs. Thus, overlap of two or more faults should be envisioned as the consequence of thrusts propagating throughout the thrust belt, rather than a special mechanism that links two or a few individual faults. In

light of this, zones of thrust overlap should be termed 'overlap zones' and the misleading term 'transfer zones' abandoned.

The composite mechanism comprising the overlap mechanism and the spreading simple shear mechanism is comprehensive because it operates at all times and throughout the thrust belt, and conforms in most regards to current knowledge about thrust fault propagation.

Consequences of thrust fault propagation

Layer-parallel strain along individual thrust sheets has been described by Bielenstein (1969), Coward and Kim (1981), Coward and Potts (1983) and several others. Complex strain patterns might be found not only at the frontal and lateral tips of thrust faults but also within hinterland thrust sheets as a consequence of thrust propagation and layer parallel simple shear strain imposed as the sheet was carried piggyback above underlying thrusts. Microstructures observed within particular thrust sheets sometimes show ambiguous kinematic indicators such as cross-cutting en échelon shear veins of opposed shear sense (see Chapter Four of this thesis). Such ambiguous indicators may have resulted from strain reversals due to layer-parallel shear strain applied during piggyback thrusting.

As noted above, the initial location of the fault nucleation point and the propagation rate of the various faults in the active thrust zone will affect the geometry of the thrust belt. In the case of thrust faults, among other things, the rheology of the rocks is a key factor that will govern the number and spacing of the thrust faults. Other factors such as pore pressure, thickness, and taper of the orogenic wedge are important and well described by the critically tapered Coulomb wedge model presented by Davis *et al.* (1983), Dahlen (1984) and Dahlen *et al.* (1984).

To improve the realism and comparative validity of the overlap mechanism, several features need to be considered. For instance, if a thick rock package could be simulated,

the foreland propagation of thrust faults induced by the rise of a hinterland of a thrust belt could be modeled (the higher taper angle of Dahlen *et al.*, 1984). This type of model should account for ramping through a thick rock package, the formation of folds and the eventual layer-parallel shear of various thrust sheets through stacking and piggyback transport of thrust sheets as indicated in structure sections.

Although the overlap mechanism presented here was applied to thrust belts, it can also be used to explain the distribution of extension faults during the evolution of an extension belt (rift) since the factors leading to fault propagation are similar for normal faults and thrust faults (Walsh and Watterson, 1988).

CONCLUSIONS

Two computer programs, with graphical simulations, demonstrate a new model of thrust propagation and thrust belt development that fits current knowledge about fault propagation. The new model is a composite of two mechanisms:

1) The spreading simple shear mechanism applies a form of layer-parallel simple shear strain symmetrical about the center of the leading edge of a thrust fault to its lateral tips, as the fault propagates laterally and forward.

2) The overlap mechanism is a conceptual model derived from computer simulations and thrust fault theory that predicts when each fault might propagate when a group of thrust faults are linked through a common décollement. The mechanism is an analog of local stress buildup and its eventual relaxation by slip on a fault best-situated to accommodate this stress release.

The OVERLAP program shows that thrust faults propagate laterally and do not intentionally transfer displacement from one thrust to another; variations in displacements along strike are the consequence of multiple thrust initiation sites. Thus, a composite mechanism of the overlap and spreading simple shear mechanisms provides a better way

of visualizing the evolution of thrust belts than the thrust transfer zone concept of Dahlstrom (1969, 1970).

The computer simulations provide useful information about the behavior of multiple faults:

1) the number of faults and the location of their nucleation points (their density), and the rheology and consequent speed of fault propagation govern the uniformity of the shortening along the thrust belt.

2) The branch lines and hanging wall strain pattern of two intersecting thrust faults can be used to unravel the sequence of thrusting of the two faults.

3) The OVERLAP computer simulations show that shortening along a thrust belt can be distributed more evenly by means of propagation of a large number of small faults than by a few large thrusts.

4) The THREE THRUSTS computer simulations also demonstrate that the final geometry of a large thrust fault on a geological map leaves few clues about its origin, whether it was produced by the coalescence of multiple, en échelon, thrust faults or from only a single fault.

TECHNICAL INFORMATION

The programs were written in the V.I.P. language (Visual Interactive Programming, Copyright 1986, 1987 by Mainstay) and run on a Macintosh microcomputer. They are available from D. Lebel either as a Run-time file along with the V.I.P. Run-time interpreter or as an ASCII file. To obtain a copy please send $25.Cnd for duplication and handling costs.

CHAPTER FOUR

MESOFABRIC RECORD OF STRAIN IN LARGE THRUST SHEETS OF THE CENTRAL CANADIAN ROCKY MOUNTAINS, ALBERTA.

ABSTRACT

Thrust faults of the Rocky Mountain thrust-fold belt generally show a decrease in displacement from the center of their map length to their lateral tips. Because of this, some internal strain must develop within the thrust sheets which permits greater forward motion of material situated in the central parts relative to the lateral ends of a thrust sheet. The results of a structural analysis of the Nikanassin and Fiddle River thrust sheets of the central Front Ranges show that within these thrust sheets mesoscale structures or fabric elements (veins, shear zones, mesoscale faults), especially subtle brittle-ductile shear zones, indicate the differential motion of elongated blocks oriented perpendicular to the thrust fault mean strike. The blocks are separated by vein sets that form small shear zones, which together with the obliquity of the S_1 cleavage to the regional folds, indicate that progressive deformation was non-coaxial. The enveloping surface of the different calculated orientations of regional $ß_1$ (bedding) fold axes along each thrust sheet shows the sinusoidal shape of the thrust sheets, coincident with their mapped fault traces. This anomalous shape is interpreted as indicating subsequent deformation of the early formed structures in the Nikanassin and Fiddle River thrust sheets, resulting from the varying values of forward motion by piggyback transport above younger, underlying Foothills thrust faults.

INTRODUCTION

In Chapter Three of this thesis, some possible effects of forward and lateral propagation of thrust faults carried piggyback by other propagating and underlying thrust faults situated further in the foreland of thrust-fold belts were discussed. Such phenomena may cause significant variations in strain along the width of thrust sheets. Some critical questions for a geometric model of thrust fault propagation were also discussed: 1) the manner by which a single fault evolves (fault propagation), and 2) the deformation that is caused by a single fault (displacement patterns in the hanging wall). This paper summarizes the results of a structural analysis of mesoscale fabric elements of two thrust sheets of the Canadian Rocky Mountain thrust-fold belt and provides some data and answers concerning these questions. The study area, in the Front Ranges of the central Rocky Mountains, is situated 60 km east of Jasper, Alberta, and straddles part of eastern Jasper National Park and the adjacent area (Figs. 2.3, 2.4).

Mesofabrics or mesoscale fabric elements (1 cm to few metres in size) include planar structures such as bedding, cleavage, small faults (mesofaults), shear zones, veins, joints, and linear structures such as intersection and stretching lineations, and small fold axes (Turner and Weiss, 1963; Hancock, 1985). The study of mesofabrics in thrust-fold belts permits the analysis of stress and strain patterns in local and regional structures and provides important clues about the kinematics of folds and thrust faults (Muecke and Charlesworth 1966; Price, 1967; Bielenstein, 1969; Siddans, 1977; Brown and Spang, 1978; Reks and Grey, 1983; Dunne, 1985; Marshak and Engelder, 1985; Wojtal, 1986; Cooper, 1992, and others). These structures are particularly useful in areas of low strain containing few strain markers such as the Front Ranges and Foothills of the Canadian Rocky Mountains.

The purpose of the study is to outline and compare the geometry and spatial orientation of the mesofabrics in two adjacent thrust sheets of the Front Ranges, the

Nikanassin and the Fiddle River thrust sheets to: (1) determine the relations between mesofabrics and regional folds and thrust faults, (2) evaluate the role of mesofabrics in the strain history induced by thrust fault motion, and (3) detect any superimposed late deformation.

STRATIGRAPHY AND REGIONAL STRUCTURE

The stratigraphy, structure and tectonic history of the foreland thrust belt of the Canadian Cordillera in the central Rocky Mountains has been thoroughly described by many researchers (Bally *et al.*, 1966; Dahlstrom, 1970; Price and Mountjoy, 1970; Price, 1981). It involves a westerly thickening wedge of Proterozoic to early Cenozoic sedimentary rocks deposited on the Hudsonian crystalline basement (Figs. 2.3, 2.4) and deformed episodically from mid-Jurassic to the late Paleocene (Underschulz and Erdmer, 1992). These deformations resulted from the accretion of a series of exotic terranes to the Pacific Margin of North America (Monger *et al.*, 1982). The Front Ranges and Foothills of the foreland thrust belt represent the more external zones of deformation that were deformed only during the latest Late Cretaceous to Paleocene compression. This deformation event was caused by the advancement of an easterly tapered orogenic wedge above a basal décollement, that formed a series of imbricated, internally deformed thrust sheets along the toe of this wedge, in the foreland. In this external zone of deformation, the sedimentary cover can be divided into two lithotectonic units with differing mechanical properties, the Paleozoic and Mesozoic-Cenozoic units (Figs.4.1, 2.4).

The Paleozoic lithotectonic unit is largely composed of carbonates and has reacted as a rigid, competent 'beam' during deformation through the development of simple thrust sheets, underlain by low-angle thrust faults, and extending for tens to hundreds of kilometres along the belt (Price and Mountjoy, 1970; Elliott, 1976a). Prominent folds are observed in thrust sheets of the Front Ranges adjacent to the North Saskatchewan River (Douglas, 1956a) and in the Jasper segment of the Rocky Mountains (Mountjoy, 1960a,

1960b, Mountjoy *et al.*, 1992) and described and discussed in some detail recently (Mountjoy, 1992). As discussed in the latter paper, in these areas, the Paleozoic lithotectonic unit changes from a single layer to a multi-layer due to the presence of Upper Devonian off-reef shales in the middle of this sequence. In both areas, competent Devonian limestones and dolomites of the Fairholme reef complex pass into off-reef shales. This incompetent shale unit (≈ 250 m thick) is sandwiched between two competent carbonate beams comprising a lower beam of Middle and Upper Cambrian carbonate and an upper beam of Upper Devonian strata (Palliser Formation, ≈ 270 m thick). Above this, the Carboniferous (Banff Formation and Rundle Group, ≈ 500 m thick) forms another multi-layer that favors the development of folds.

The overlying Mesozoic-Cenozoic lithotectonic unit comprises incompetent shales, for the most part with thin to thick-bedded sandstones, conglomerates and coal beds, that were deposited in the foreland basin situated ahead of the advancing Cordilleran orogenic wedge. This thick sequence (≈4 km) has been deformed into closely spaced folds and imbricates that crop out mostly in the Foothills. Exploration for oil and gas has delineated numerous thrust sheets in the subsurface which display a simple geometry (Price and Fermor, 1985; Fermor, 1993), similar to thrust sheets observed at the surface in the Front Ranges. The disharmony in structural style and shortening measured within the two lithotectonic units outlines the presence of one or more extensive décollements at the base of the Mesozoic sequence in addition to the décollement at or near the base of the sedimentary sequence (Bally *et al.*, 1966; Jones, 1982; Price and Fermor, 1985; Lebel, Chapter Two of this thesis).

The Nikanassin and Fiddle River thrusts

The Nikanassin and overlying Fiddle River thrusts are adjacent thrust sheets, which are situated at the northeastern edge of the Front Ranges in central Alberta (Figs. 2.3, 2.4 and 4.2). Both are well exposed and are representative examples of Front Range

thrust sheets because of their relatively simple structure. These thrust sheets also display relatively homogeneous lithologies along strike, mainly of the Paleozoic and lower part of the Mesozoic lithotectonic units, and therefore it can be assumed that both thrust sheets deformed in a comparable manner. In plan view, both fault traces are arcuate and the presence of folds at the extremities of the thrust sheets is typical of a number of faults in the Front Ranges. These folds have been interpreted as classical examples of folds propagating ahead of a laterally developing thrust fault by Elliott (1976a, fault-propagation folds of Jamison, 1987).

The two faults emanate from a wide and relatively flat décollement near the base of the Mesozoic sequence, situated above an underlying thrust sheet that glides in turn above the basal décollement of the orogenic wedge (Fig. 2.6, see Chapter Two, this thesis, for discussion). The structurally higher décollement transported Cambrian and overlying rocks of the Nikanassin and Fiddle River thrust sheets along a layer-parallel glide zone situated about 300-500 m above the base of the Mesozoic sequence (Late Jurassic-Early Cretaceous Nikanassin Formation; Douglas and Lebel, 1993; Mountjoy *et al.*, 1992; Chapter Two, this thesis). At the surface the faults are separate near the McLeod River but merge in the northwestern part of the study area, near the Miette Hotsprings. The Nikanassin thrust fault extends for 70 km towards the southeast and decreases in displacement from its mapped center to both of its lateral tips. Its southeast tip overlaps the northwest tip of the Bighorn thrust fault which in turn increases displacement towards the southeast, and extends for a similar map length and glides along the same décollement (in the Nikanassin Formation) as the Nikanassin and Fiddle River thrust faults (Fig. 2.4). The Fiddle River thrust fault is shorter in map length (37 km) and terminates near the McLeod River, close to the center of the Nikanassin thrust fault. The dip of the Nikanassin thrust fault plane, near the surface, changes from moderate to steep in the southeast, near section C-C' (Fig. 2.6), to shallow dips west of Cadomin, steepening

again near its northwest termination (Fig. 2.3). The steep dips appear to be the result of rotation by underlying folds and thrusts.

Cambrian strata are brought to the surface in the hanging wall of the Fiddle River thrust fault near Luscar (Mount Berry area) and were encountered in a well, at the base of the Nikanassin thrust sheet (Aquit Mich 6-23-46-22W5). This thrust sheet exposes a wide band (1-5 km) of Paleozoic rocks, mostly homoclinal with little internal deformation (Fig. 2.3). The Nikanassin thrust sheet also contains mostly Paleozoic rocks but by contrast, is narrower at the surface (<2 km wide) and contains numerous splay faults and folds. Around Mountain Park, in the higher portion of the Nikanassin thrust sheet, the Jurassic and younger hanging wall rocks are detached from the Triassic and Paleozoic rocks and imbricated in a series of folded thrust faults (Charlesworth and Kilby, 1982; Mountjoy *et al.*, 1992; Chapter Two, this thesis).

Folds are usually well exposed and are observed along most of the hanging wall of the Nikanassin thrust fault. Most fold traces are sub-parallel to the local trend of the fault and can be followed for several kilometres before gradual broadening and disappearing. Some folds end abruptly against small faults or against the main thrust fault. Axial planes are generally upright to overturned towards the northeast. Usually, folds are cylindrical, concentric, and flexural-slip (Class I folds, Ramsay, 1967).

In the southeastern portion of the Nikanassin thrust sheet, the tight and upright Redcap anticline has a shallow plunge toward the southeast. Further northwest near Cadomin, the immediate hanging wall contains a tight asymmetric and overturned southeast-plunging fold in the Paleozoic. This fold continues northwest across the McLeod River and becomes broader. Additional folds that are cut by minor fault splays appear there (Fig. 4.3; section I-I', Fig. 2.6). Further northwest, the overlying Fiddle River thrust sheet is folded by these structures, which are responsible for the klippe of Cambrian rocks near Mount Berry (Fig. 4.4). In the Miette area, near the intersection between the Nikanassin and Fiddle River thrust faults, Mountjoy (1960a) outlined a

complex set of fault splays emanating from the Nikanassin thrust fault, that are folded by footwall structures. In the northwest, east of the Miette Hotsprings, the combined Nikanassin-Fiddle River thrust fault terminates in a fault-propagated anticline-syncline fold pair (Figs. 2.3 and 4.2).

In addition, the Nikanassin and Fiddle River thrust sheets have also been rotated into steeper dips by the motion of these thrust sheets along the underlying listric (concave upward) thrust faults and the stacking of underlying thrust sheets (see section C-C', Fig. 2.6). This rotation has caused the development of a broad syncline, with its axial plane inclined to the southwest (northeast-dipping) and outcropping just northeast of the Miette thrust (section I-I', Fig. 2.6). Mountjoy (1960a, 1992) observed and discussed rotated thrust faults and folds towards the southwest within adjacent thrust sheets in the Miette area ('southwest overfolds'). The origin of these folds is identical to the broad inclined syncline involving the Nikanassin and Fiddle River thrusts. The southwest overfolds are interpreted as part of a single, progressive compression of the Front Ranges, and not the result of separate phases of deformation (Mountjoy, 1992).

Minor thrust splays outline thrust slices of limited extent and thickness that are mostly restricted to the immediate hanging wall or footwall of the major thrust faults. Exceptionally, small duplexes were observed (e.g. Little MacKenzie Creek, 1 km wide, 400 m high, Fig. 3.6).

DATA COLLECTION

One hundred and sixty stations for mesofabric analysis were located along the Nikanassin and Fiddle River thrust sheets. Since exposure is generally excellent, stations were located using three criteria: (1) limited to the Paleozoic lithotectonic unit, especially limestone and dolomite lithologies, (2) wide distribution in the thrust sheets, and (3) around limbs and hinges of folds, and away from the immediate hanging wall of the main thrust faults. Data collection at each station consisted of three steps: (1) collection of

orientation data, (2) mesostructural description, and (3) measurements of spacing and thickness of veins in vein sets, stylolitic cleavage and spacing of joint sets.

Orientation data were collected by determining three or more measurements of the orientation of each type of mesofabric. The description of mesostructures included morphological character, relative ages, type and attitude of vein fills, sense and amount of displacement on mesoscale faults and shear zones. Also, the spacing of veins and joints within sets was measured normal to the fractures. In all, close to 1100 structural measurements were made of bedding planes (conventionally labeled S_0), two intersecting cleavages, first and second phases (S_1 and S_2), intersection lineations between bedding and cleavages (L_1^0, L_2^0), L_2^1), minor fold axes (B_1), veins, minor faults, minor shear zones and joints (Fig. 4.2, in pocket).

MESOFABRICS DESCRIPTION

Stratification (S_0) and mesoscopic folds (B_1)

Stratification (or bedding) is the most prominent fabric element measured in the field. Bedding orientations (Fig. 2.3) strike northwest and dip southwest in general, but have a variety of attitudes depending on the occurrence of macroscopic (regional) folds that plunge either northwest or southeast. Regionally, the stratification follows the curvature of the thrust faults as determined from the orientation of the stratigraphic contacts (Fig. 2.3). Mesoscopic folds (B_1) are rarely observed, but generally conform in orientation and structural style to the macroscopic folds.

Cleavage (S_1) and intersection lineation (L_1^0))

First phase cleavage (S_1) is dominated by disjunctive, spaced cleavages (Powell, 1979; Engelder and Marshak, 1985) in non-folded areas of the Nikanassin and Fiddle River thrust sheets. In carbonate units, 'sutured' (or 'stylolitic') and 'non-sutured'

('solution') cleavages (Wanless, 1979; Engelder and Marshak, 1985) were both observed. The stylolites are usually less then 1 mm in amplitude, coalescing into discrete planes of insoluble material that are generally spaced every 30 cm or more (a 'weak' spacing, Alvarez *et al.*, 1978). Stylolites and solution cleavage were observed throughout the thrust sheets, but with a closer spacing in the core of folds.

In the tighter cores of meso- or macroscale folds, or next to faults, especially in shaly units, often the spacing of cleavage planes is reduced to less that 1 mm and can be termed 'slaty' (Powell, 1979), but this slaty cleavage is not widely distributed. In these zones and in most areas, cleavage is axial planar to folds, and cleavage refraction and fanning on the fold limbs was frequently observed (Fig. 4.5). In other areas, such as west of Cadomin, cleavage was observed to cross-cut fold limbs ('transected folds').

The intersection lineation L_1^0 between stratification (S_0) and the S_1 cleavage, is defined by a simple line on either of these planes.

Second cleavage (S_2)

Rarely, a second cleavage (S_2) crenulates the first cleavage. The origin of this cleavage is not readily apparent although it appeared in some cases to be related to fault ramps as determined from field observations and cross-sections. Few measurements have been obtained of this fabric, most of them showed northeast-southwest trends with variable dips, almost perpendicular to S_1. The best examples occur in the immediate hanging wall of the Nikanassin thrust, near the radio antenna west of Cadomin. Not enough L_2^1 and L_2^0 intersection lineations were observed to make any relevant analysis.

Veins and shear zones

Veins filled with calcite cements were observed most often in carbonate lithologies. Most vein sets are oriented approximately perpendicular to the regional fold

axes and thrust faults. They occur in brittle-ductile shear zones as the consequence of simple shear (Ramsay, 1980). In the area mapped, vein sets are grouped within three types of shear zones: (1) narrow (5-30 cm) shear zones of en échelon veins of varying thickness (≤ 2 cm) (Fig. 4.7), (2) small conjugate shear zones with intersecting vein sets, and (3) broad zones (≥ 10 m) with long (1-3 m), thin (1-10 mm), and widely spaced (≥ 30 cm) veins. This last type of vein set is not easily recognizable as part of a shear zone, but extensive outcrops show that individual veins have slightly sigmoidal shapes that are typical of narrower shear zones (Type 1). Few vein sets are strictly related to pure extension, except for some rare axial planar veins observed in fold hinges (e.g. in Domains X and XI, Fig. 4.2).

Overall, the average width of measured veins varied from 0.1 mm to 20 mm. Mean vein width is 1.8 ± 2.0 mm with a statistical mode in the class ranging from 0.9 and 1.4 mm and includes 55.9 % of the measurements. The average spacing between veins in each set varies from 10 mm to 1 m, with a mean spacing of 152 mm; the statistical mode is in the class ranging from 50 to 70 mm and includes 21.5 % of the measurements (Fig. 4.9). The majority of the vein sets has a spacing ranging between 10 and 70 mm.

On average, most veins show an extension of 1 mm per 40 mm of rock length perpendicular to the vein set, which represents an extension of 2.5 %. This extension occurred along the entire Nikanassin and the Fiddle River thrust sheets, perpendicular to the transport direction.

Joints and mesofaults

Joints are abundant but only consistent sets were measured in the field. If slickensides were present on the fractures, they were classified as mesofaults (mesoscale faults) and their relative motion recorded. Mesofaults are rare in the studied area and were

not sufficiently numerous for a significant stereographic analysis. The more important mesofaults are included on Fig. 4.2.

ORIENTATION ANALYSIS

Bielenstein (1969) studied the mesoscale structures of the Rundle thrust sheet situated in the Front Ranges of the southern Rocky Mountains near Banff, Alberta, a thrust sheet comparable in geometry and map length to the Nikanassin. Individual bedding and cleavage measurements were plotted against their relative position along the map trace of the Rundle thrust fault and a regression analysis was done to test for lcorrelation. Results showed that there was a good and significant correlation between the orientation of stylolitic cleavage, veins and various families of mesoscale faults at any sample site and the position of the sample site along the Rundle thrust sheet or in other words that the thrust fault displayed a regular curvature (see Fig. 4.15). Only bedding measurements showed a lack of correlation. Bielenstein (1969) interpreted these results as indicating translation of the thrust sheet along divergent displacement trajectories, resulting in extension of the Rundle thrust sheet perpendicular to the direction of forward motion.

The results of regression analysis for some mesoscale fabric elements versus distance along the Nikanassin and Fiddle River thrust sheets are listed in Table 4.1. Bedding orientations lack correlation with distance along the Nikanassin and Fiddle River thrusts, similar to what occurs in the Rundle thrust sheet. In addition, cleavage and lineation orientations in the Nikanassin and Fiddle River thrust sheets also lack a significant correlation. This difference of mesoscale structures between the Nikanassin-Fiddle River and the Rundle thrust sheets is interpreted to be the consequence of superimposed deformation on the initial tectonic fabrics due to the forward translation of the Nikanassin and Fiddle River thrust sheets. Later phase, non-coaxial folds or intersecting cleavages are good indicators of superimposed deformation. As shown below

Mesostructures	n	r
S_0 NK	226	0.203
S_0 FR	215	0.108
S_1 NK	108	0.172
S_1 FR	97	0.200
L_1^0 NK	64	0.224
L_1^0 FR	62	0.196

Table 4.1: Results of statistical analysis comparing individual mesostructural measurements versus distance along the Fiddle River (FR) and Nikanassin (NK) thrust sheets. (see Figs. 4.2 and 2.3). S_0: Bedding S_1: First cleavage, L_1^0: intersection lineation between S_0 and S_1. n: number of measurements

the geometric and kinematic relationships between cleavage and regional folds suggest that later deformation rotated and moved the earlier mesoscale structures.

Conventionally, cleavage planes are considered to be sub-parallel to the *XY* plane of the strain ellipsoid (*X*, *Y* and *Z* are the maximum, intermediate and minimum elongation directions, respectively) and are axial planar to folds. However, because axial planar cleavage often fans around a fold axis, only cleavage planes which intersect a fold hinge should be considered parallel to the *XY* plane. Quantitative strain evaluation in little metamorphosed fold-and-thrust belts shows that the *X* axis of the finite strain ellipsoid is usually oriented perpendicular to the local fold axis (Reks and Grey, 1982) and average fold axes calculated from orientation analysis of the mesoscale fabrics within each domain provide an estimate of the orientation of *Y*. The orientation of this axis in individual domains is used here to evaluate the variations in finite strain along the strike of the studied thrust sheets. In folds with axial planar cleavage, mesoscale fabrics such as bedding, cleavage, intersection lineations, and minor fold axes can be used to calculate the mean fold axis of a structural domain (Suppe, 1985, p.54). The orientation of the mean fold axes of individual domains is calculated here from stereographic π-diagrams (poles to planes) and line projections from: (1) the pole to the best fit great circle of poles to bedding (labeled β_1 fold axis), (2) the pole to the best fit great circle of poles to the S_1 cleavage (labeled ∂_1 structural axis), (3) the mean orientation of the intersection lineation L_1^0 (labeled Δ_1 structural axis). These three methods have been used concurrently to determine if cleavage fans are coaxial to folds. All these axes were calculated using a conventional stereographic computer program (Stereo 4.0™, David B. McEachran), that permits statistical calculation of the best fit great circle of poles to planes and the mean orientation of lineations. In addition, rose diagrams were prepared for veins to relate the orientation of the principal vein sets to the orientation of the finite strain ellipsoid. Stereograms of the vein sets orientation were also prepared for each domain but only the mean stretching axes obtained from these diagrams are reported here since most veins

showed subvertical orientations. Insufficient data were obtained in some domains for analysis of all types of mesofabrics.

Overall, fourteen domains were delimited within the Nikanassin (Domains I to VII, Figs. 4.2, 4.10) and Fiddle River (Domains IX to XIV) thrust sheets. Domain VIII corresponds to an imbricate fault slice underlying the Nikanassin thrust sheet near its northwest extremity. Structural domains were selected so that they had relatively uniform plunge as determined from field observations of the macroscopic folds.

Stereographic diagrams

Macroscopic folds occur within the Nikanassin and Fiddle River thrust sheets. The broad, southwest-inclined syncline discussed earlier and some other internal tighter folds within the Nikanassin and Fiddle River thrust sheets, explain why the stereographic diagram of S_0 poles generally outlines a good to weak girdle distribution allowing for the calculation of $ß_1$ (Fig. 4.10).

The mean orientation of the S_1 cleavage has been calculated for each domain where there are sufficient data. S_1 cleavage strikes west-northwest to northwest in each domain, dipping northeast between 47° and 85° (Table 4.1), generally making a significant dihedral angle (30 to 90°) to bedding that generally strikes northwest and dips southwest (Fig. 4.10). Fanning of cleavage is observed within most domains, and for this reason the stereographic projection of S_1 poles generally outlines a good to weak girdle distribution, permitting the calculation of the ∂_1 axis (pole to the best fit great circle of S_1 poles, Fig. 4.10). Diagrams of the L_1^0 intersection lineations generally show a single-point maximum distribution, which is used to calculate the Δ_1 axis (Fig. 4.10).

Rose diagrams

Rose diagrams of vein sets (Fig. 4.10) show that vein set orientations vary from one domain to another and that two vein sets are dominant. Most veins are sub-vertical

and a north-northeast/south-southwest *a-c* vein set (approximately normal to fold axes) is invariably present, and a north-south to north-northwest/south-southeast set is present in most domains. In addition, several other orientations of vein sets were measured within the different domains that appear to be related to local structures because of their local distribution in the Nikanassin and the Fiddle River thrust sheets. Rose diagrams of all vein set orientations (Fig. 4.11) show a statistical mode between 210° and 215° for the Fiddle River thrust sheet, and between 205° and 210° for the Nikanassin thrust sheet. The strike of these vein sets are nearly perpendicular to the average map trend of each thrust sheet. Thus, the maximum horizontal extension direction, represented approximately by the direction perpendicular to the statistical mode of these vein sets, is close to being parallel to the trend of the Nikanassin and Fiddle River thrust faults and at a right angle to the transport direction.

Field observations of cross-cutting veins suggest a chronology for the dominant vein sets where the *a-c* vein set is older than the north-south set. The north-south vein set is associated with northeast-southwest trending sinistral shear zones. These sinistral shear zones occur throughout the Nikanassin and Fiddle River thrust sheets (Fig. 4.2). Dextral shear zones were observed locally but have no systematic orientation, varying from northwest-southeast to northeast-southwest (Fig. 4.2).

Synoptic diagrams

Synoptic diagrams of the $ß_1$ fold axes, and the ∂_1 and Δ_1 structural axes of the different domains of the Nikanassin thrust sheet (Fig. 4.12 (a, b, c), Table 4.2) reveal that most structural elements plunge southeast in the southeastern part of the thrust sheet and plunge northwest for those situated northwest of Domain IV (Fig. 4.10). The calculated mean trend and plunge of all $ß_1$ fold axes (poles to great circle for bedding, Fig. 4.12 (a)) is [119.1°/1.3°]. Most $ß_1$ axes trend at a significant angle (up to 13°) from this mean trend of the $ß_1$ axes or from the map trace of the Nikanassin fault. The average

Domain	β_1	n (S_0)	∂_1	mean S_1	n (S_1)	Δ_1	n (L_1^0)
Nikanassin thrust sheet							
I	124.6°/ 5.6°	58	304.8°/ 1.6°	303°/ 62°	18	123.2°/ 9.6°	12
II	286.4°/ 5.2°	14	119.9°/ 19.5°	319°/ 47°	7	120.1°/ 8.7°	7
III	121.3°/ 8.1°	33	-	-	-	-	-
IV	132.4°/ 13°	25	-	308°/ 85°	18	-	-
V	302.1°/ 5.5°	52	287.8°/ 4.1°	279°/ 47°	34	291.9°/ 12.5°	16
VI	290.6°/ 14.5°	35	304.8°/ 0.1°	305°/ 69°	25	306.1°/ 7.2°	13
VII	-	29	275.1°/ 0.7°	96°/ 67°	7	276.9°/ 5.9°	5
VIII	116.4°/ 7.2°	29	292.2°/ 28.6°	279°/ 69°	9	272.1°/ 9.1°	3
Fiddle River thrust sheet							
IX	124°/ 8.7°	16	126.6°/ 7.4°	126°/ 89°	8	125.1°/ 7.7°	8
X	-	37	133°/ 22.6°	318.8°/ 76.4°	19	129.1°/ 16.8°	14
XI	276.8°/ 6.5°	53	-	304°/ 70°	22	298.7°/ 7.2°	13
XII	285.8°/ 8.1°	15	296.8°/ 17.6°	292.1°/ 75.4°	7	296.8°/ 8.3°	3
XIII	292.2°/ 44.2°	36	290°/ 21°	156°/ 28°	11	282.6°/ 28.1°	10
XIV	296.4°/ 12.7°	29	297.4°/ 7.3°	128°/ 34°	8	304.9°/ 15.8°	6

Table 1: Summary of calculated mesofabric axes and mean orientations for the Nikanassin and Fiddle River thrust sheets (from Fig. 4.10). β_1 : Pole to best fit great circle to bedding poles; n (S_0): number of bedding measurements; ∂_1 : Pole to best fit great circle to S_1 cleavage poles; mean S_1: mean orientation of the S_1 cleavage; n (S_1): number of S_1 measurements; Δ_1: Mean trend and plunge of the intersection lineations between S_0 and S_1; n (L_1^0): number of lineations.

trend of the Nikanassin thrust fault on the map is about 117°, and about 115° for the Fiddle River thrust fault, each estimated from the envelope of the sinuous trace of both faults (i.e. estimated from measured fault strikes).

The calculated mean trend/plunge of all the ∂_1 structural axes (pole to great circle of S_1 cleavage) is [294.2°/2.4°], making a slight angle in strike and plunge with the mean $ß_1$ fold axis. The Δ_1 structural axes (mean intersection lineation) generally fall close to their relative ∂_1 structural axes on the stereograms (e.g. ∂_1 from Domain II falls close to Δ_1 from the same domain, Fig. 3.12 (b, c), Table 4.2) and have a similar mean orientation for all domains (291.8°/2.8°), but most differ from the the corresponding $ß_1$ fold axes.

From southeast to northwest, there is a change of orientation of the various types of fold axes along the Nikanassin fault, but this change is not simple and gradual. The fold axes of the more southeastern domains generally make a dextral (clockwise) angle with the average fault trace, while the northwestern domains make a sinistral (anticlockwise) angle. Also, $ß_1$, ∂_1 and Δ_1 axes of the different domains of the Fiddle River thrust sheet (Fig. 4.12 (e, f, g)) display the same geometry, where southeast domains plunge southeast and northwestern domains plunge northwest and differ from the average fault trace. There is a discrepancy in orientation between the $ß_1$ fold axes and the ∂_1 and Δ_1 structural axes. Together, the $ß_1$, ∂_1 and Δ_1 fold axes do not lie along a great circle for both the Nikanassin and the Fiddle River thrust sheets (Fig. 4.12). The pole to the mean orientation of all vein sets was calculated for each domain to estimate the axes of longitudinal extension along the thrust sheets. On synoptic diagrams for the Nikanassin and Fiddle River thrust sheets domains (Fig. 4.13 (a, b)), these poles display a geographic variation in orientation similar to fold axes. The change in plunge and curvature of the two thrust sheets occurs in the same area, near the McLeod River. This change does not coincide with a regional culmination since most folds observed in the

thefootwall of the Nikanassin thrust fault plunge southeast, southeast of the Miette Hotsprings (northwest termination of the Nikanassin-Fiddle River thrust fault, Fig. 2.3).

Summary plots and discussion

Plots of the orientation of the calculated structural axes (β_1, ∂_1, and Δ_1) and poles to the mean vein sets for each domain of the Nikanassin and Fiddle River thrust sheets, versus distance (d) of the domain from a common point origin, situated at the northwestern tip of the Nikanassin-Fiddle thrust fault, are shown in Fig. 4.14. To interpret these diagrams properly, one must understand the relationship between the angle and distance along the arc of a circle (Fig. 4.15). Within a cartesian reference frame (xy frame), the x coordinates of the arc of a circle, with tangents oriented at a low angle from the x axis (shaded area, Fig. 4.15) versus the relative orientation of these tangents plot as a straight line (see shaded area, Fig. 4.15). The slope of this line is proportional to the length of the ray between the center of curvature and the arc, and the sign of this slope indicates outward or inward curvature (Fig. 4.15).

Visual observation of the plotted structural axes versus distance (Fig. 4.14) permits one to check that none display a linear relationship for the whole map length of each thrust sheet. Some data points fall on a straight line or a line with uniform slope (e.g. Fig. 4.14 (a)), which represents a regular curvature of the structural axes for a specific segment of the thrust sheet. Further along strike (d), other data points fall on straight lines with a differing slope, indicating that the structural axes of different segments of each thrust sheet change in axis of curvature along strike. Overall, the broken lines that tie the data points suggest that the Fiddle River and Nikanassin thrusts sheets have changing curvatures of structural axes along strike and that three to four consecutive and aligned points (Fig. 4.14) represent segments of a thrust sheet with a constant curvature (Fig. 4.14 (a) to (d)),

The comparative plot of the β_1 fold axes for the domains of the Nikanassin and the Fiddle River thrusts sheets (Fig. 4.14 (a)) shows that these axes follow a sinusoidal and sub-parallel path when projected on the horizontal plane (on the map), and have at least one inflection point situated in the same region from the point of origin (d =30 to 45 km). The northwest segment of the Fiddle River thrust sheet shows an open outward curvature (center of curvature toward the foreland), as displayed by a low negative slope, an observation which is in agreement with the general curved-outward shape of the present fault and fold mapped axial traces within the thrust sheet (Fig. 4.2). The central part of the Nikanassin thrust sheet displays a tight outward curvature in the area situated southeast of the McLeod River (d >40 km), and a tight inward curvature northwest of the McLeod River. Also, as outlined on the synoptic stereographic diagrams (Fig. 4.12 (a, d)), β_1 axes vary in plunge from southeast to northwest and this variation follows sinusoidal paths of changing curvature for both thrust sheets (Fig. 4.14 (e)).

Models of thrust fault propagation, such as the Bow and Arrow rule (Elliott, 1976a) or based on observations of faults (Cowie and Scholz, 1992) indicate that thrust faults display a generally inward curvature (curved toward the hinterland of the thrust belt). If the Nikanassin and Fiddle River thrust sheets are presumed to have formed initially with such an inward and regular curvature, their sinusoidal curvature and subparallel inflexion points revealed by the β_1 fold axes and the regional along-strike variation of these faults and mapped fold axial traces (Fig. 4.2) indicate that both thrust sheets have been subject to a common overprinted deformation that modified their initial curvature. The change in orientation of the β_1 axes suggests that the initial configuration of each thrust sheet probably had a regular curvature that was later locally modified by the superimposition of varying strain.

The S_1 cleavage axes and mean intersection lineations (∂_1, Δ_1) together with poles to mean vein sets from domains of the Nikanassin and the Fiddle River thrust sheets are plotted on Fig. 4.14 (b) to (d). A significant discrepancy appears between the regional

curvature of these elements and that of the β_1 fold axes (Fig. 4.14 (f, g)). The relative ∂_1 and Δ_1 axes have the same orientation in the different domains and outline a broad inward curvature of these axes along the thrust sheets (orientation generally increase in absolute orientation towards the southeast, Fig. 4.14 (b, c)). This discrepancy with the β_1 axes is in agreement with field observations of S_1 cleavage planes oblique to the local strike of fold traces and fault planes and the local obliquity of the L_1^0 lineation with the local fold axis. Also, the trend of the pole to the mean orientation of the vein sets tends to follow the orientation of the ∂_1 and Δ_1 axes rather than the β_1 fold axes. In domains where the S_1 cleavage does not show very well developed cleavage fans, stereographic diagrams show that the mean orientation of S_1 does not contain the β_1 fold axis (Fig. 4.10, e.g.Domain XI).

In summary, in the Nikanassin and Fiddle River thrust sheets, there is a mismatch between the regional curvature of the ∂_1, Δ_1 and the pole to mean veins sets with respect to the β_1 fold axes, and an obliquity of β_1 fold axes relative to the mean orientation of S_1 cleavage. This mismatch can be explained as indicating that regional folding was not coeval with cleavage formation (cleavage formed early or late), or that some kind of non-coaxial deformation permitted the rotation of folds during a common deformation and continued cleavage development.

Because cleavage has been observed in the field to be closely related to folds (e.g. common observation of cleavage fans), it is unlikely that cleavage formed later than the deformation that caused the folding within the Nikanassin and Fiddle River thrust sheets. Recent studies concerning the timing of cleavage in thrust-fold belts indicates that cleavage is initiated early during the development of these belts, and continues to develop throughout the development of other structures (Marshak and Engelder, 1985). The transecting relationship between cleavage and some particular folds has been observed and discussed in several papers (Powell, 1974; Stringer, 1975; Borradaile, 1978, Stringer and Treagus, 1980). Commonly, transected folds occur where cleavage and folding are

not precisely contemporaneous, and thus that each element is the result of different strain fields, where the axes of deformation are different within each deformation event or gradually rotated during deformation (non-coaxial strain history).

Other field observations suggest that some of the deformation at the mesoscale occurred within a non-coaxial progressive strain history. Steeply dipping shear veins and associated shear zones within the Nikanassin and Fiddle River thrust sheets are evidence that some simple shear deformation occurred, oriented sub-parallel to the transport direction. The internal strain involved in permitting the translation of material within these thrust sheets to the curved regional shapes described above, must occur at either the mesoscale or the microscopic scale. Mesoscopic vertical shear zones and mesofaults oriented broadly northeast-southwest and vertically, more or less perpendicular to the long axis of the thrust sheets are prime candidates for much of the accommodation of this strain, because they are observed throughout the area. These structures allowed the shearing of the thrust sheets into a large number of elongated sheared compartments with centimetre displacements, of both dextral and sinistral sense that account for most of the required internal deformation. The observed intersection of shear zones of opposite sense attest to the fact that the progressive deformation was non-coaxial. The material needed to fill the numerous thin veins likely came from dissolution of material by other transgranular strain (Groshong *et al.*, 1984) during the continued formation of stylolitic cleavage in the carbonate units and/or grain-to-grain pressure solution.

The fact that relatively few mesofaults were observed in the field relative to shear veins indicates that brittle-ductile deformation (Ramsay, 1980) was the main type of rock deformation within the Paleozoic sequence. The stretching of about 2.5% due to veins perpendicular to the thrust faults provides another indication that these structures are an important component of the strain partitioning between macroscale (major thrusts) and microscale structures (dissolved grain boundaries). The internal deformation observed in

the Nikanassin and Fiddle River thrust sheets is probably representative of other Paleozoic thrust sheets in the Rocky Mountains.

Also, these faults have an anomalous trend relative to adjacent regional thrust faults to the northeast and southwest (Fig. 2.4). The Miette thrust fault has a similar map trend to that of the Nikanassin and Fiddle River thrust faults but the McConnell, Brazeau and Folding Mountain thrust faults have a more northerly trend (up to 15°, Table 4.3) from the other faults. From the regional map (Fig. 2.4), the mean strike of the thrust belt and other important faults is sub-parallel to these last thrust faults (≈125°), which suggests that the Nikanassin, Fiddle River and Miette thrusts have been rotated as a whole, counterclockwise, relative to this presumably initial orientation.

A regional sinistral shear, oriented parallel with the observed shear zones (northeast-southwest), and applied to the Nikanassin and Fiddle River thrusts of the Front Ranges of the area could explain this rotation. A model of evolution and thrust fault propagation of the Front Ranges and Foothills of the Athabasca-Brazeau area was outlined in the Chapter Three of this thesis (Figs. 3.8 and 3.9), based on the measured map lengths of the major thrust faults and simple approximations about the rate of lateral and forward propagation of these faults. This model showed that a series of sinistral and dextral shears, applied to hinterland thrust sheets developed during the successive development of foreland thrust faults and piggyback thrust transport, produces a regional geometry of fault traces with changing curvatures, similar to those observed in the studied area. In particular, the regional orientation of the Nikanassin and Fiddle River thrusts generated by the model are subjected to an important layer-parallel sinistral shear due to the gradual development of thrust faults associated with the Brazeau thrust. This study of mesoscopic fabrics strengthens this model by showing that the Nikanassin and Fiddle River thrust sheets were subjected to significant shear strains, along planes subparallel to the transport direction. The exact reason explaining the development of the Brazeau

Thrust fault	Map trend
Nikanassin	117° (297°)
Fiddle River	115° (295°)
McConnell	128°
Miette	120°
Folding Mountain	130°
Luscar	113°
Brazeau	125°

Table 4.3 : Comparison of the average trend of major thrusts measured in the Athabasca-Brazeau area (north of 52°00' N)

Structure is unknown now, but future work dealing with the detail of the subsurface structural geology may reveal some particular cause (e.g. major thrust lateral ramp).

CONCLUSIONS

The geometry and spatial orientation of the mesoscale structures within the Paleozoic lithotectonic unit of the Nikanassin and Fiddle River thrust sheets of the Front Ranges show that :

(1) Solution cleavage (S_1) is observed throughout the Nikanassin and Fiddle River thrust sheets, and fans around an axis parallel to the local fold axis.

(2) In some domains, the axis of fanning of the S_1 cleavage and the mean intersection lineation between S_1 cleavage and bedding are not parallel to the fold axis calculated from bedding orientations. This is interpreted to result from the rotation of early folds just before some new cleavage planes formed. A second cleavage (S_2) is superimposed upon the early formed S_1 cleavage in some areas and attest to the fact that the strain history is complicated.

(3) Wide and narrow shear zones mainly composed of spaced, thin and long en échelon veins are observed throughout the thrust sheets, and display a statistical mode of vein set orientations nearly perpendicular to the mean map trend of the thrust fault. These shear zones are subvertical and indicate that layer-parallel simple shear was an active deformation mechanism in the thrust sheets. Because these shear zones are present throughout the area, and not only close to folds, they are considered to have originated from the progressve emplacement of the thrust sheets. Volume dilation by the veins within these shear zones is considered to be balanced by the solution of material along cleavage planes. Shear zones of opposite dextral and sinistral sense intersect each other.

The progressive strain history involves: (1) the formation of early folds, probably related to the propagation of the thrust faults (fault-propagation folds), together with the inception of some early cleavage planes. (2) The continued lateral and forward

propagation of the Nikanassin and Fiddle River thrust faults resulted in internal deformation within the thrust sheets by layer-parallel simple shear through a series of dextral and sinistral shear zones, sub-parallel to the transport direction, and (3) the stacking of underlying thrust sheets and piggyback transport above Foothills thrust faults during the latest phase of deformation, in some areas rotated fold axes and other mesoscale structures to positions oblique to the regional stress field. This rotation explains the local transection of folds and early cleavage by later formed cleavage planes.

CHAPTER FIVE

GENERAL CONCLUSIONS

The three papers presented in this thesis give new insights about the geometry, kinematics and theory of thrust faulting, in particular within the Athabasca-Brazeau area of the central Canadian Rocky Mountains.

Three types of décollements can be deduced from the current geometry of the Canadian Cordilleran foreland thrust belt, namely basal, intermediate internal and upper décollements. Geological data and interpretations presented in Chapter Two suggest that:

1) An internal décollement is recognized by a layer-parallel glide horizon that correspond to an extensive flat segment above a ramp that links it to a portion of the basal décollement situated further in the hinterland of the thrust belt. Many fault imbricates emanate from an internal décollement. The internal décollement is underlain by the continuation of the basal décollement towards the foreland and overlain in most cases by an upper décollement surface.

2) The basal décollement of the Front Ranges and Foothills changes both laterally and towards the foreland. It has two ramps, one that cuts up section from the base of the stratigraphic pile to a slippage zone in the Devonian, and another that cuts up section from the Devonian to another flat in the Upper Cretaceous.

3) When considered overall, the shortening within the Mesozoic sequence in the Foothills is equivalent to that in the Paleozoic sequence. However, the two sequences exhibit discrepancies in relative shortening when only short segments of the cross-sections are

considered. Section balancing using restored bed lengths is thus only applicable to the whole of the Foothills.

4) In the Athabasca-Brazeau region six extensive layer-parallel glide horizons are recognized: the Sassenach-Lower Palliser Formation, the Fernie Group, the upper portion of the Nikanassin Formation, the Blackstone Formation, the Wapiabi Formation and the lower part of the Brazeau Formation.

5) Successive forward shifts of the basal décollement to new positions within the stratigraphic pile led to the formation of internal décollements, some of which may be cross-cut, folded by the stacking of thrust sheets of younger faults rising from deeper and more northeastward décollements.

6) The upper, more forward segment of an early décollement appears to have been utilized as a roof thrust during the development of deeper seated duplexes (i.e. the Folding Mountain and Luscar duplexes underlying the Blackstone décollement).

7) The abandonment and forward shift of basal décollements in the external part of the Rocky Mountain belt appears to be related to the development of the upper décollement and can be explained by the Coulomb orogenic wedge model. It is interpreted that the formation of the upper décollement caused increased friction along the composite basal-upper décollement surface that gradually raised the critical taper angle of the orogenic wedge. Renewed internal deformation within the wedge eventually led to a shift of the basal décollement downwards to a new basal décollement to reduce friction. This allowed for renewed foreland accretion until friction again built up sufficiently to cause another cycle of basal décollement abandonment.

In Chapter Three, two computer programs demonstrate a model of thrust propagation and thrust belt development that fits current knowledge about fault propagation. This numerical model is based on two mechanisms:

1) The spreading simple shear mechanism applies a simple form of layer-parallel shear strain symmetrical about the center of the leading edge of a thrust fault to its lateral tips that follows the lateral and forward propagation and motion of this single thrust fault.

2) The overlap mechanism is a conceptual model that predicts how and when each fault might propagate when a group of thrust faults are linked through a common décollement. The mechanism is an analog of local stress buildup and its eventual relaxation by slip on the fault best-situated for this stress release.

The OVERLAP program shows that thrust faults propagate laterally and do not intentionally transfer displacement from one thrust to another; variations in displacements along strike are the consequence of multiple thrust initiation sites. A composite mechanism of the overlap and spreading simple shear mechanisms provides a better way of visualizing the evolution of thrust belts than the thrust transfer zone concept of Dahlstrom (1969, 1970).

The computer simulations provide useful information about the behavior of multiple faults:

1) the number of faults, the locations of their nucleation points, and hence their density, the rheology and consequent speed of fault propagation govern the uniformity of the shortening along the thrust belt.

2) The branch lines and hanging wall strain pattern of two intersecting thrust faults can be used to trace back the thrusting sequence of two thrusts.

3) The OVERLAP computer simulations show that shortening along a thrust belt can be distributed more evenly by means of propagation of a large number of small faults than few large thrusts.

4) The THREE THRUSTS computer simulations also demonstrate that the final geometry of a large thrust fault on a geological map leaves few clues about its origin, whether it was produced by the coalescence of multiple, en échelon thrust faults or from only a single nucleation point.

The study, presented in Chapter Four, of the geometry and spatial orientation of the mesoscale structures within the Paleozoic lithotectonic unit and along the strike of the Nikanassin and Fiddle River thrust sheets of the Front Ranges shows that :

(1) Solution cleavage (S_1) is observed throughout the Nikanassin and Fiddle River thrust sheets, most of the time and fans around an axis parallel to local fold axes.

(2) In some domains, the axis of fanning of the S_1 cleavage and the mean intersection lineation between S_1 cleavage and bedding are not parallel to the fold axis calculated from bedding orientations. This is interpreted to result from the rotation of early folds just before some new cleavage planes formed. A second cleavage (S_2) is superimposed upon the early formed S_1 cleavage in some areas and attest to the fact that the strain history is complicated.

(3) Wide and narrow shear zones mainly composed of spaced, thin and long en échelon veins are observed throughout the thrust sheets, and display a statistical mode of vein set orientations nearly perpendicular to the mean map trend of the thrust fault. These shear zones are subvertical and indicate that layer-parallel simple shear was an active deformation mechanism in the thrust sheets. Because these shear zones are present throughout the area, and not only close to folds, they are considered to have originated from the progressve emplacement of the thrust sheets. Volume dilation by the veins within these shear zones is considered to be balanced by the solution of material along cleavage planes. Shear zones of opposite dextral and sinistral sense intersect each other.

The progressive strain history involves: (1) the formation of early folds, probably related to the propagation of the thrust faults (fault-propagation folds), together with the inception of some early cleavage planes. (2) The continued lateral and forward propagation of the Nikanassin and Fiddle River thrust faults resulted in internal deformation within the thrust sheets by layer-parallel simple shear through a series of dextral and sinistral shear zones, sub-parallel to the transport direction, and (3) the stacking of underlying thrust sheets and piggyback transport above Foothills thrust faults

during the latest phase of deformation, in some areas rotated fold axes and other mesoscale structures to positions oblique to the regional stress field. This rotation explains the local transection of folds and early cleavage by later formed cleavage planes.

REFERENCES

Aitken, J. D. 1989. Birth, growth and death of the Middle Cambrian Cathedral carbonate lithosome, southern Rocky Mountains. Bulletin of Canadian Petroleum Geology, v. 37, pp. 316-333.

Aitken, J. D., Fritz, W. H. and Norford, B. S. 1972. Cambrian and Ordovician biostratigraphy of the southern Canadian Rocky Mountains: Excursion A-19, Guidebook, 24th International Geological Congress, Montreal, Quebec, Canada.

Allan, J. A. and Rutherford, R. L. 1923. Geology along Blackstone, Brazeau, and Pembina Rivers, in the Foothills belt, Alberta. Science and Industrial Research Council of Alberta, Report no. 9.

Alvarez, W., Engelder, T. and Geiser, P. 1978. Classification of solution cleavage in pelagic limestones. Geology, v. 6, pp. 263-266.

Bally, A. W., Gordy, P. L. and Stewart, 1966. Structure, seismic data, and orogenic evolution of the southern Canadian Rocky Mountains. Bulletin Canadian Petroleum Geology, v. 18, pp. 337-381.

Beaumont, C., Fullsack, P. and Hamilton, J. 1992. Erosional control of active compressional orogens. *In:* Thrust Tectonics, (K. R. McClay, ed.), Chapman and Hall, London, UK, pp. 1-31.

Berberian, M. 1982. Aftershock tectonics of the 1978 Tabas-e-Golshan (Iran) earthquake sequence: a documented active 'thin-and-thick skinned tectonic' case. Geophysical Journal of the Royal Astronomical Society, v. 68, pp. 499-530.

Berryman, K. and Beanland, S. 1991. Variation in fault behavior in different tectonic provinces of New Zealand. Journal of Structural Geology, v. 13, pp. 177-189.

Best, E. W. 1958. The Triassic of the North Saskatchewan-Athabasca Rivers area. Alberta Society of Petroleum Geologists, Guidebook Eight Annual Field Conference, pp. 39-49.

Bielenstein, H. U. 1969. The Rundle thrust sheet, Banff, Alberta. Unpub. Ph. D. Thesis, Queen's University, Kingston. Ont. 149 pages

Bombolakis, E. G. 1992. A development stage of a foreland thrust belt. *In:* Thrust Tectonics, (K. R. McClay, ed.), Chapman and Hall, London, UK, pp. 33-40.

Borradaile, G. J. 1978. Transected folds: A study illustrated with examples from Canada and Scotland. Geological Society of America Bulletin, v. 89, pp. 481-493.

Boyer, S. E. 1992. Geometric evidence for synchronous thrusting in the southern Alberta and northwest Montana thrust belt. *In:* Thrust Tectonics (K. R. McClay, ed.), Chapman and Hall, London, UK, pp. 377-390.

Boyer, S. E. and Elliott, D. 1982. Thrust systems. American Association of Petroleum Geologists Bulletin, v. 66, pp. 1196-1230.

Brown, R. L., Carr, S. D., Johnson, B. J., Coleman, V. J., Cook, F. A. and Varsek, J. L. 1992. The Monashee décollement of the southern Canadian Cordillera: a crustal-scale shear zone linking the Rocky Mountain Foreland belt to lower crust beneath accreted terranes. *In:* Thrust Tectonics, (K. R. McClay, ed.), Chapman and Hall, London, UK, pp. 357-364.

Brown, R. L., Journeay, J. M., Lane, L. S., Murphy, D. C. and Rees, C. J. 1986. Obduction, backfolding and piggyback thrusting in the metamorphic hinterland of the southeastern Canadian Cordillera. Journal of Structural Geology, v. 8, pp. 255-268.

Brown, R. L., Journeay, J. M. and Lane, L. S. 1991. The Monashee Terrane. *In:* Part D, Omineca Belt, Structural Styles, Chapter 17 (Gabrielse, H., Compiler), *In:* Geology of the Cordilleran Orogen in Canada (Gabrielse, H. and Yorath, C. J.) Geological Survey of Canada, Geology of Canada, no. 4, pp. 605-607. (also Geological Society of America, The Geology of North America, v. G-2).

Brown, S. P. and Spang, J. H. 1978. Geometry and mechanical relationship of folds to thrust fault propagation using a minor thrust in the Front Ranges of the Canadian Rocky Mountains. Bulletin of Canadian Petroleum Geology, v. 26, pp. 551-571.

Carr, S. D. 1989. Implications of Early Eocene Ladybird granite in Thor-Odin-Pinnacles area, southern British Columbia. *In:* Current Research, Part E. Geological Survey of Canada, Paper 89-1E, pp. 69-77.

Chapple, W.M. 1978. Mechanics of thin-skinned fold-and-thrust belts. Geological Society of America Bulletin, v. 89, p. 1189-1198.

Charlesworth, H. A. K. and Gagnon, L. G. 1985. Intercutaneous wedges, the triangle zone and structural thickening of the Mynheer coal seam at Coal Valley in the Rocky Mountain Foothills of central Alberta. Bulletin of Canadian Petroleum Geology, v. 33, pp. 22-30.

Charlesworth, H. A. K. and Kilby, W. E. 1981. Thrust nappes in the Rocky Mountain Foothills near Mountain Park, Alberta. *In:* Thrust and Nappe Tectonics (McClay, K. R. and Price, N. J., eds.), Special Publication Geological Society of London. No. 9, pp. 475-482.

Charlesworth, H. A. K., Johnston, S. T. and Gagnon, L. G. 1987. Evolution of the triangle zone in the Rocky Mountain Foothills near Coalspur, central Alberta. Canadian Journal of Earth Sciences, v. 24, pp. 1668-1678.

Coletta, B., Letouzey, J., Pinedo, R., Ballard, J. F. and Balé, P. 1991. Computerized X-ray tomography analysis of sandbox models: Examples of thin-skinned thrust systems. Geology, v. 19, pp. 1063-1067.

Cook, F. A. 1988. LITHOPROBE seismic reflection structure of the southeastern Canadian Cordillera: initial results. Tectonics, v. 7, pp. 157-180.

Cook, H. E. 1972. Miette Platform evolution and relationship to overlying bank ('reef') localization, Upper Devonian, Alberta. Bulletin of Canadian Petroleum Geology, v. 20, pp. 375-411.

Cooper, M. 1992. The analysis of fracture systems in subsurface thrust structures from the Foothills of the Canadian Rockies. *In:* Thrust Tectonics (K. R. McClay, ed.), Chapman & Hall, London, UK, pp. 391-405.

Cooper, M. A. and Trayner, P. M. 1986. Thrust-surface geometry: implications for thrust-belt evolution and section-balancing techniques. Journal of Structural Geology, v. 8, pp. 305-312.

Coward, M. P. and Kim, J. H. 1981. Strain within thrust sheets. *In:* Thrust and nappe tectonics (McClay, K. R. and Price, N. J., eds), Geological Society of London Special Publ. 9, pp. 275-291.

Coward, M. P. and Potts, G. J. 1983. Complex strain patterns at the frontal and lateral tips to shear zones and thrust zones. Journal of Structural Geology, v. 5, pp. 383-399.

Cowie, P. A. and Scholz, C. H. 1992a. Physical explanation for the displacement-length relationship of faults using a post-yield fracture mechanics model. Journal of Structural Geology, v. 20, pp. 1133-1148.

Cowie, P. A. and Scholz, C. H. 1992b. Displacement-length scaling relationship for faults: data synthesis and discussion. Journal of Structural Geology, v. 20, pp. 1149-1156.

Dahlen, F.A. 1984, Noncohesive critical Coulomb wedges; An exact solution. Journal of Geophysical Research, v. 89, p. 5389-5396.

Dahlen, F.A. 1990. Critical taper model of fold-and-thrust belts and accretionary wedges. Annual Review of Earth and Planetary Sciences, v. 18, p. 55-99.

Dahlen, F.A. and Suppe, J. 1988. Mechanics, growth, and erosion of mountain belts. In: Processes in continental lithospheric deformation (Clark, S.P. Jr., Birchfiel, B.C. and Suppe, J. eds.). Geological Society of America Special Paper 218, p. 161-178.

Dahlen, F.A., Suppe, J. and Davis, D. 1984. Mechanics of fold-and-thrust belts and accretionary wedges. Journal of Geophysical Research, v. 88, p. 10,087-10,101.

Dahlstrom, C. D. A. 1969. Balanced cross sections. Canadian Journal of Earth Sciences, v. 6, pp. 743-757.

Dahlstrom, C. D. A. 1970. Structural geology in the eastern margin of the Canadian Rocky Mountains. Bulletin of Canadian Petroleum Geology, v. 18, pp. 332-406.

Davis, D., Suppe, J. and Dahlen, F. A. 1983. Mechanics of fold-and-thrust belts and accretionary wedges. Journal of Geophysical Research, v. 88, pp. 1153-1172.

Dechesne, R. G. and Mountjoy, E. W. 1992. Multiple decollements at deep levels of the southern Canadian Rocky Mountain Main Ranges, Alberta and British Columbia. *In:* Structural Geology of Fold and Thrust Belts (S. Mitra and G. W. Fisher, eds), John Hopkins University, Baltimore, pp. 225-238.

de Paor, D. STRAIN SAMPLER. Mac computer program. Department of Earth and Planetary Sciences, The John Hopkins University, Baltimore, MD, U. S. A.

Diegel, F. A. 1986. Topological constraints on imbricate thrust networks, examples from the Mountain City window, Tennessee, U. S. A. Journal of Structural Geology, v. 8, pp. 269-279.

Dixon, J. M. and Liu, S. 1992. Centrifuge modelling of the propagation of thrust faults. In: Thrust Tectonics (K. R. McClay, ed.), Chapman and Hall, London, UK, pp. 53-69.

Douglas, R. J. W. 1950. Callum Creek, Langford Creek, and Gap map-areas, Alberta. Geological Survey of Canada Memoir 255.

Douglas, R. J. W. 1956a. Nordegg, Alberta; Geological Survey of Canada, Paper 55-34, 31 pages.

Douglas, R. J. W. 1956b. George Creek, Alberta; Geological Survey of Canada, Paper 55-39.

Douglas, R. J. W. 1958a. Mount Head map area, Alberta. Geological Survey of Canada Memoir 291, 241 pages.

Douglas, R. J. W. 1958b, Chungo Creek map-area, Alberta; Geological Survey of Canada, Paper 53-3.

Douglas, R. J. W. Unpublished. Cadomin area (East). Geological Survey of Canada, manuscript map

Douglas, R. J. W. and Lebel, D. 1993. Geology and structure cross-section, Cardinal River, Alberta. Geological Survey of Canada, map 1828A, NTS 83C/15, scale 1: 50, 000.

Dunne, W. M. 1986. Mesostructural development in detached folds: an example from West Virginia. Journal of Geology, v. 94, pp. 473-488.

Elliott, D. 1976a. The energy balance and deformation mechanisms of thrust sheets. Philosophical Transactions of the Royal Society of London, v. 283A, pp. 289-312.

Elliott, D. 1976b. The motion of thrust sheets. Journal of Geophysical Research, v. 81, pp. 949-963.

Ellis, M. A. and Dunlap, W. J. 1988. Displacement variation along thrust faults: implications for the development of large faults. Journal of Structural Geology, v. 10, pp. 183-192.

Engelder, T. and Marshak, S. 1985. Disjunctive cleavage formed at shallow depths in sedimentary rocks. Journal of Structural Geology, v. 7, pp. 327-343.

Eschelby, J. D. 1973. Dislocation theory for geophysical applications. Philosophical Transactions of the Royal Society of London, v. 274A, pp. 331-338.

Fermor, P. 1993. Some aspects of the three-dimensional structure of the Alberta Foothills. (*Abs*) 19th Annual Cordilleran Tectonics Workshop, Queen's University, February 19-21, 1993, Abstracts with program.

Frebold, H. 1957. The Jurassic Fernie Group in the Canadian Rocky Mountains and Foothills. Geological Survey of Canada, Memoir 287, 197 pages.

Frebold, H., Mountjoy, E. W. and Reed, R. 1959. The Oxfordian beds of the Jurassic Fernie Group, Alberta and British Columbia. Geological Survey of Canada Bulletin 53.

Gardner, D. A. C. and Spang, J. H. 1973. Model studies of the displacement transfer associated with overthrust faulting. Bulletin of Canadian Petroleum Geology, v. 21, pp. 534-552.

Geiser, P. H. 1988. Mechanisms of thrust propagation: some examples and implications for the analysis of overthrust terrains. Journal of Structural Geology, v. 10, pp. 829-845.

Gibson, D. W. 1968. Triassic stratigraphy between the Athabasca and Brazeau Rivers of Alberta, Geological Survey of Canada, Paper 68-11. 84 pages.

Gibson, D. W. 1978. The Kootenay-Nikanassin lithostratigraphic transition, Rocky Mountain foothills of west-central Alberta. Geological Survey of Canada, Paper 78-1A, pp. 379-381.

Gillespie, P. A., Walsh, J. J. and Watterson, J. 1992. Limitations of dimension and displacement data from single faults and the consequences for data analysis and interpretation. Journal of Structural Geology, v. 20, pp. 1157-1172.

Gretener, P. E. 1972. Thoughts on overthrust faulting in a layered sequence. Bulletin of Canadian Petroleum Geology, v. 25, pp. 110-122.

Groshong, R. H. Jr., Pfiffner, O. A. and Pringle, L. R. 1984. Strain partitioning in the Helvetic thrust belt of eastern Switzerland from the leading edge of the internal zone. Journal of Structural Geology, v. 6, pp. 5-18.

Hake, B. F., Willis, R. and Addison, C. C. 1942. Folded thrust faults in the Foohills of Alberta. Bulletin of the Geological Society of America. v. 53, pp. 291-334.

Hancock, P. L. 1985. Brittle microtectonics: principles and practice. Journal of Structural Geology, v. 7, pp. 437-457.

Hatcher, R. D. and Hooper, R. J. 1992. Evolution of crystalline thrust sheets in the internal parts of mountain chains. *In:* Thrust Tectonics, (K. R. McClay, ed.), Chapman and Hall, London, UK, pp. 217-233.

Hill, K. 1980. Structure and stratigraphy of the coal-bearing and adjacent strata near Cadomin, Alberta. Masters thesis, University of Alberta, Edmonton. 188 pages.

Hossack, J. R. 1983. A cross-section through the Scandinavian Caledonides constructed with the aid of branch line maps. Journal of Structural Geology, v. 5, pp. 103-111.

House, W. M. and Gray, D. R. 1982. Displacement transfer at thrust terminations in Southern Appalachians. American Association of Petroleum Geologists Bulletin, v. 66, pp. 830-842.

Hubbert, M. K. 1937. Theory of scale models as applied to the study of geologic structures. Geological Society of America Bulletin, v. 48, pp. 1459-1520.

Hubbert, M. K. and Rubey, W. W. 1959. Role of fluid pressure in mechanics of overthrust faulting-I. Mechanics of fluid filled porous solids and its application to overthrust faulting. Geological Society of America Bulletin, v. 70, pp. 115-166.

Huiqi, L., McClay, K. R. and Powell, D. 1992. Physical models of thrust wedges. *In:* Thrust Tectonics (K. R. McClay, ed.), Chapman and Hall, London, UK, pp. 71-81.

Irish, E. J. W. 1965. Geology of the Rocky Mountain Foothills, Alberta (between latitudes 53°15' and 54°15'). Geological Survey of Canada, Memoir 334. 238 pages.

Jamison, W. R. 1987. Geometric analysis of fold development in overthrust terranes. Journal of Structural Geology, v. 9, pp. 207-219.

Jerziekiewicz, T. 1985. Stratigraphy of the Saunders Group in the central Alberta Foothills- a progress report. *In:* Current Research, Part B, Geological Survey of Canada, Paper 85-1B, pp. 247-258.

Jerziekiewicz, T. and McLean, J. R. 1980. Lithostratigraphical and sedimentological framework of coal-bearing Upper Cretaceous and Lower Tertiary strata, Coal Valley area, Central Alberta Foothills. Geological Survey of Canada, Paper 79-12, 47 pages.

Jones, P. B. 1971. Folded faults and sequence of thrusting in Alberta Foothills. American Association of Petroleum Geologists Bulletin, v. 55, pp. 292-306.

Jones, P. B. 1982. Oil and gas beneath east dipping underthrust faults, Alberta Foothills. *In:* Geologic studies of the Cordilleran Thrust Belt (R. B. Powers, ed.), Rocky Mountain Association of Geologists, pp. 61-74.

Jones, P. B. and Linsser, H. THRUSTBELT. IBM Computer program, Thrustbelt systems, Calgary, Alberta.

Jones, P. B., Schink, E. A. and Downey, M. E. 1992. Winchell Coulee, case history of an integrated structural-stratigraphic play using computer-balanced cross-sections. Bulletin of Canadian Petroleum Geology, v. 40, pp. 60-67.

Kilby, W. E. 1978. Structural geology of the coal-bearing and adjacent strata near Mountain Park, Alberta. Masters thesis, University of Alberta, Edmonton. 154 pages.

Kilby, W. E. and Charlesworth, H. K. 1980. Computerized downplunge projection and the analysis of low-angle thrust-faults in the Rocky Mountain Foothills of Alberta, Canada. Tectonophysics, v. 66, pp. 287-299.

Klapper, G. and Lane, H. R. 1988. Frasnian (Upper Devonian) conodont sequence at Luscar Mountain and Mount Haultain, Alberta Rocky Mountains. *In:* Devonian of the world, Vol. II (N. J. McMillian, A. F. Embry and D. J. Glass, eds.). Canadian Society of Petroleum Geologists, Memoir 14, pp. 469-478.

Klapstein, B. R. FLTBND. IBM computer program. Department of Geology, University of Alberta, Edmonton, Alberta.

Kligfield, R., Geiser, P. and Geiser, J. GEOSEC-10. Apple Lisa program. Geo-Logic Systems, Inc., New Paltz, N. Y.

Kryzca, A. A. W. 1959. The Nikanassin Formation at the type area, near Cadomin, Alberta. Masters thesis, University of Albera.

Langenberg, C. W. 1985. The geometry of folded and thrusted rocks in the Rocky Mountain Foothills near Grande Cache, Alberta. Canadian Journal of Earth Sciences, v. 22.

Langenberg, C. W. and Fietz, D. 1990. Geology of the Cadomin East (83F/3) map sheet. Alberta Research Council, Open File Report 1990-12.

Langenberg, C. W. and McMechan, M. E. 1985. Lower Cretaceous Luscar Group (revised) of the northern and north-central Foothills of Alberta. Bulletin of Canadian Petroleum Geology, v. 33, pp. 1-11.

Liu, S. and Dixon, J. M. 1991. Centrifuge modelling of thrust faulting: Structural variation along strike in fold-thrust belts. Tectonophysics, v. 188, pp. 39-62.

MacKay, B. R. 1929a. Mountain Park, Alberta; Geological Survey of Canada, Map 208A.

MacKay, B. R. 1929b. Cadomin, Alberta; Geological Survey of Canada, Map 209A.

MacKay, B. R. 1940a. Pembina Forks. Geological Survey of Canada preliminary geological Map 610A.

MacKay, B. R. 1940b. Grave Flats, Alberta. Geological Survey of Canada, Paper 40-15.

MacKay, B. R. 1943. Foothills belt of central Alberta; Geological Survey of Canada, Paper 43-3.

Mackenzie, W. S. 1965a. Upper Devonian carbonate mounds and lenses, vicinity of Mount MacKenzie, Alberta. *In:* International Symposium on the Devonian System, (D. H. Oswald, ed.). Alberta Society of Petroleum Geologists, Vol. II, pp. 409-420.

Mackenzie, W. S. 1965b. Upper Devonian carbonates of the Southesk-Cairn Complex and associated strata, eastern Rocky Mountains and Foothills, Alberta, Bulletin of Canadian Petroleum Geology, v. 13, pp. 457-481.

Mackenzie, W. S. 1969. Devonian Southesk-Cairn Carbonate Complex, Alberta. Geological Survey of Canada, Bulletin 184.

Macqueen, R. W. 1966. Mississippian stratigraphy and sedimentology at Cadomin *In:* Alberta. Edmonton Geological Society (ed), Eighth Annual Field Trip Guide Book, pages 39-59.

Macqueen, R. W. 1967. Stratigraphy of the Banff Formation and Lower Rundle Group (Mississippian), southwestern Alberta. Geological Survey of Canada Paper 67-47. 37 pages.

Marshak, S. and Engelder, T. 1985. Development of cleavage in limestones of a fold-thrust belt in eastern New York. Journal of Structural Geology, v. 7, pp. 345-359.

McClay, K. R. 1992. Glossary of thrust tectonics terms. *In:* Thrust Tectonics (K. R. McClay, ed.), Chapman & Hall, London, UK, pp. 419-433.

McDonough, M. R. and Simony, P. S. 1988. Structural evolution of basement gneisses and Hadrynian cover, Bulldog Creek area, Rocky Mountains, British Columbia. Canadian Journal of Earth Sciences, v. 25, pp. 1687-1702.

McEachran, D. B. 1985. Strain-graphics programs. Macintosh computer programs, Rockware, Inc., Denver, CO.

McLean, J. R. 1977. The Cadomin Formation: stratigraphy, sedimentology and tectonic implications. Bulletin of Candian Petroleum Geology, v. 25, pp. 792-897.

McLean, J. R. 1982. Lithostratigraphy of the Lower Cretaceous coal-bearing sequence, Foothills of Alberta. Geological Survey of Canada, Paper 80-29. 46 pages.

McMechan, M. E. 1985. Low-taper triangle-zone geometry: an interpretation for the Rocky Mountain Foothills, Pine Pass-Peace River area, British Columbia. Bulletin of Canadian Petroleum Geology, v. 33, pp. 31-38.

Mitra, G. and Elliott, D. 1979. Deformation of basement in the Blue Ridge and the development of the South Mountain Cleavage. In: The Caledonides in the U. S. A. (edited by Wones, D. R.). Dept. Geol. Sci. Virginia Tech. Mem., pp. 307-311.

Monger, J. W. H., Price, R. A., and Templeman-Kluit, D. J. 1982. Tectonic accretion and the origin of two major metamorphic and plutonic welts in the Canadian Cordillera. Geology, v. 16, pp. 70-75.

Mountjoy, E. W. 1960a. Structure and stratigraphy of the Miette and adjacent areas, eastern Jasper National Park, Alberta. Ph. D. thesis, University of Toronto. 234 pages.

Mountjoy, E. W. 1960b. Miette map-area. Geological Survey of Canada, Map 40-1959, scale 1: 63, 360.

Mountjoy, E. W. 1962. Mount Robson (southeast) map-area, Rocky Mountains of Alberta and British Columbia, 83E/SE. Geological Survey of Canada, Paper 61-31, 114 pages.

Mountjoy, E. W. 1965. Stratigraphy of the Devonian Miette Reef Complex and associated strata, eastern Jasper National Park, Alberta. Geological Survey of Canada, Bulletin 110.

Mountjoy, E. W. 1980a. Mount Robson, Alberta-British Columbia. Geological Survey of Canada Map 1499A, scale 1: 250, 000.

Mountjoy, E. W. 1980b. Some questions about the development of Upper Devonian buildups (reefs), western Canada. Bulletin of Canadian Petroleum Geology, v. 28, pp. 315-344.

Mountjoy, E. W. 1989. Miette reef complex (Frasnian), Jasper National Park, Alberta. *In:* Reefs, Canada and Adjacent areas (H. H. J. Geldsetzer, N. P. James and G. E. Tebbutt, eds.). Canadian Society of Petroleum Geologists, Memoir 13, pp. 497-505.

Mountjoy, E. W. 1992. Significance of rotated folds and thrust faults, Alberta Rocky Mountains. *In:* Structural Geology of Fold and Thrust Belts (G. Mitra and G. W. Fisher, eds.), John Hopkins University Press, pp. 207-223.

Mountjoy, E. W. and Aitken, J. D. 1978. Middle Cambrian Snake Indian Formation (New) Jasper region, Alberta. Bulletin of Canadian Petroleum Geology, v. 26, pp. 343-361.

Mountjoy, E. W. and Price, R. A. 1976. Geology, Medicine Lake, Alberta. Geological Survey of Canada Open file map 372, scale 1: 50, 000.

Mountjoy, E. W., Price, R. A and Lebel, D. 1992. Geology and structure cross-sections, Mountain Park, Alberta. Geological Survey of Canada map 1830A, NTS 83C/14, scale 1:50, 000.

Muecke, G. K. and Charlesworth, H. A. K. 1966. Jointing in folded Cardium Sandstones along Bow River, Alberta. Canadian Journal of Earth Sciences, v. 3, pp. 579-596.

Nabalek, J. 1985. Geometry and mechanism of faulting of the 1980 El Asnam Algeria earthquake from inversion of teleseismic body waves and comparison with field observations. Journal of Geophysical Research, v. 90, pp. 12713-12728.

O'Brien, C.A.F. (1960). The structural geology of the Boule and Bosche Ranges in the Canadian Rocky Mountains. Quarterly Journal of the Geological Society of London, v. 116, pp. 409-436.

Okulitch, A. V. 1984. The role of the Shuswap Metamorphic Complex in Cordilleran tectonism: a review. Canadian Journal of Earth Sciences, v. 21, pp. 1171-1193.

Ollerenshaw, N. C. (Compiler). 1978. Geology, Calgary West of Fifth Meridian, Alberta and British Columbia. Geological Survey of Canada Map 1457A. (scale 1: 250, 000 with structure sections).

Platt, J.P. 1986. Dynamics of orogenic wedges and the uplift of high-pressure metamorphic rocks. Geological Society of America Bulletin, v. 97, p. 1037-1053.

Powell, C. McA. 1974. Timing of slaty cleavage during folding of Precambrian rocks, northwest Tasmania. Geological Society of America Bulletin, v. 85, pp. 1043-1060.

Powell, C. McA. 1979. A morphological classification of rock cleavage. Tectonophysics, v. 58, pp. 21-34.

Price, R. A. 1967. The tectonic significance of mesoscopic subfabrics in the southern Rocky Mountains of Alberta and British Columbia. Canadian Journal of Earth Sciences, v. 4, pp. 39-70.

Price, R. A. 1981. The Cordilleran foreland thrust and fold belt in the southern Rocky Mountains. *In* : Thrust and nappe tectonics (McClay, K. and Price, N. J., eds.). Geological Society of London, Special Paper no. 9, pp. 427-448.

Price, R. A. 1986. The southeastern Canadian Cordillera: thrust faulting, tectonic wedging, and delamination of the lithosphere. Journal of Structural Geology, v. 8, pp. 239-254.

Price, R. A. and Fermor, P. R. 1985. Structure section of the Cordilleran foreland thrust and fold belt west of Calgary, Alberta. Geological Survey of Canada Paper 84-14.

Price, R. A. and Mountjoy, E. W. 1970. Geologic structure of the Canadian Rocky Mountains between Bow and Athabasca Rivers- a progress report. *In:* Structure of the south Canadian Cordillera (J. O. Wheeler, ed.), Geological Association of Canada, Special Paper 6, pp. 7-25.

Price, R. A., Stott, D. F., Campbell, R. B., Mountjoy, E. W. and Ollerenshaw, N. C. 1977. Athabasca River. Geological Survey of Canada, Geological Atlas Series, Map 1339A, Scale 1: 1, 000, 000.

Pugh, D. C. 1971. Subsurface Cambrian stratigraphy in southern and central Alberta. Geological Survey of Canada, Paper 70-10.

Ramberg, 1981. Gravity deformation and the Earth's crust (second edition): London, Academic Press, 452 pages.

Ramsay, J. G. 1967. *Folding and Fracturing of Rocks*. McGraw-Hill, New York, 568 pages.

Ramsay, J. G. 1980. Shear zone geometry: a review. Journal of Structural Geology, v. 2, pp. 83-99.

Ramsay, J. G. and Huber, M. I. 1983. *The techniques of modern structural geology. Volume 1: Strain analysis*. Academic Press Inc., London, 307 pages.

Read, P. B. and Brown, R. L. 1981. Columbia River fault zone: southeastern margin of the Shuswap and Monashee complexes, southern British Columbia. Canadian Journal of Earth Sciences, v. 18, pp. 1127-1145.

Reks, I. J. and Grey, D. R. Strain patterns and shortening in a folded thrust sheet: an example from the southern Appalachians. Tectonophysics, v. 93, pp. 99-128.

Rich, J. L. 1934. Mechanics of low-angle overthrust faulting as illustrated by Cumberland thrust block, Virginia, Kentucky and Tennessee. American Association of Petroleum Geologists Bulletin, v. 1, pp. 1584-1596.

Sanderson, D. A. and Spratt, D. A. 1992. Triangle zone and displacement transfer structures in the Eastern Front Ranges, Southern Canadian Rocky Mountains. American Association of Petroleum Geologists Bulletin, v. 76, pp. 828-839.

Sanderson, D. J. 1982. Models of strain variation in nappes and thrust sheets: a review. Tectonophysics, v. 88, pp. 201-224.

Sanderson, J. O. G. 1939. Geology of the Brazeau area. Canadian Institute of Mining and Metallurgy, Transactions, v. XLII, pp. 429-442.

Scholtz, C. H., Aviles, C. A. and Wesousky, S. G. 1986. Scaling differences between large interplate and intraplate earthquakes. Bull. seism. Soc. Am. v. 76, pp. 65-70.

Schultheis, N. H. and Mountjoy, E. W. 1978. Cadomin conglomerate of western Alberta- a result of Early Cretaceous uplift in the Main Ranges. Bulletin of Canadian Petroleum Geology, v. 26, pp. 297-342.

Schwartz, D. P. and Coopersmith, K. J. 1984. Fault behavior and characteristic earthquakes: examples from the Wasatch and San Andreas fault zones. Journal of Geophysical Research, v. 89, pp. 5681-5698.

Scott, J. C. 1951. Folded faults in Rocky Mountain Foothills of Alberta, Canada. American Association of Petroleum Geologists, v. 35, pp. 2316-2347.

Seeber, L. Armbruster, J. G. and Quittmayer, R. C. 1981. Seismicity and continental subduction in the Himalayan arc. American Geophysical Union Geodynamic Series 3, pp. 215-242.

Shields, M. J. and Geldsetzer, H. H. J. 1992. The MacKenzie margin, Southesk-Cairn carbonate complex: depositional history, stratal geometry and comparison with

other Late Devonian platform-margins. Bulletin of Canadian Petroleum Geology, v. 40, pp. 274-293.

Siddans, A.W.B. 1977. The development of slaty cleavage in a part of the French Alps. Tectonophysics v. 39, p. 533-557.

Simony, P. S., Ghent, E. D., Craw, D., Mitchell, W. and Robbins, D. B. 1980. Structural and metamorphic evolution of northeast flank of Shuswap complex, southern Canoe River area, British Columbia. *In:* Cordilleran Metamorphic Core Complexes (Crittenden, M. D., Jr., Coney, P. J. and Davis, G. H., eds), Geological Society of America Memoir, 153, pp. 445-461.

Skuce, A. G., Goody, N. P., and Maloney, J. 1992. Passive-roof duplexes under the Rocky Mountain foreland basin, Alberta. American Association of Petroleum Geologists, v. 76, pp. 67-80.

Spratt, D. A., Lawton, D. C. and MacKay, P. A. 1993. The Triangle Zone and Turner Valley Structure west of Calgary. Geological Association of Canada/ Mineralogical Association of Canada Annual Meeting, Field Trip Guidebook A1.

Stott, D. F. 1963. The Cretaceous Alberta Group and equivalent rocks, Rocky Mountain Foothills, Alberta. Geological Survey of Canada Memoir 317.

Stott, D. F. 1984. Cretaceous sequences of the Foothills of the Canadian Rocky Mountains. In The Mesozoic of Middle North America, D. F. Stott and D. J. Grass ed., Canadian Society of Petroleum Geologists Memoir 9, pp. 85-107.

Stringer, P. 1975. Acadian slaty cleavage noncoplanar with fold axial surfaces in the northern Appalachians. Canadian Journal of Earth Sciences, v. 12, pp. 949-961.

Stringer, P. and Treagus, J. E. 1980. Non-coaxial planar S1 cleavage in the Hawick Rocks of the Galloway area, Southern Uplands, Scotland. Journal of Structural Geology, v. 2, pp. 317-332.

Suppe, J. 1985. *Principles of Structural Geology*. Prentice-Hall, Englewood Cliffs, New Jersey, USA, 537 pages.

Thompson, R. I. 1979. A structural interpretation across part of the northern Rocky Mountains, British Columbia, Canada. Canadian Journal of Earth Sciences, v. 16, pp. 1228-1241.

Thompson, R. I. 1981. The nature and significance of large 'blind' thrusts within the northern Rocky Mountains of Canada. *In:* Thrust and Nappe Tectonics (McClay, K. R. and Price, N. J., eds.), Geological Society of London, Special Publication 9, pp. 449-462.

Turner, F. J. and Weiss, L. E. 1963. *Structural Analysis of Metamorphic Tectonites*. McGraw-Hill, New York, 545 pages.

Tysdal, R. G. 1986. Thrust faults and back thrusts in Madison Range of southwestern Montana foreland. American Association of Petroleum Geologists Bulletin, v. 70, pp. 360-376.

Underschultz, J. R. and Erdmer, P. 1991. Tectonic loading in the Canadian Cordillera as recorded by mass accumulation in the foreland basin. Tectonics, v. 10, pp. 367-380.

Usdansky, S. and Groshong, R. H. THRUSTRAMP. IBM and Mac computer program. Wilkerson and Associates, Champaign, IL, U. S. A.

Walsh, J. J. and Watterson, J. 1988. Analysis of the relationship between displacements and dimensions of faults. Journal of Structural Geology, v. 10, pp. 239-247.

Wanless, H. 1979. Limestone response to stress: pressure solution and dolomitization. Journal of Sedimentary Petrology, v. 49, pp. 437-462.

Webb, J. B. 1955. Cross-section of Foothills belt east of Jasper Park. Alberta Society of Petroleum Geologists 5th Annual Field Conference Guidebook, p. 130a.

Weissenberger, J. A. W. and McIlreath, I. A. 1989. Southesk-Cairn reef complex, Upper Devonian of Alberta. *In:* Reefs, Canada and Adjacent areas (H. H. J. Geldsetzer, N. P. James and G. E. Tebbutt, eds.). Canadian Society of Petroleum Geologists, Memoir 13, pp. 535-542.

Wheeler, J. O. and McFeely, P. (compilers). 1992. Terrane Assemblage map of the Canadian Cordillera and adjacent parts of the United States. Geological Survey of Canada, Map 1712A. Scale 1: 2, 000, 000.

Wilkerson, M. S. and Usdansky, S. I. FAULT. IBM and Mac computer program. Wilkerson and Associates, Champaign, IL, U. S. A.

Williams, G. and Chapman, T. 1983. Strains developed in the hangingwalls of thrusts due to their slip/propagation rate: a dislocation model. Journal of Structural Geology, v. 5, pp. 563-571.

Wojtal, S. 1986. Deformation within foreland thrust sheets by populations of minor faults. Journal of Structural Geology, v. 8, pp. 341-360.

Zhao, W.-L., Davis, D., Dahlen, F.A. and Suppe. J. 1986. The origin of convex accretionary wedges; Evidence from Barbados. Journal Geophysical Research, v. 91, 10,246-10,258.

Ziegler, P. A. 1969. The development of sedimentary basins in Western and Arctic Canada. Alberta Society of Petroleum Geologists, 89 pages.

Illustrations

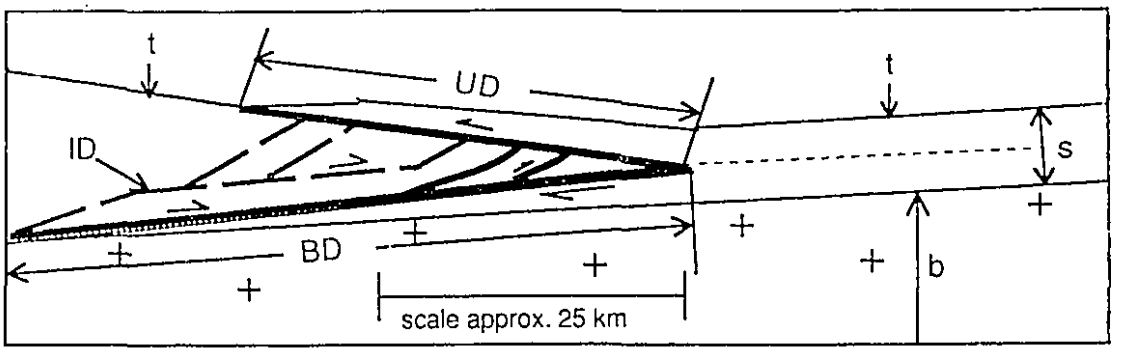

Figure 2. 1: Structural positions of observed décollements in the Cordilleran foreland thrust belt: BD: basal décollement; UD: upper décollement; ID: internal décollement; other surfaces and volumes include: t: topographic surface; b: crystalline basement; s: sedimentary stratigraphic pile.

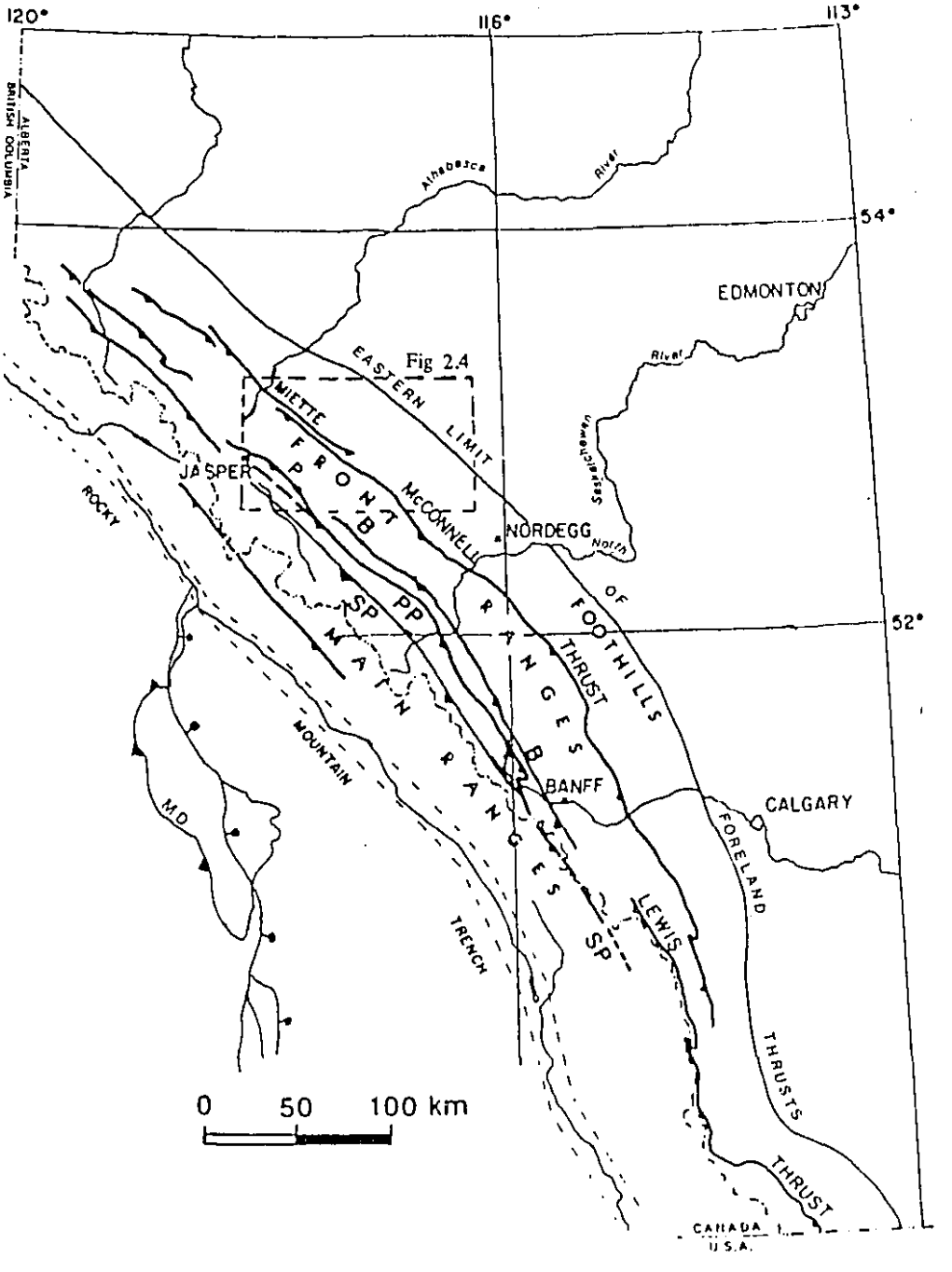

Figure 2. 2: Regional tectonic map of western Alberta and adjoining British Columbia. P - Pyramid thrust, B - Bourgeau thrust, PP - Pipestone thrust, SP - Simpson Pass thrust, MD - Monashee Décollement. Dashed frame indicates location of the Athabasca-Brazeau region and Fig. 2. 4. Adapted from Mountjoy, 1992 and Brown *et al.*, 1992.

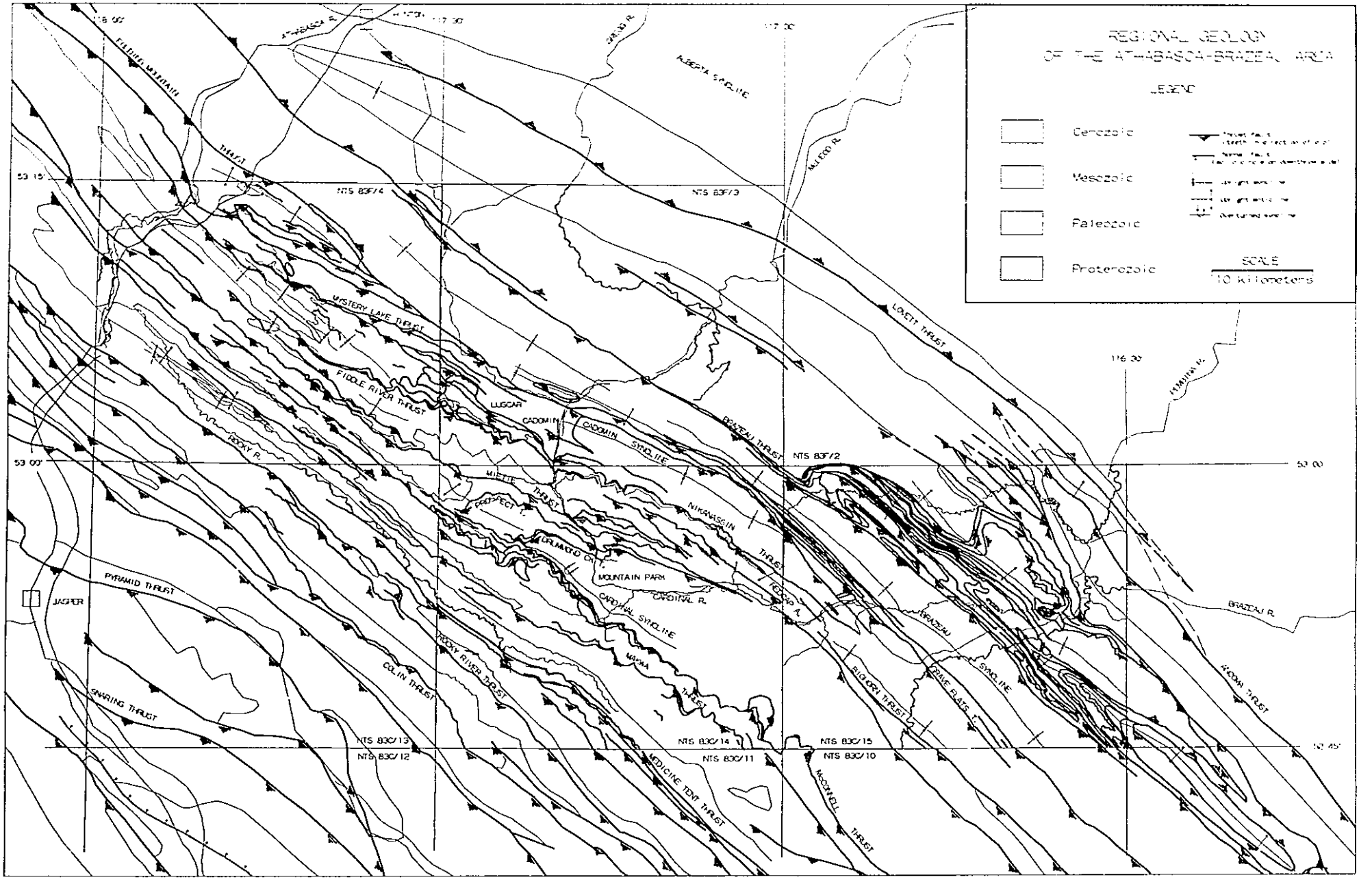
REGIONAL GEOLOGY
OF THE ATHABASCA-BRAZEAU AREA
LEGEND
Cenozoic
Mesozoic
Paleozoic
Proterozoic
SCALE
10 kilometers
ATHABASCA R.
ALBERTA SYNCLINE
MIETTE R.
FITZHUGH MOUNTAIN
THRUST
NTS 83F/4
NTS 83F/3
MYSTERY LAKE THRUST
FIDDLE RIVER THRUST
LUSCAR
CADOMIN
CADOMIN SYNCLINE
ROCKY R.
LOVETT THRUST
RESTAL THRUST
NTS 83F/2
MIETTE THRUST
CRESCENT
NIKANASSIN
THRUST
CHUNGO CR.
MOUNTAIN PARK
CAPITAL R.
CAPITAL SYNCLINE
MAYNA
THRUST
PYRAMID THRUST
JASPER
ROCKY RIVER THRUST
COLLIN THRUST
SNARING THRUST
NTS 83O/13
NTS 83O/12
NTS 83O/14
NTS 83O/11
NTS 83O/15
NTS 83O/10
MEDICINE TENT THRUST
MACDONELL THRUST
BIGELOW THRUST
PEAK FLATS
SYNCLINE
BRAZEAU
BRAZEAU R.
HOOKE THRUST
53 15'
53 00'
52 45'
116 30'
117 30'

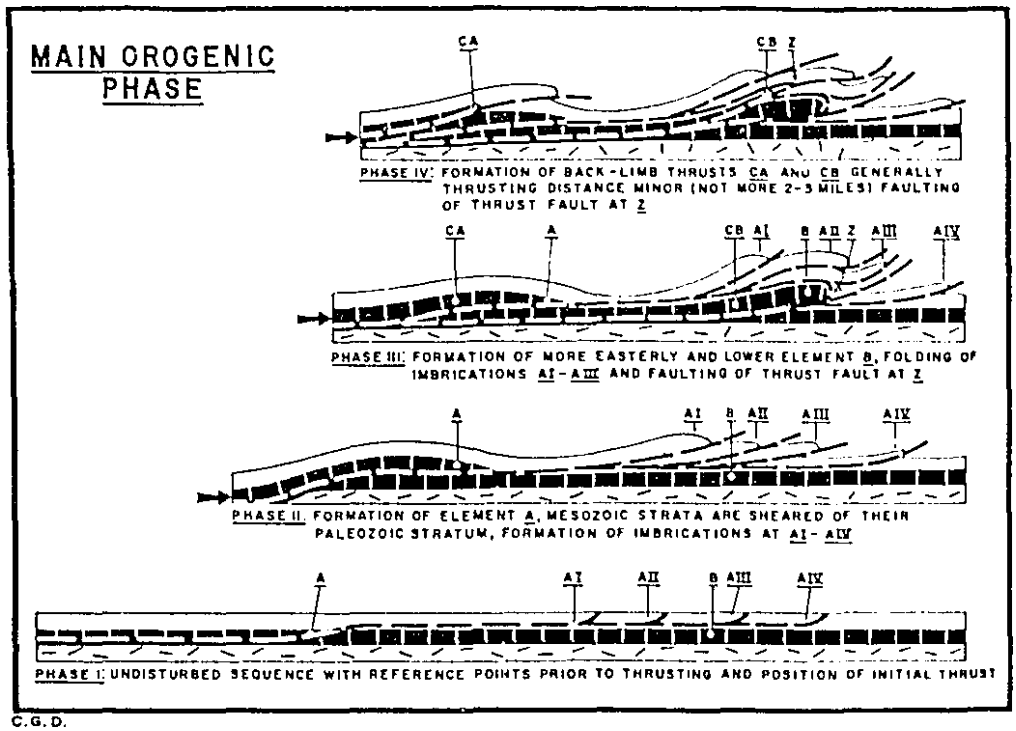

Figure 2. 5: Bally et al (1966, Figure 13, p. 370) model of evolution of the Mesozoic-Paleozoic décollement.

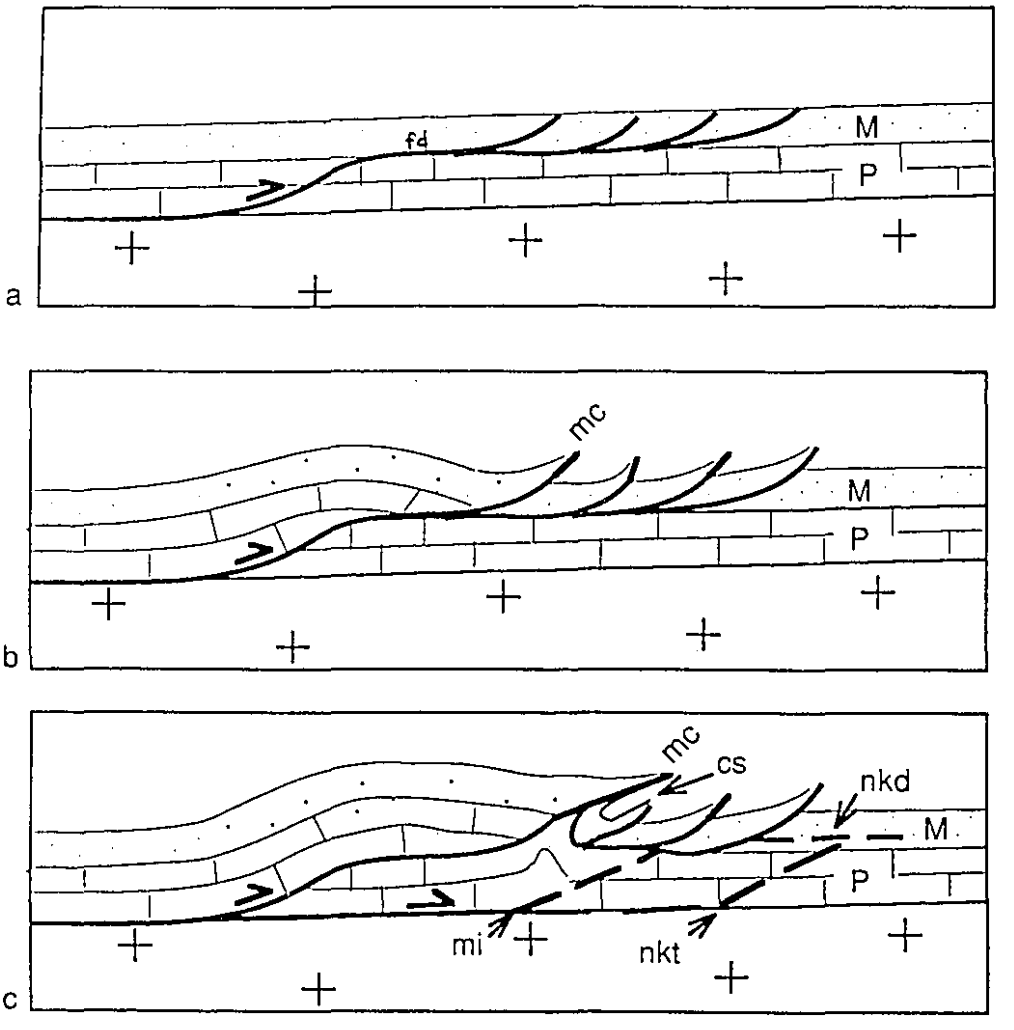

Figure 2. 7: Schematic kinematic model of the Fernie décollement (fd), Mountain Park thrust network leading to the formation of the Nikanassin décollement (nkd). (a): location of the future Fernie décollement; (b) motion along the Fernie décollement permits early motion of the McConnell thrust (mc) and the formation of the Mountain Park thrust network in front (right); (c) renewed motion along the McConnell thrust caused the folding of the Fernie décollement in the Cardinal syncline (cs); the Fernie décollement is then abandoned and a new basal décollement is formed, from which the Miette (mi) and Nikanassin (nkt) thrusts emanate. The upper segment of these faults follow a flat within the Nikanassin Formation, the Nikanassin décollement. M: Mesosoic clastic rocks; P: Paleozoic platformal carbonates.

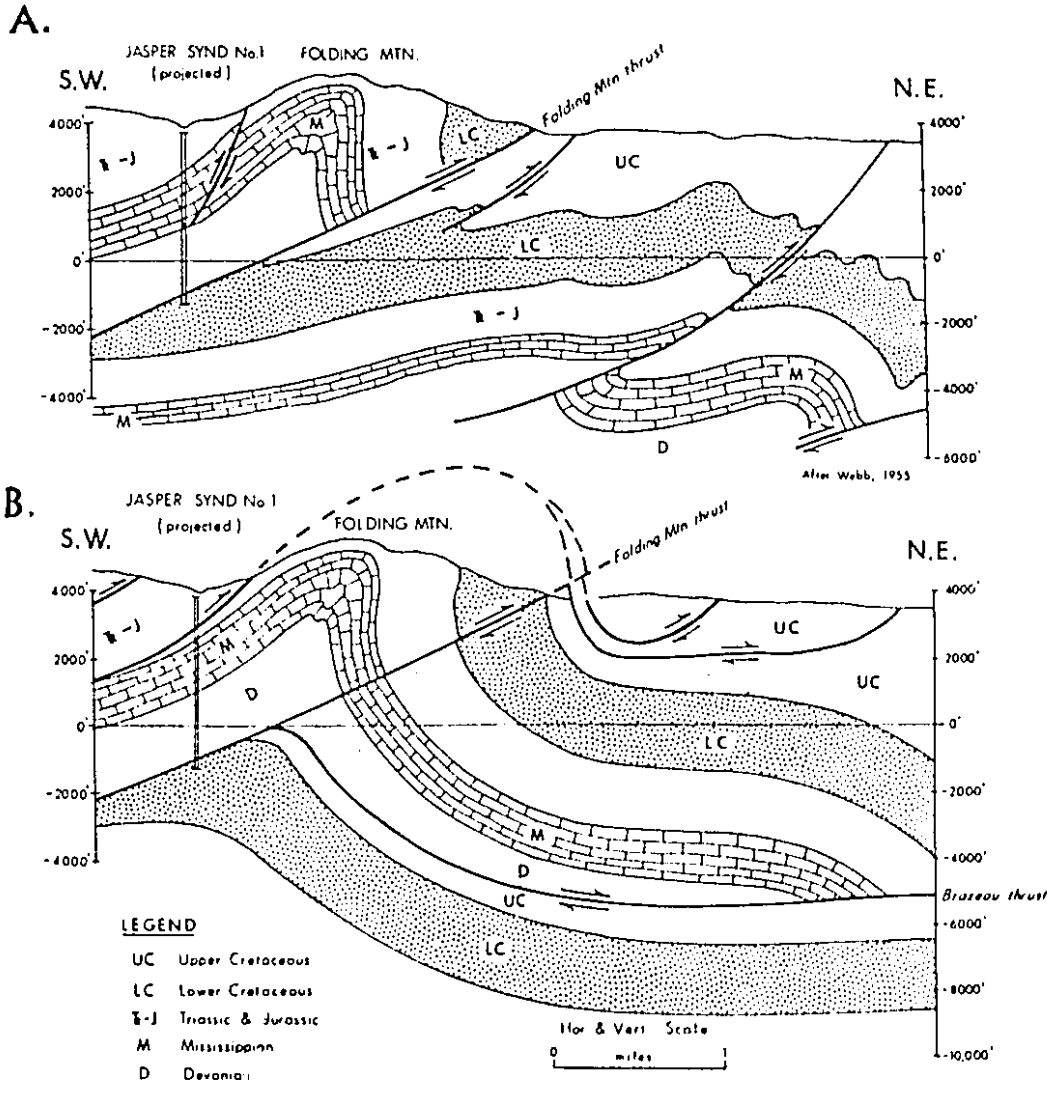

Figure 2. 8 : Various interpretations of the Folding Mountain structure

Figure 2. 8 (A): Simple thrust fault -Webb (1955) and Mountjoy (1960a, b)-(reproduced from Jones (1971).

Figure 2. 8 (B): Folded thrust fault interpretation- Jones, 1971-(reproduced from Jones (1971).

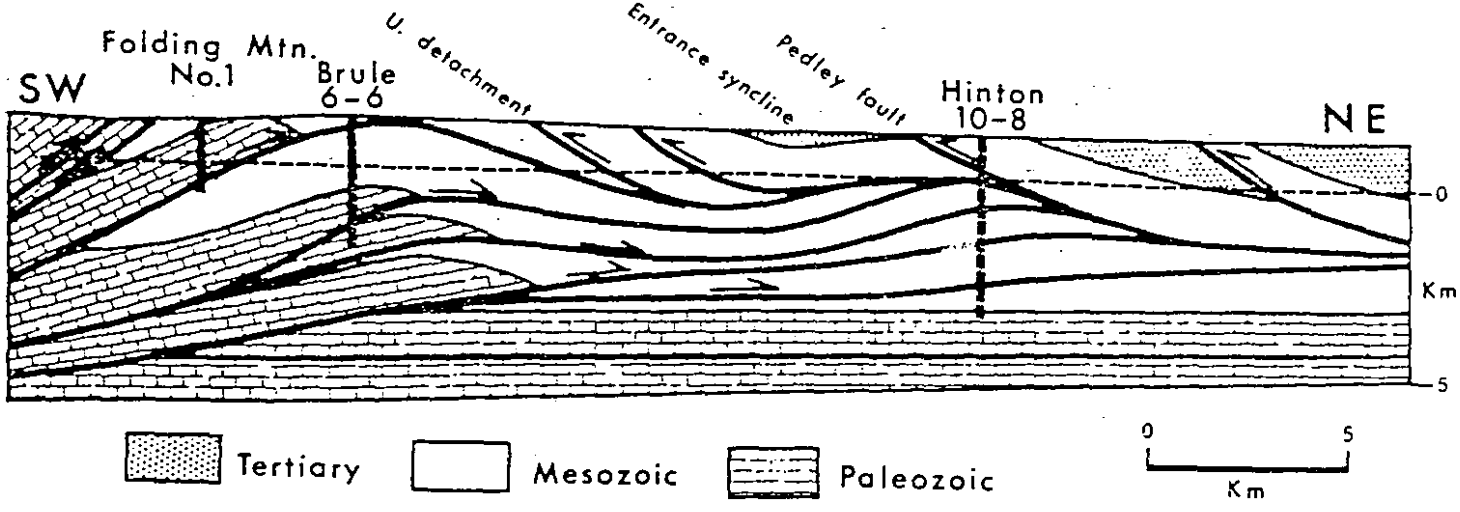

Figure 2. 8 (C): Interpretation of the Folding Mountain structure. Folded thrusts and blind thrusts branching with an upper detachment interpretation from Ziegler (1969) and Jones (1982)- (reproduced from Jones (1982).

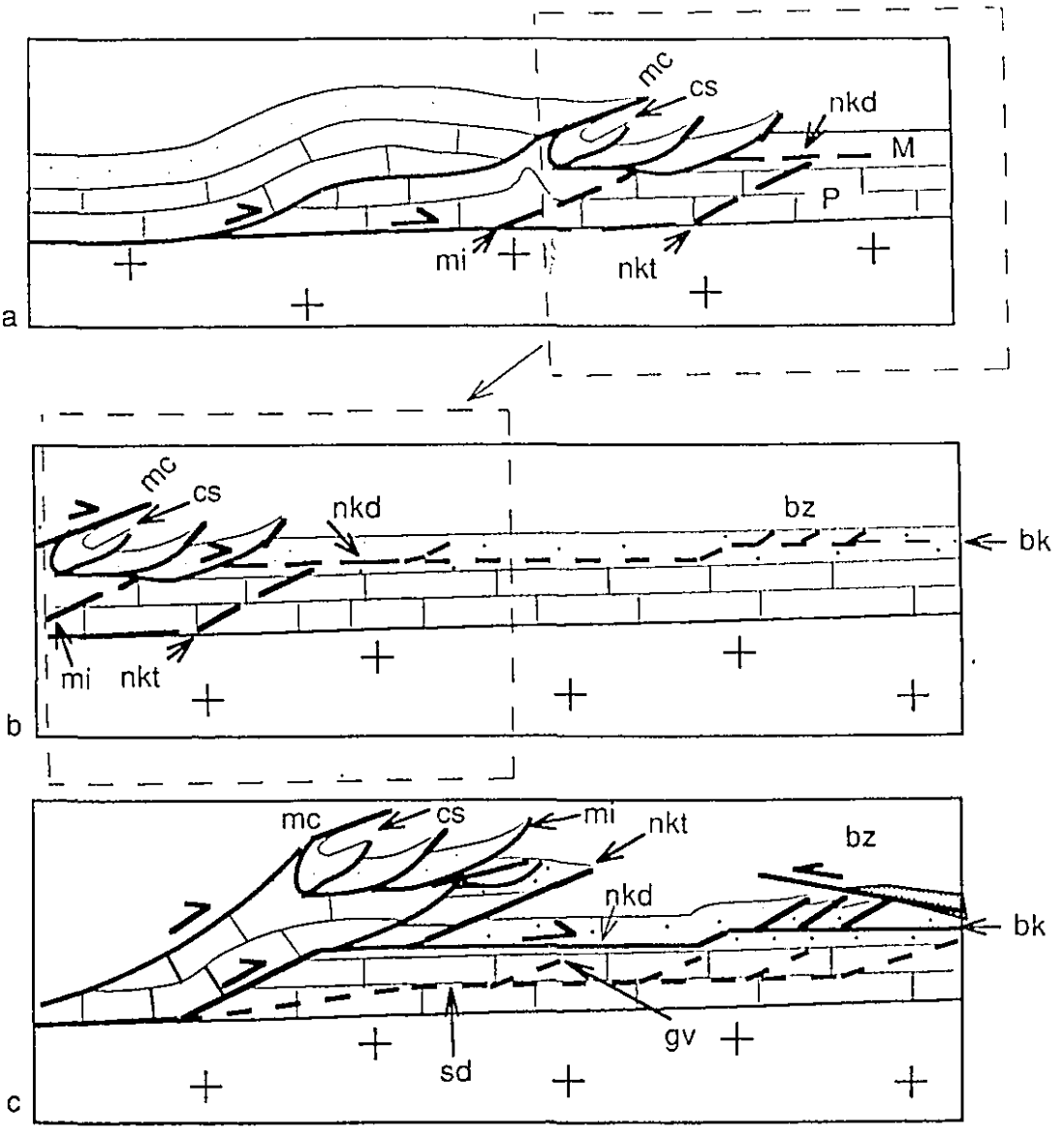

Figure 2. 9: Kinematic model of evolution of the Foothills thrust belt in the Brazeau area. (a) Location of future Nikanassin décollement (nkd) after the formation of the Fernie décollement (i. e. see Fig. 2. 7). (b) Location of future Blackstone décollement (bk) and Brazeau thrust network (bz) in front of the propagating Nikanassin décollement. (c) Motion along the Nikanassin décollement first allows for motion of the Miette thrust (mi) and intersection with the Fernie décollement, secondly motion on the Nikanassin thrust (nkt), and thirdly the formation of the Brazeau thrust network. The development of the upper décollement (UD) causes the eventual abandonment of the Nikanassin décollement and the shift to a new basal décollement along the Sassenach Formation (sd). Motion along the Sassenach décollement eventually led to cross-cutting of the Nikanasin décollement (nkd) by thrusts such as the Grave Flats thrust (gv) and the development of the Folding Mountain-Luscar duplex. This final deformation event leads to the structural geometry similar to Section A-A' (Fig. 2. 6).

Figure 2. 10 (next page) : Schematic model of evolution of the Cordilleran orogenic wedge in the foreland thrust belt. (a) The rise of the orogenic wedge leads to the formation of a foreland basin beginning in middle Jurassic. α is the dip of the topographic slope of the wedge, β is the dip of the basal décollement. (b) erosion of the orogenic wedge leads to molasse deposition over the toe of the orogenic wedge. Further advancement of the wedge will cause the formation of the intercutaneous wedge under the upper décollement represented by the plane of deposition. (c) Emplacement of the intercutaneous wedge leads to increase friction along the basal and upper décollement surfaces and a consequent increase in critical taper. The subsequent internal deformation will cause an isostatic response to the increased wedge weight thus increasing of β. These combined factors will lead to abandonment of the older basal décollement and downward shift to a new basal décollement lower in the stratigraphic pile. (d) The propagation of the new basal décollement is gradual and is accomplished by imbricate faults propagating sequentially (1→2→3), sometimes through the older basal décollement and overlying wedge.

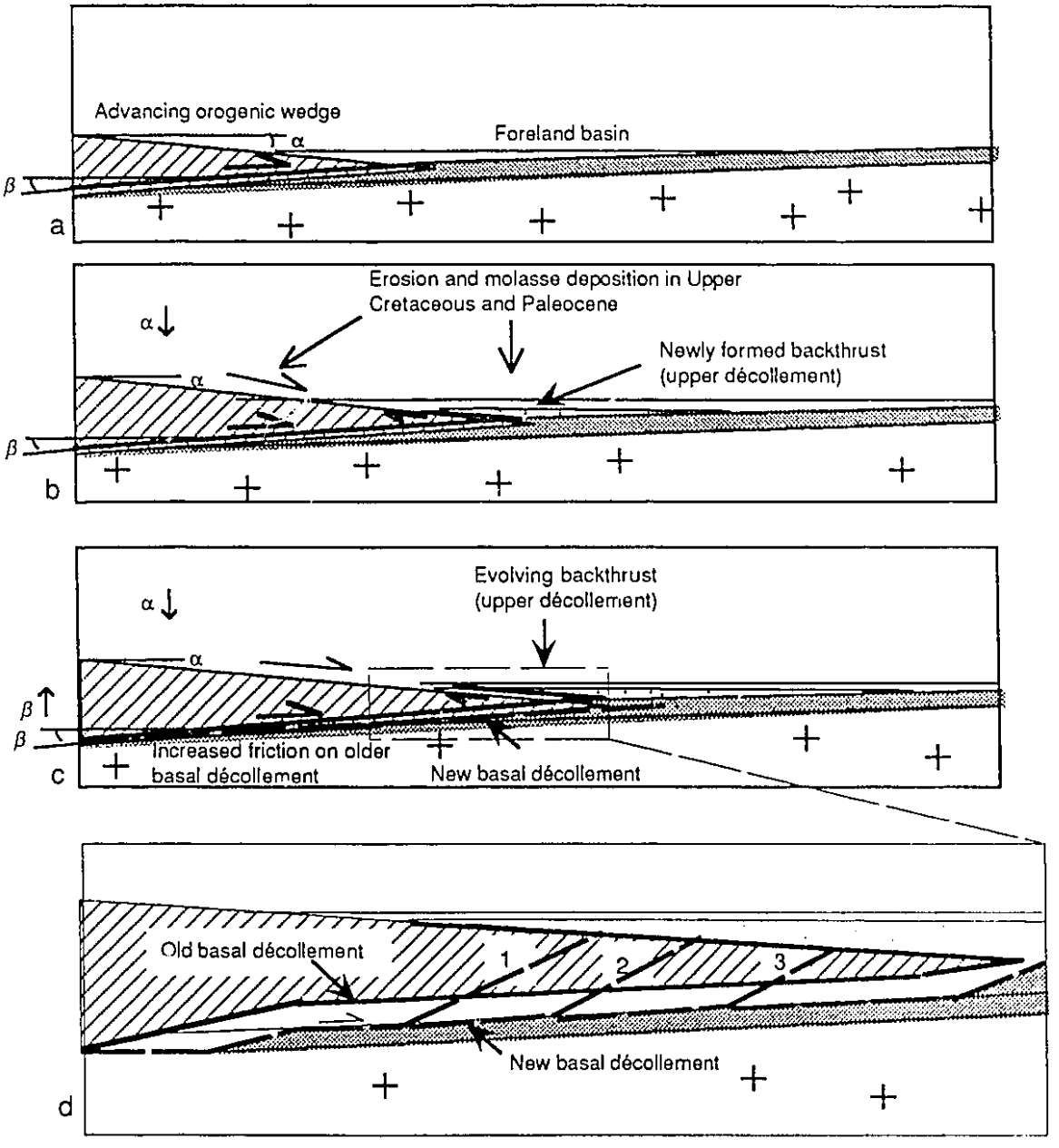
Advancing orogenic wedge
Foreland basin
α
β
a
Erosion and molasse deposition in Upper Cretaceous and Paleocene
Newly formed backthrust (upper décollement)
b
Evolving backthrust (upper décollement)
Increased friction on older basal décollement
New basal décollement
c
Old basal décollement
1
2
3
New basal décollement
d
Orogenic wedge of accreted strata
Upper Cretaceous and Paleocene molasse
Undisturbed Paleozoic and Mesozoic strata
Precambrian crystalline basement

Figure 2.10

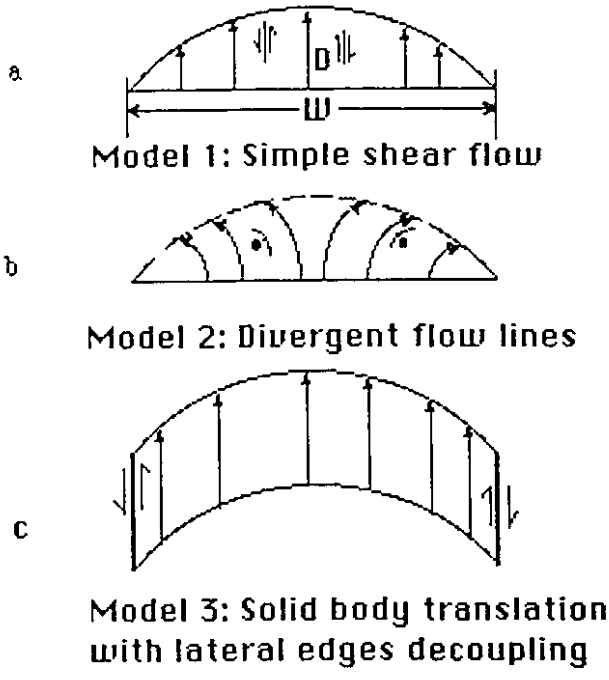

Figure 3. 1 (a-c): Comparison between various possibilities of simple models of kinematic patterns leading to a bow shape of a thrust fault in map view. These models neglect the effect of lateral thrust propagation. W is the thrust width measured perpendicular to the line of maximum displacement (D) of the thrust fault (see Walsh and Watterson, 1988, Fig. 1) . Here D is always considered to be in the center of W.

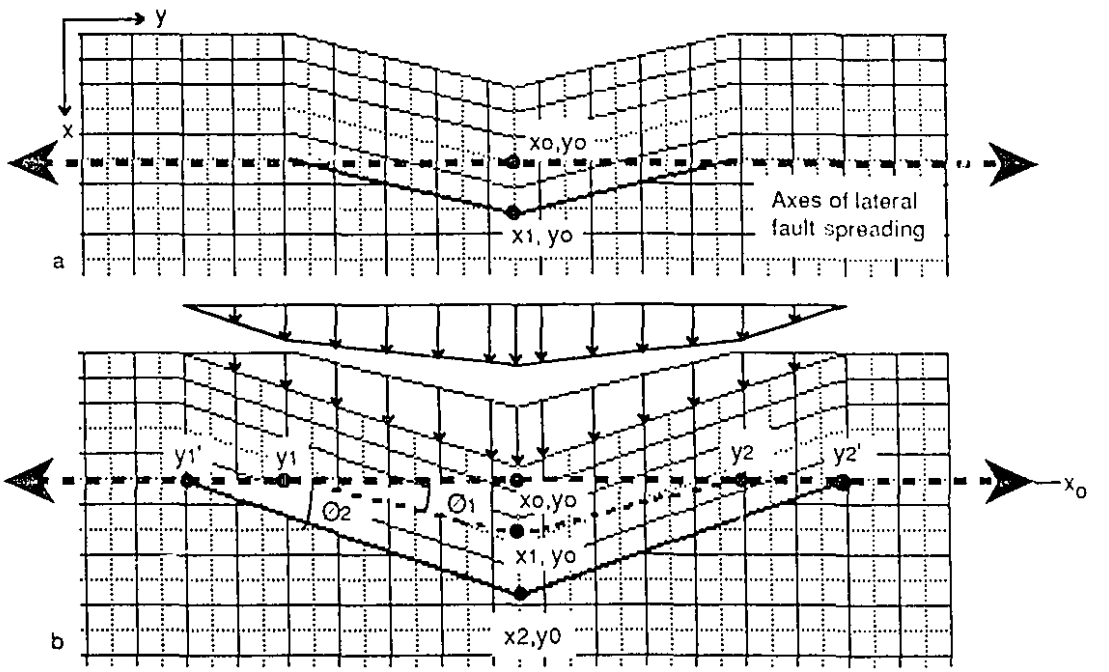

Figure 3. 2: The spreading simple shear deformation mechanism during thrust fault propagation.

Figure 3. 2(a): Initial nucleation point and first fault slip increment. x_0y_0, the location of the fault nucleation point; x_1y_0, location of the frontal thrust tip after the first slip increment; x_0y_1 and x_0y_2, location of the left and right lateral thrust tips after the first increment. The axes of lateral fault spreading control the location of future left and right thrust tips. The calculated location of the frontal thrust tip and the location of the lateral thrust tips control the shape of the fault, and consequent hanging wall deformation. The first increment of fault slip applies two symmetrical simple shear deformations on the hanging wall of the thrust, dextral on the compartment left of y_0, sinistral on the right one.

Figure 3. 2(b): The spreading simple shear mechanism controls each increment of fault slip. x_0, y_1 and x_0, y_2 , position of fault lateral tips before slip increment; x_0, y_1' and x_0, y_2' new positions of fault lateral tip; $\emptyset_1$ and $\emptyset_2$: angle between the axis of lateral fault spreading and the frontal thrust center, before and after slip increment. Arrows in the upper part of the figure show the variation in value of the vectors of incremental slip. The rate of incremental deformation is higher between the old and the new lateral thrust tips because the fault is assumed to show a linear decrease in displacement from its frontal center point to its lateral tips.

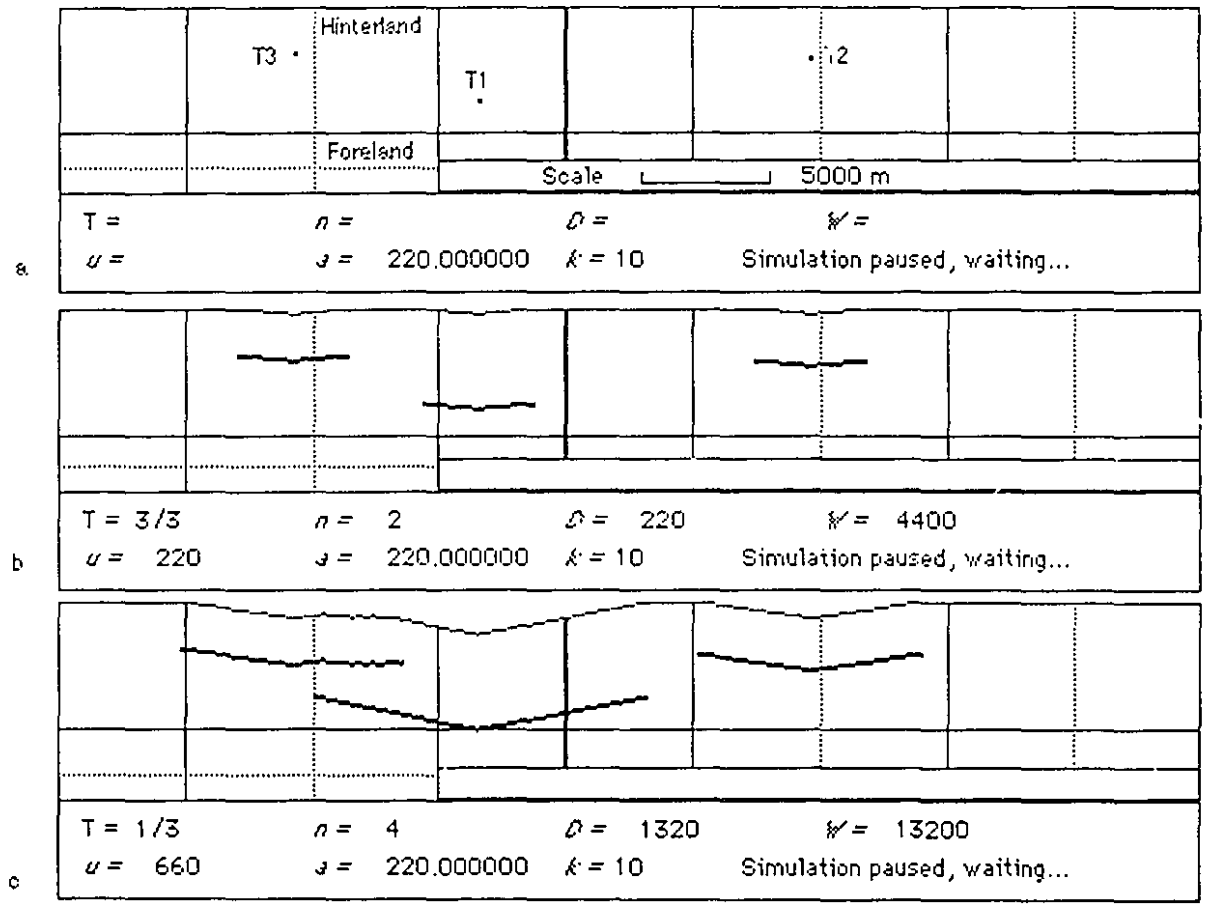

Figure 3. 3: Example of a THREE THRUSTS simulation. T1 to T3 are three thrusts ordered by their position relative to the foreland (Fig. 3 (a)); T is the currently active thrust; a is the arithmetical growth factor (set by the user); k is the rheological constant (also set by the user); n , current number of slip events of T; D , maximum displacement of T; W , total width of T; u , current incremental slip. D, W, u and a are in meters. The thick vertical line represents the location of the schematic cross-section drawn on the extreme left. The simulations are scale-dependent. In all figures, the foreland is at the bottom.

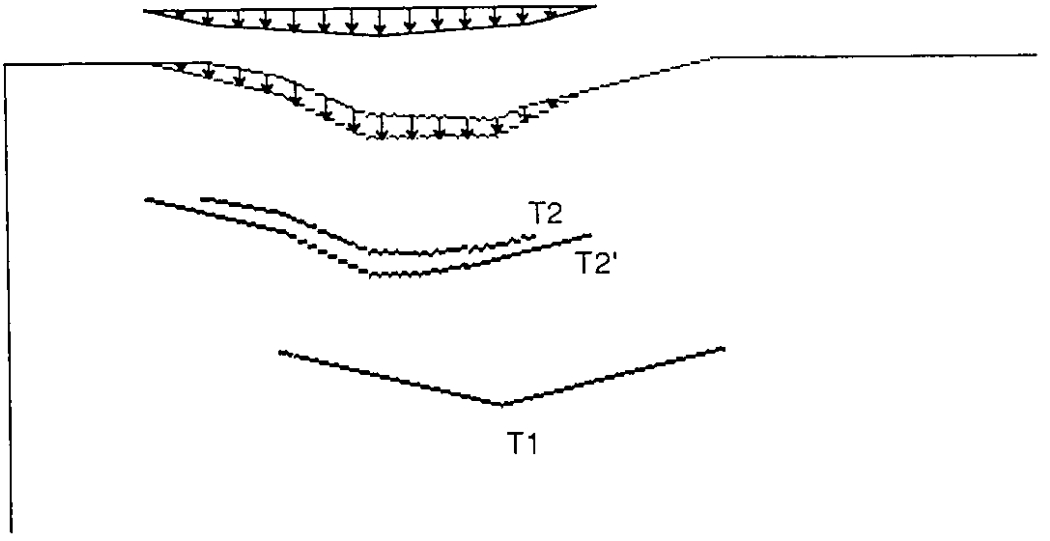

Figure 3. 4: Example of vectorial addition of the incremental displacement on a non-rectilinear thrust. After being subject to asymmetrical layer-parallel shear strain by T1, T2 has been deformed. From its new position, T2 advances to T2' through spreading simple shear. The distribution of the incremental displacement in the hanging wall of T2' (shown by the displacement vectors in the upper part of the figure) conforms to the spreading simple shear mechanism and is identical to the one of a rectilinear thrust (see Fig. 3. 2).

Figure 3. 5: Special geometric case where one tip of a hinterland thrust (T3) propagates in front of one tip of a foreland thrust. Three thrusts initially ranked T1 to T3, from their position relative to the foreland (5a) propagate to a new position on Fig. 3. 5b. After incremental layer-parallel shear strain by T1 on T3, T2's left lateral tip becomes situated in a more hinterland position than T3 right lateral tip (5b). Eventually, after more lateral propagation from its position on Fig. 3. 5c, T3 will become a footwall fault of T2. In turn, the left part of T2 will be carried piggyback by both T1 and T3. In a natural setting, this phenomenon is a geometrical necessity but in the case of a computer simulation, a particular algorithm in the program needs to handle the geometric switch between T2 and T3 so that T3 does not cut through T2 while propagating. Rather T3 will continue to propagate underneath T2 and merge with T2 to form a duplex where T2 will be carried piggyback.

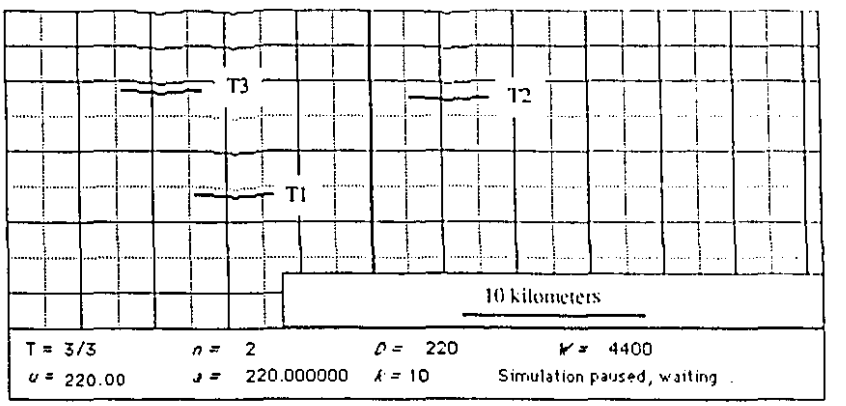

5a

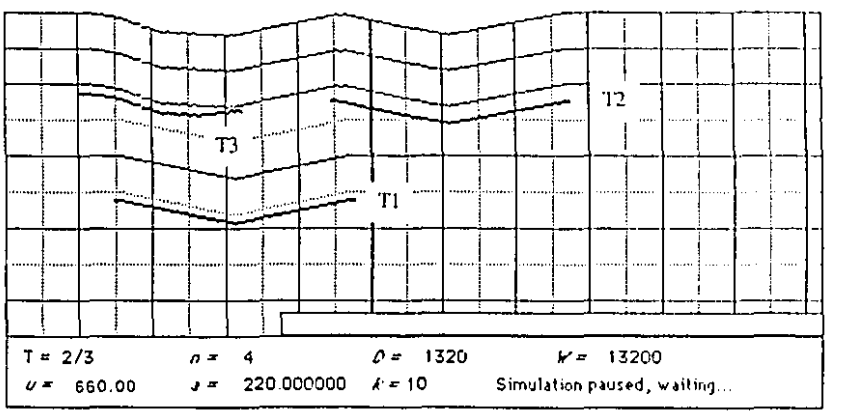

5b

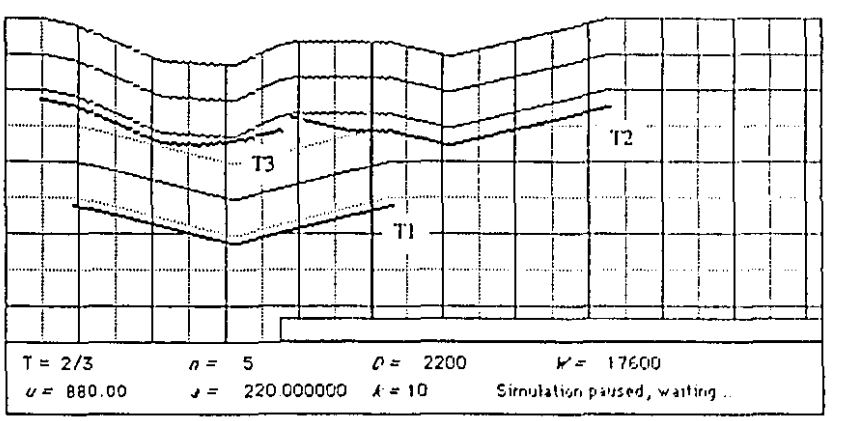

5c

Figure 3.5

Figure 3. 6: Comparison of the influence of the sequence of thrusting on the final geometry of a thrust zone. Three sequences of thrusting are represented, each starting with the same location for the nucleation points of thrusts T1 and T2, slip parameters and scale, and ending with equal numbers of slip events for each fault (N=11). Figure 3. 6(a) sequence represents a case with the hinterland T2 reaching its full width before T1 starts to form. Figure 3. 6(b) shows the opposite case. Point X on Fig. 3.6 (b2) shows the location of the initial branch point between T2 and T1. Figure 3. 6(c) represents a case of synchronous thrusting where T1 and T2 slip alternatively until N = 11. The geometries of the simulated thrust belts at the end are sharply different although equivalent shortening distributions are observed for the three cases at the back of each thrust belt (top of each graph, (a3), (b3) and (c3)). BP, branch point between the two thrust; BL, branch line; T (shaded area), torn part of T1 by the propagation of T2.

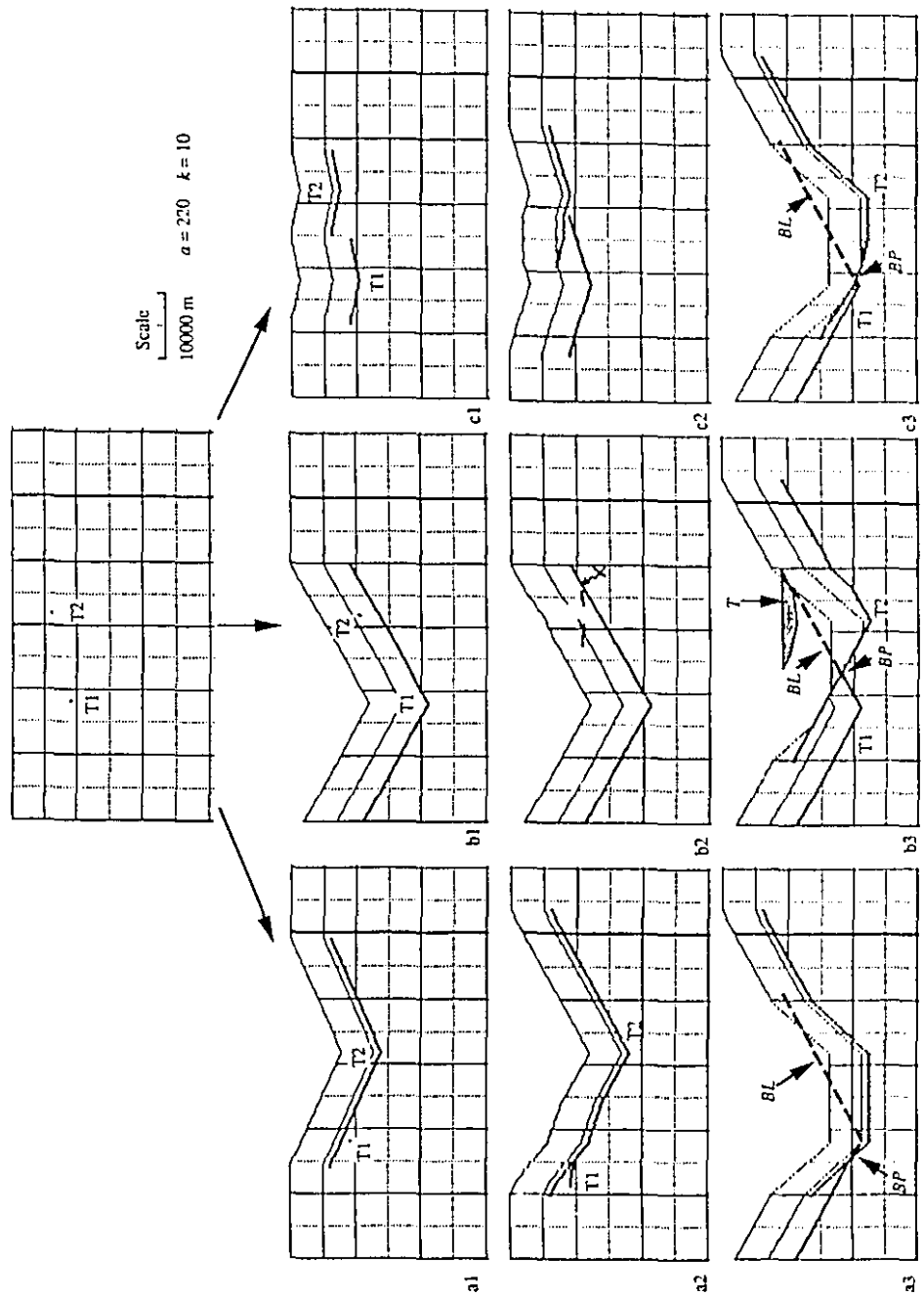

Figure 3.6

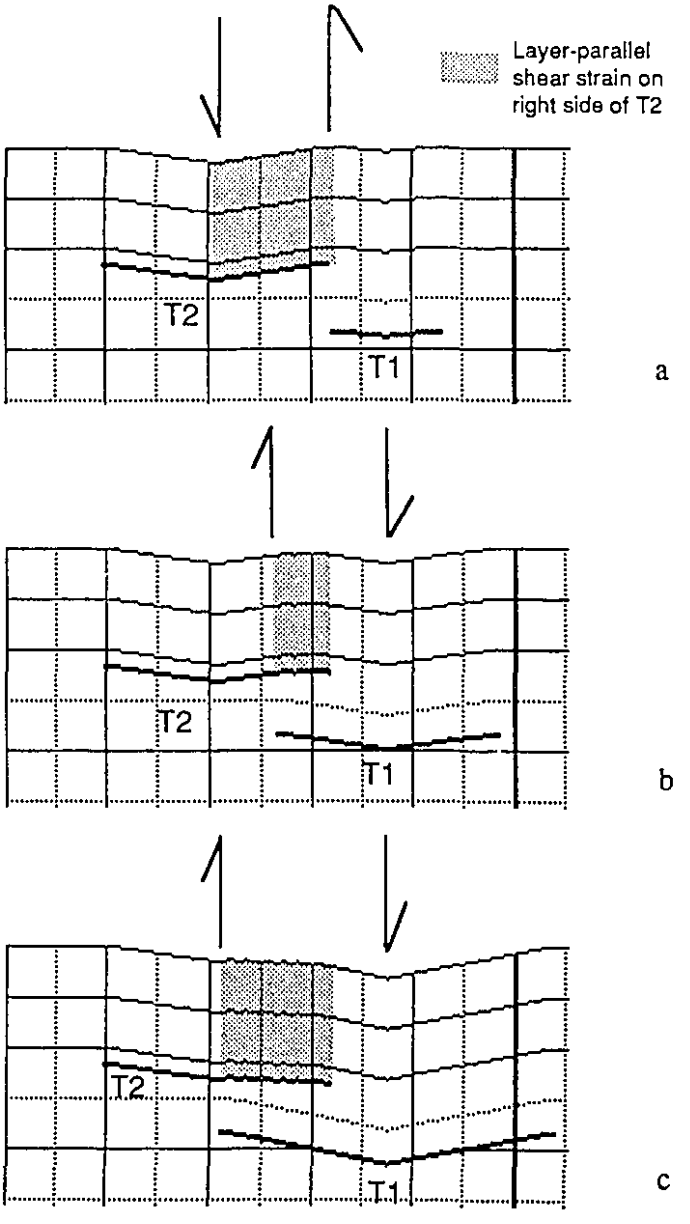

Figure 3. 7: Reversed incremental strain pattern induced by two propagating thrust faults. After sinistral simple shear in the right part of the hanging wall of T2 induced by thrust propagation and motion, the propagation of T1 leads to a dextral simple shear in the same area, although the final strain pattern of T2's thrust sheet might lead one to the conclusion that no layer-parallel shear deformation has occurred.

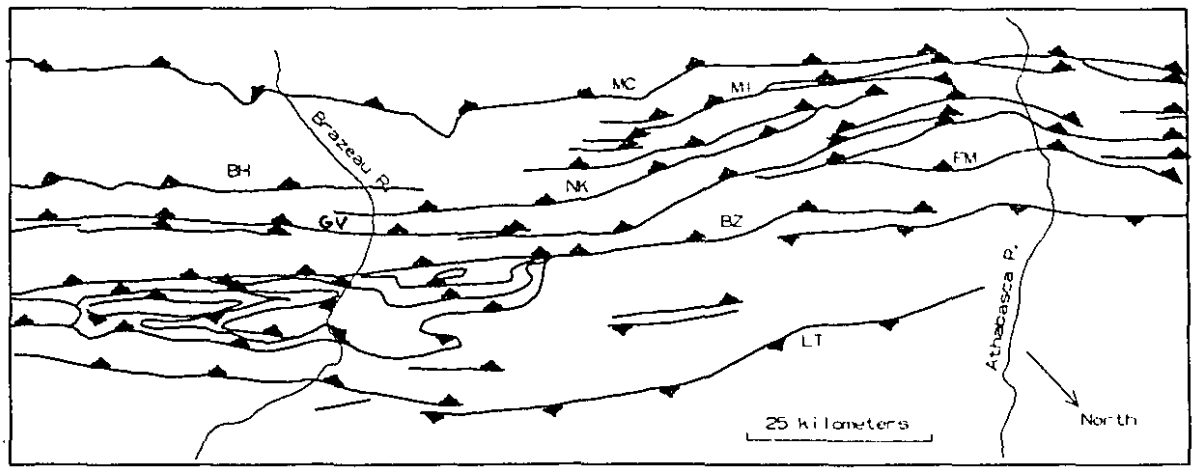

Figure 3. 8: Map of the thrust faults observed in the Canadian Rocky Mountains in the Athabasca-Brazeau region. Thrust faults: Folding Mountain (FM), Lovett (LT), Brazeau (BZ), Miette (MI), McConnell (MC), Nikanassin (NK), Bighorn (BH), Grave Flats (GV).

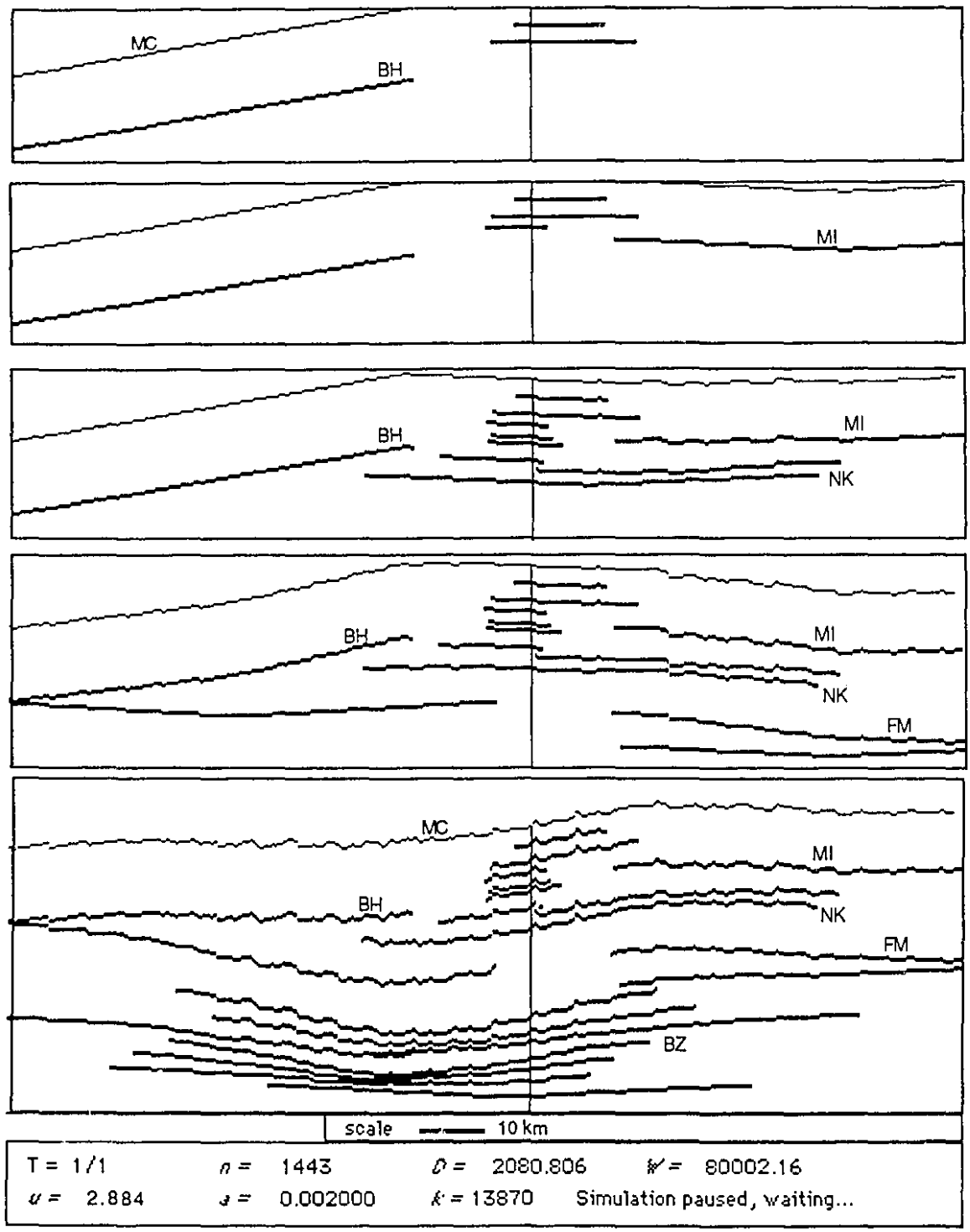

Figure 3. 9: THREE THRUST simulation leading to an approximation of the map pattern observed on Fig. 3. 8. See text for explanation. Refer to Fig. 3. 8 for thrust labels.

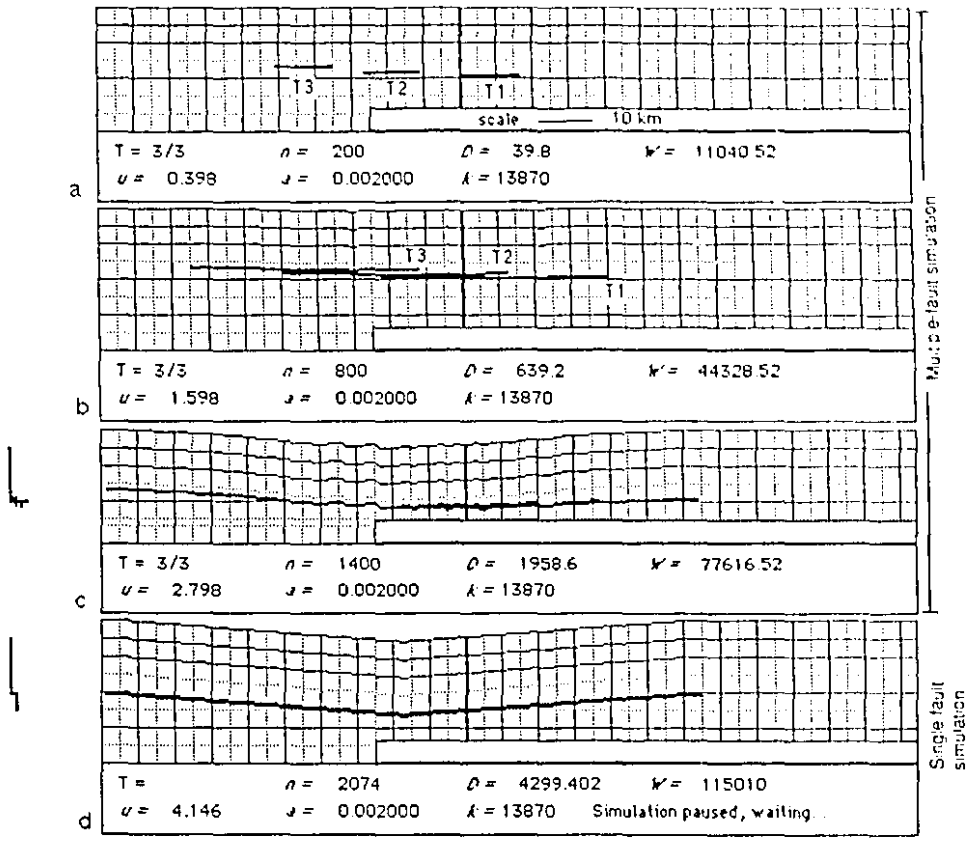

Figure 3. 10: Example of two different simulations leading to a similar configuration of a thrust fault, using realistic a and k values. The first simulation (a-c) shows three faults which after nucleation and initial propagation (a), start to overlap each other, where the more foreland ones carry the others piggyback (b). The piggyback longitudinal shear strain on the hanging wall thrust faults eventually leads to their propagation toward and against the leading edge of the lowest thrust (c) and the consequent fault coalescence. The second simulation (d) generated with only one active fault leads to almost the same final strain pattern as (c). The lines drawn on the left are schematic cross-sections along the thick line near the center of the diagram. The lines on the cross-sections represent the relative fault length of each thrust from its initial breaking point to its leading edge.

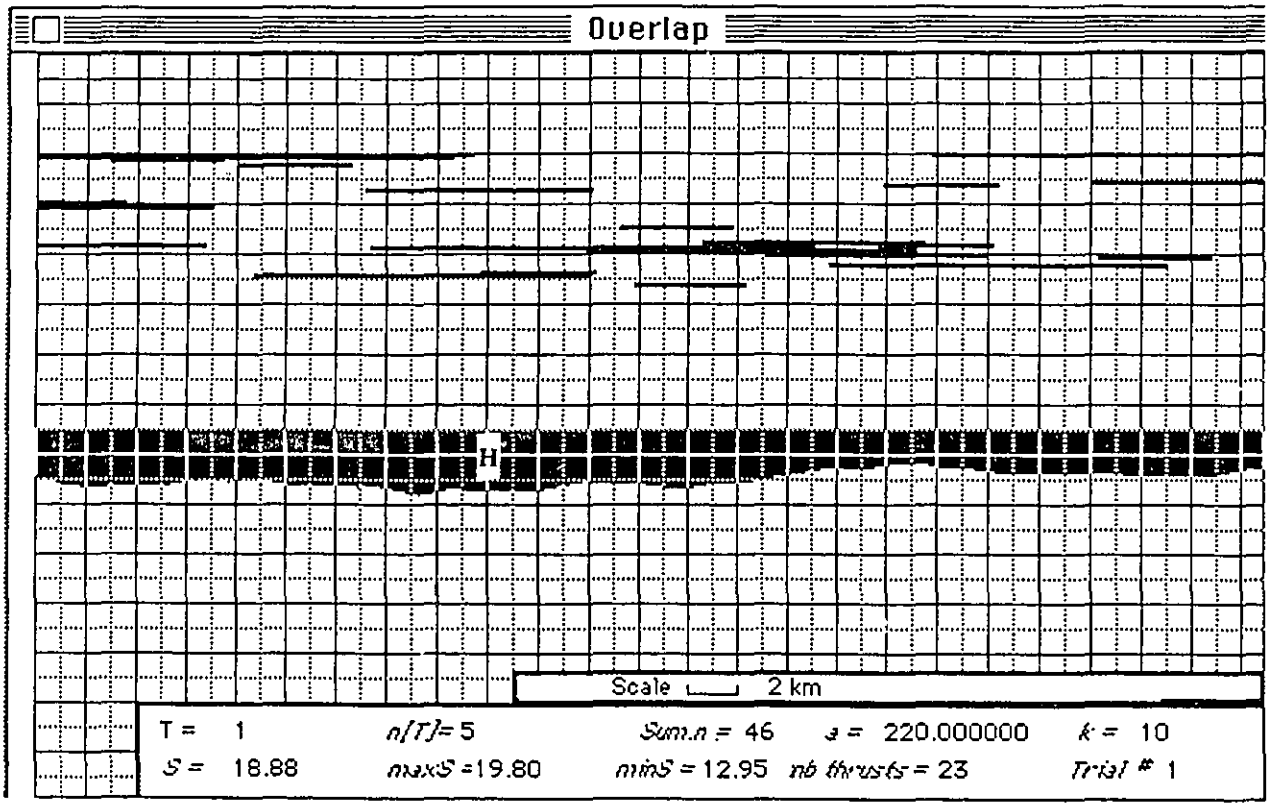

Figure 3. 11: Example of OVERLAP simulation. The program generates new faults where the shortening is the least if no other faults are close enough to permit any shortening. The shortening accommodated by the various faults situated in the upper part of the diagram is represented in the middle part of the diagram by a histogram (H) of the cumulative displacement of all overlapping faults. T: current active thrust number; *n[T]*: number of slip events reached that T has undergone; *Sum. n*: sum of all *n* that occurred within the simulation; *a* and *k*: slip and rheological variables (Walsh and Watterson , 1988); *S*, *maxS* and *minS*: average, maximum and minimum value of shortening in pixels (1 square =1000 m) ; *nb thrusts*: number of thrusts within the belt.

ERA	PERIOD	GROUP OR FORMATION / MAP UNIT			THICKNESS (metres)
		Younger rocks occur in Foothills and Plains			
MESOZOIC	Lower Cretaceous		Luscar Fm	Sandstone, fine grained, greenish grey, siltstone shale, coal	± 600
			Cadomin Fm	Conglomerate, chert and quartzite	3 to 10
	Lower Cretaceous and Jurassic		Nikanassin Fm	Sandstone, siltstone, silty mudstone dark grey	350 to 700
	Jurassic		Fernie Group	Shale, black and dark grey, concretionary, all members present	200 to 275
	Triassic		Whitehorse Fm	Carbonate, light grey, breccias, red mudstone, gypsum	30 to 450
			Sulphur Mountain Fm	Siltstone, dark brown grey, thin bedded silty mudstone	180 to 350
PALEOZOIC	Permian and/or Pennsylvanian		Rocky Mountain Fm	Massive grey chert, cherty brown sandstone	0 to 65
	Mississippian	Rundle Group	Mt. Head Fm	Dolomite, dense, cherty, medium bedded	75 to 120
			Turner Valley Fm	Dolomite, brown, porous coarse grained	50 to 120
			Shunda Fm	Limestone, dark grey, fine grained, thin bedded	60 to 110
			Pekisko Fm	Limestone, light grey, crinoidal coarse grained, thick bedded	35 to 90
			Banff Fm	Limestone and calcareous shale, dark brown, thin bedded	150 to 230
	Devonian		Palliser Fm	Limestone, dark grey, massive, fine crystalline, dolomitic	200 to 275
			Sassenach Fm	Sandstone, fine grained, siltstone, silty shale, silty carbonates	30 to 180
		Fairholme Group or Reefs	Mount Hawk Fm.	Limestone, brown grey, argillaceous and brown calcareous shale	75 to 200
			Perdrix Fm	Shale, black, fissile, thin limestone interbeds	60 to 105
			Maligne and Flume Fms	Limestone, dark grey, thin bedded, argillaceous, limestone, dark brown, cherty, with stromatoporoids	50 to 75
	sub Devonian			Unconformity	
	Middle Cambrian		Arctomys Fm	Shale, silty, red and green, siltstone brown	180 to 245
			Pika Fm	Limestone, calcareous, shale, thin bedded	150 to 200
			Eldon Fm	Limestone, dark grey, massive dolomitic	150 to 245
			Snake Indian Fm	Shale, green and red, argillaceous limestone Limestone, dark grey, resistant	425 to 550

Figure 4. 1: Statigraphic column for the Athabasca-Brazeau segment of the Front Ranges, reproduced from Mountjoy (1992). The subdivision of the Fairholme Group (Cairn and Southesk formations) are not shown. See Fig. 2. 3 for a complete stratigraphic column.

Figure 4. 3: Macroscopic, upright anticlinal fold within the Nikanassin thrust sheet involving strata of the Mississippian Pekisko (Mpk) and Shunda (Msh) formations. A minor backlimb thrust duplicates the Pekisko. View to the southeast from unnamed creek northeast of Mount Luscar (UTM coordinates: 471900E, 5875000N)

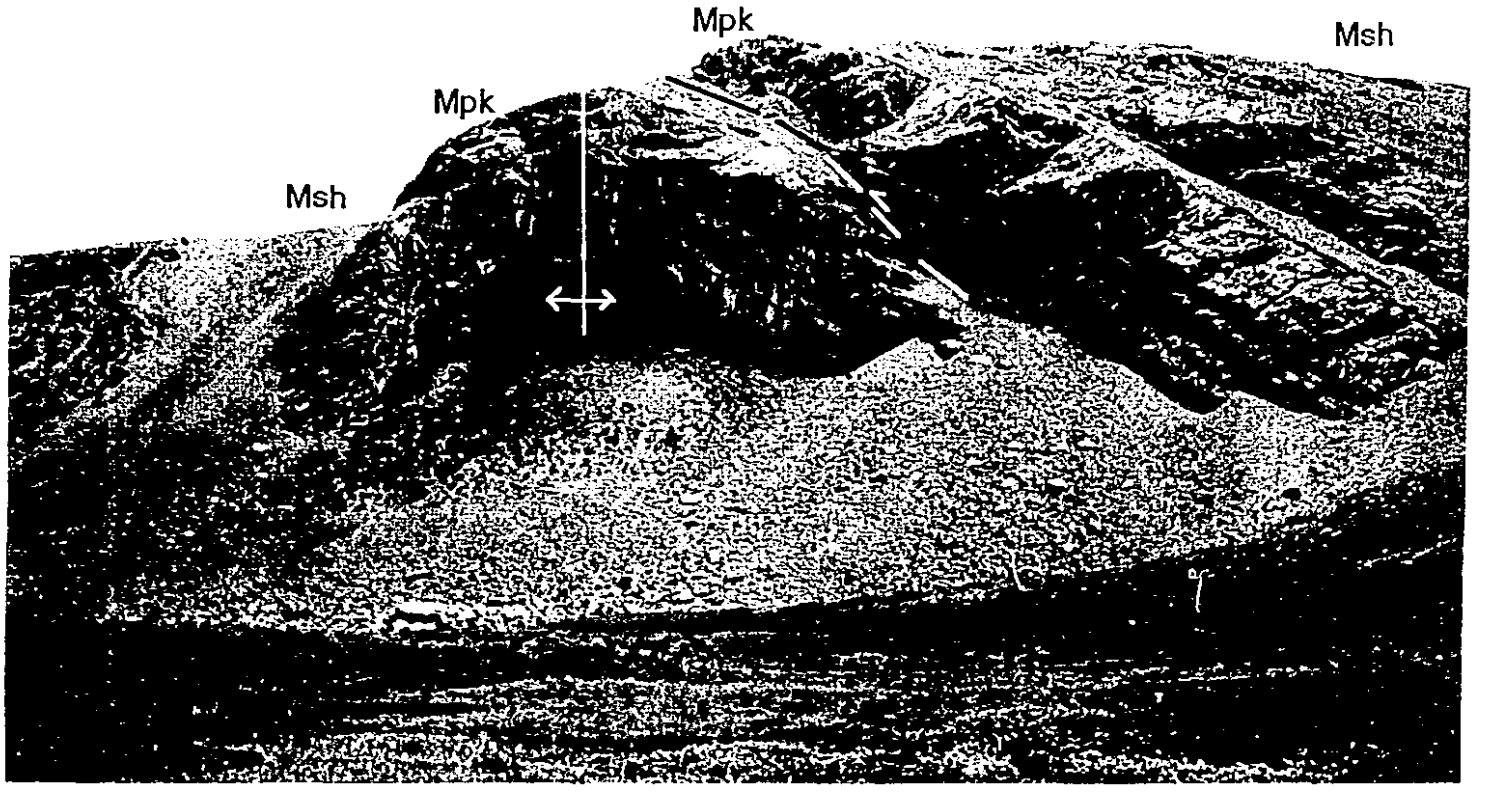

Figure 4.3

Figure 4. 4: Klippe of the folded Fiddle River thrust sheet exposed on a ridge northeast of Mount Berry (on left horizon), viewed towards the northwest from south of Cardinal River Mine (view point at UTM: 470000E, 5877000N). Note low dips of Cambrian (C) strata at Mount Berry. The klippe is composed of Cambrian Eldon Formation (Cel). Folds within the underlying Nikanassin thrust sheet involving Mississippian Rundle Group (Mr) and Triassic Sulphur Mountain Formation (TRsm) fold the Fiddle River thrust fault.

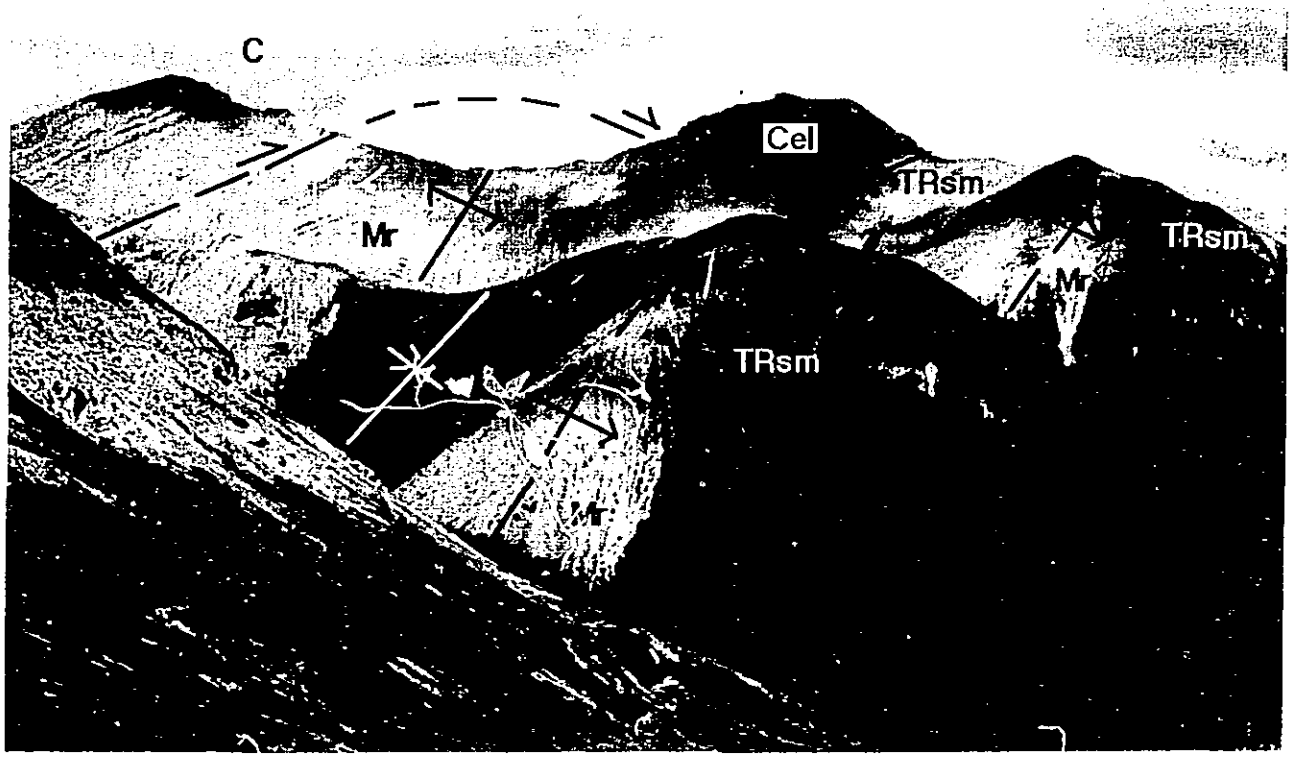

Figure 4.4

Figure 4. 5: S_1 Cleavage (S) fan in a tight macroscopic anticlinal fold northwest of Cadomin Mountain. The S_1 cleavage is only parallel to the axial plane in the hinge area of the fold. The cleavage is slaty within the Banff Formation (Mbf) and stylolitic within the Pekisko Formation (Mpk). This fold is in the hanging wall of the Nikanassin thrust and is traced for nine kilometers towards the northwest, across the McLeod River. View looking southeast from viewpoint coordinates: UTM 4793000E, 5872200N.

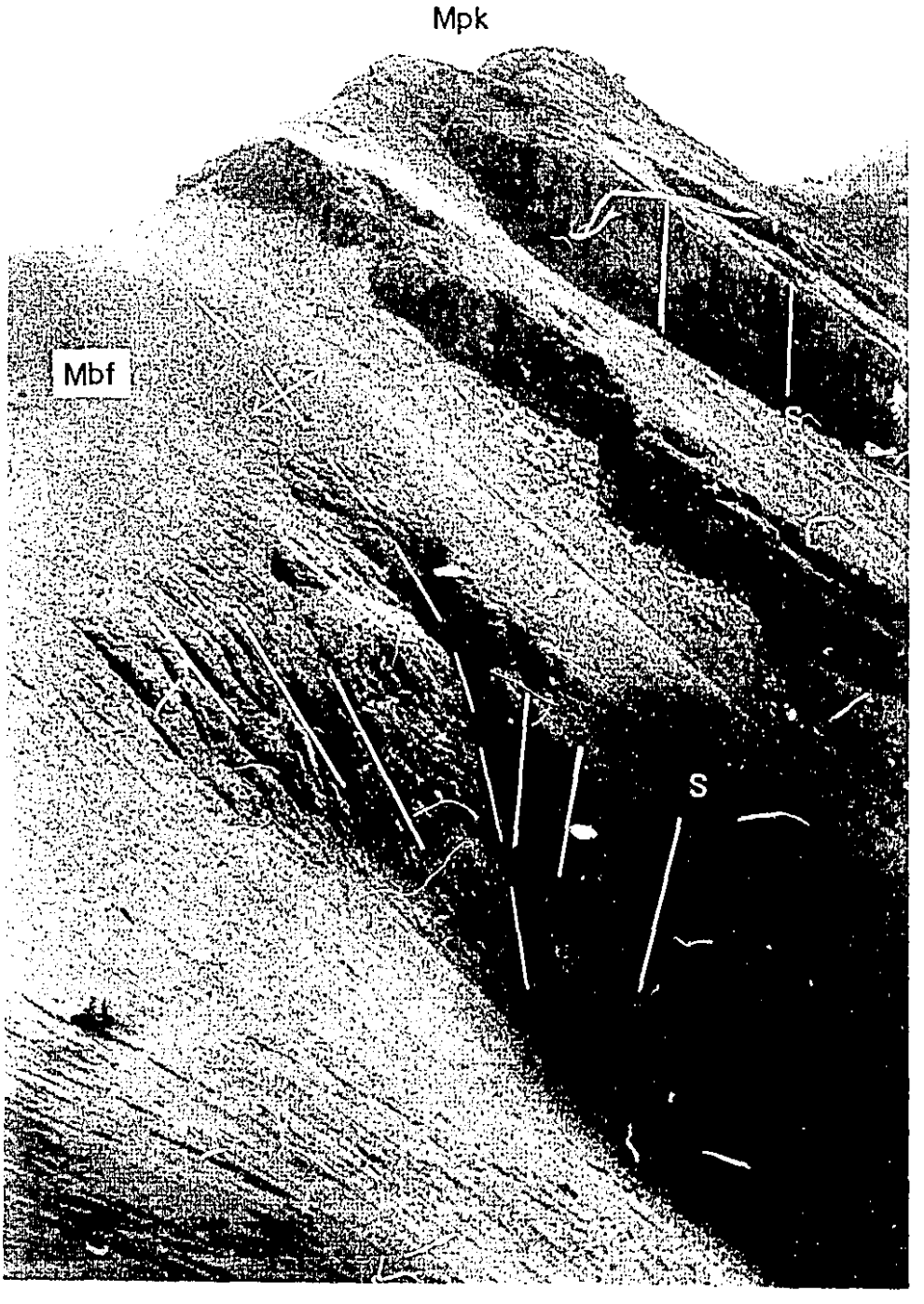

Figure 4.5

Figure 4. 6: Macroscale duplex at Little MacKenzie Creek. The sole thrust of the duplex is the Nikanassin thrust (NK T.) and the roof thrust (R) follows a ramp in the Pekisko Formation (Mpk) and a flat along the base of the overlying Shunda Formation (Msh). Strata of the Shunda and Turner Valley and Mount Head formations (Mtm) are not affected by the imbricates repeating the Pekisko and Banff (Mbf) formations. The Nikanassin thrust climbs a low-angle footwall ramp from the Nikanassin Formation to the Lower Cretaceous Cadomin and Lower Luscar Group at this location. View southeast from viewpoint at UTM 482600E, 5870600N. (Just northeast of the southeast tip of the Fiddle River thrust).

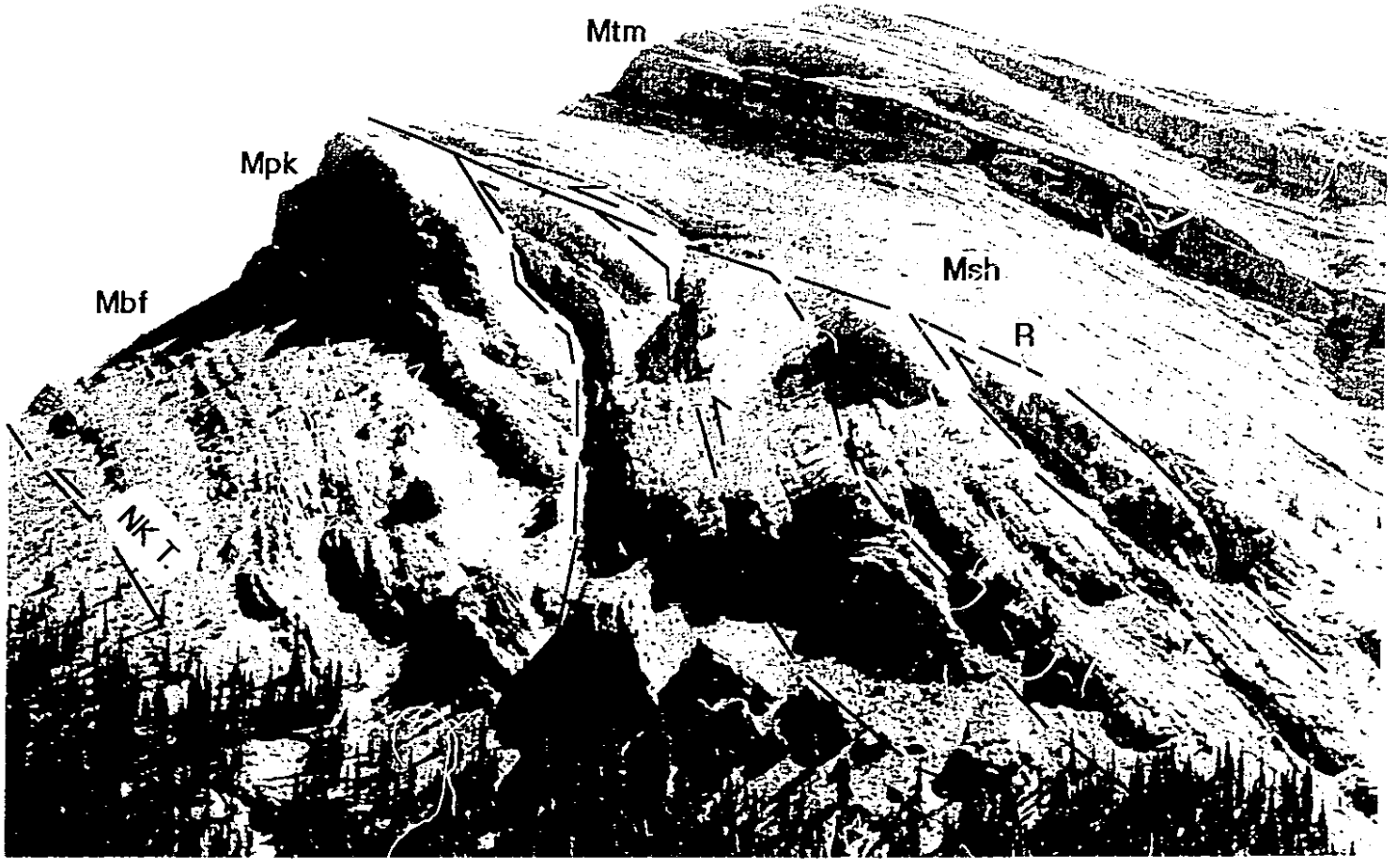

Figure 4.6

Figure 4. 7: En échelon calcite veins indicating dextral shear, along the axis of the hammer, observed frequently within Paleozoic thrust sheets of the Athabasca-Brazeau region. The shear plane is oriented at [294/90] and individual veins trend approximately NNW, within Palliser Formation at Disaster Point west of Roche Miette (along the Athabasca River valley). UTM 435500E, 5890500N.

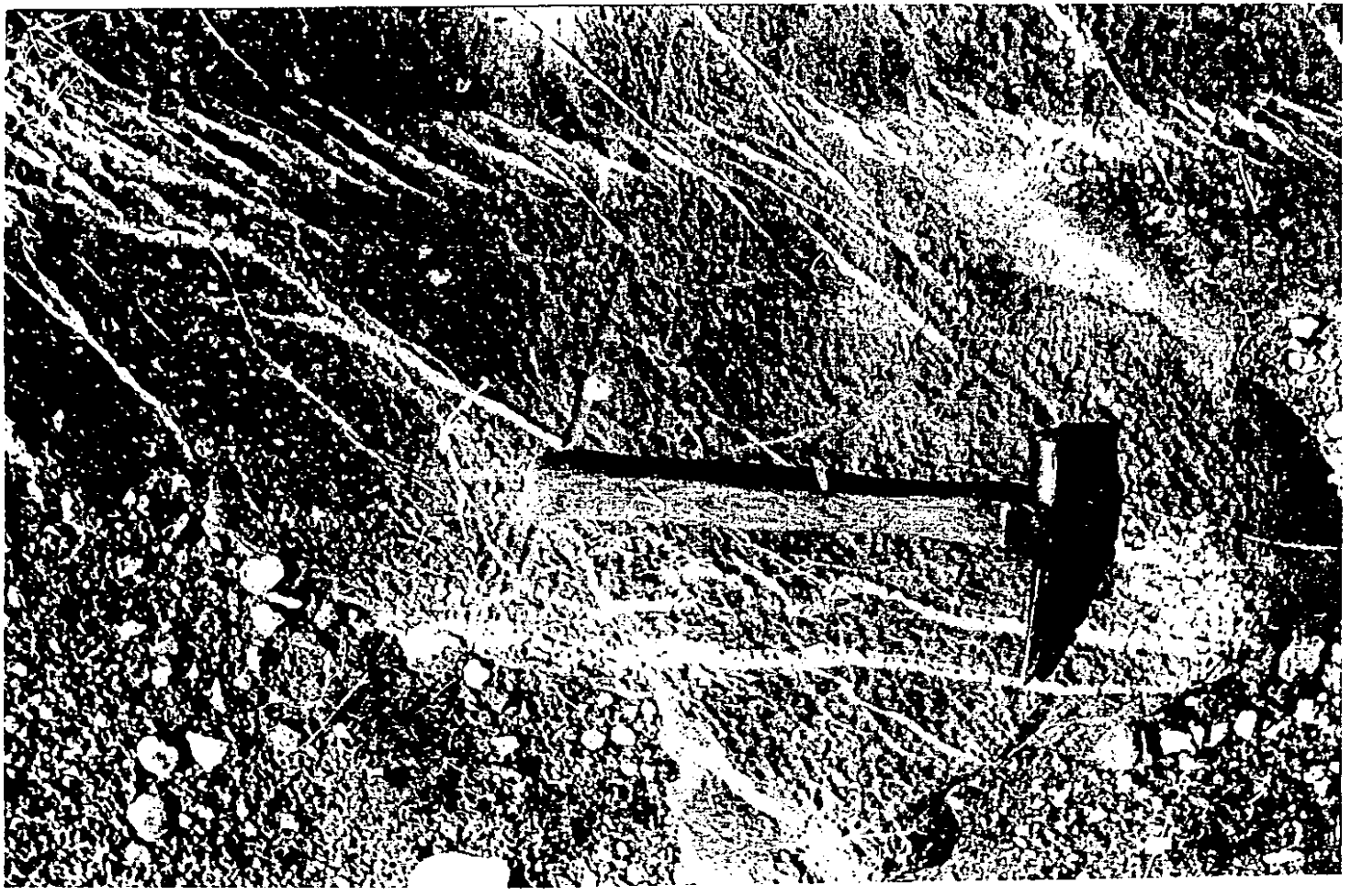

Figure 4.7

Figure 4. 8: Cross-cutting pressure-solution cleavage planes within Mount Head dolomites in the Redcap anticline. An early set of closely spaced (1-3 cm) stylolites (S_1), axial planar to the macroscopic fold, is cross-cut by a later set of en échelon shear veins (V) indicating sinistral shear along a NE-SW axis, perpendicular to the fold axis. A later cleavage (S_2) represented by thick (1-5 mm) and spaced (30-40 cm) solution planes cross-cuts both the veins and the S_1 planes. North is along an imaginary diagonal line towards the upper right corner of the photograph. UTM 461500, 5898500.

Figure 4.8

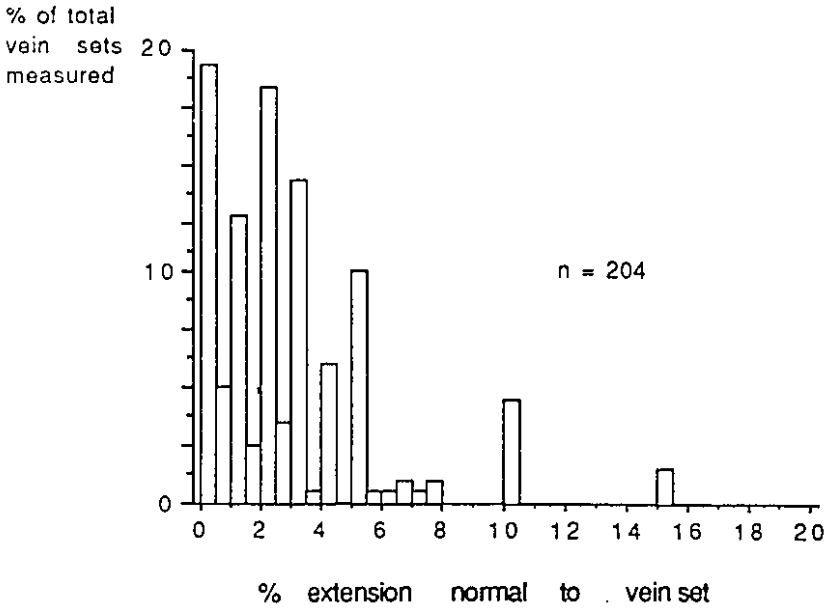

Figure 4. 9: Frequency distribution of local extension from measured veins within the Nikanassin and Fiddle River thrust sheets.

% extension = average thickness of the veins per vein set/ spacing of the veins X 100

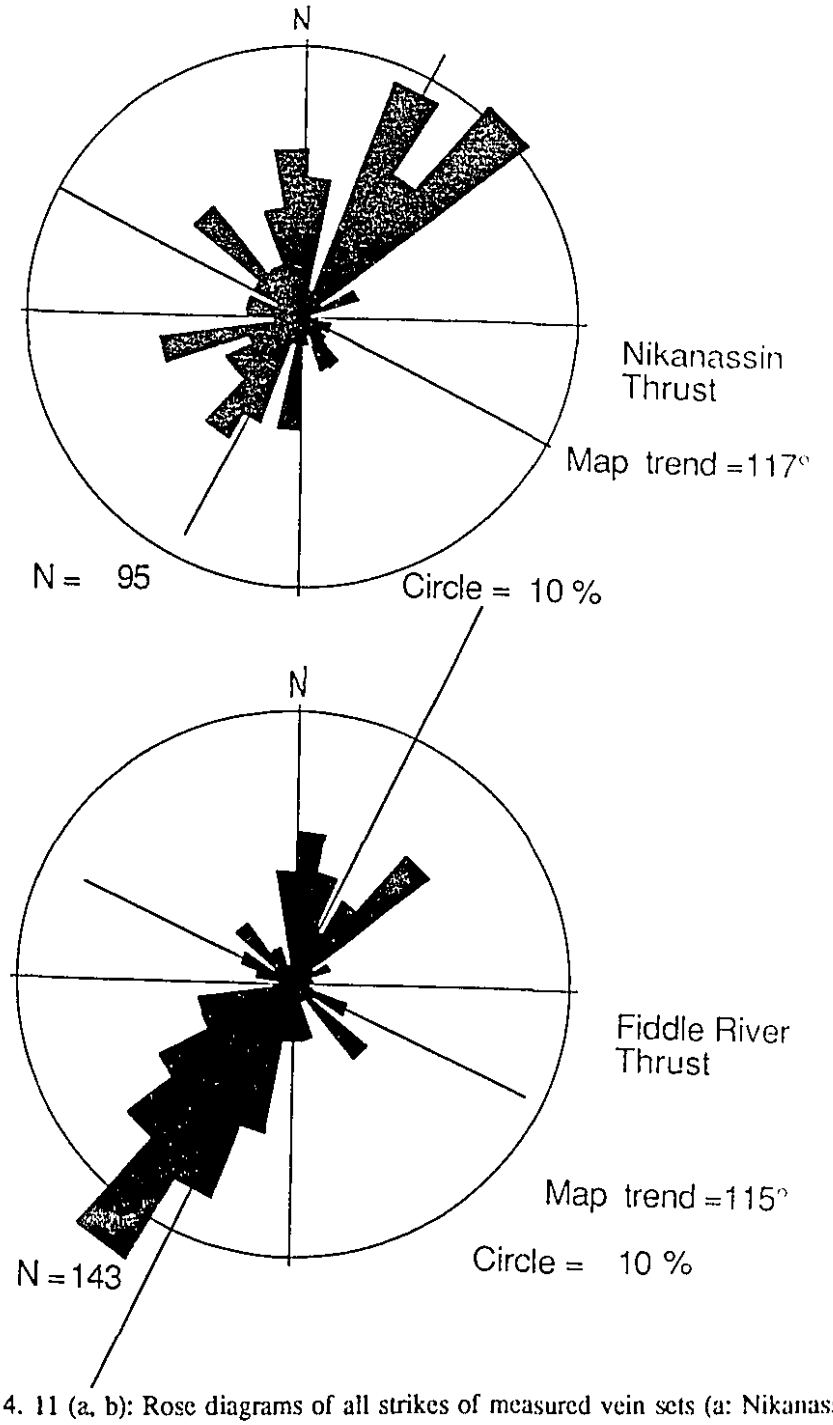

Figure 4. 11 (a, b): Rose diagrams of all strikes of measured vein sets (a: Nikanassin, b: Fiddle River thrust sheet).

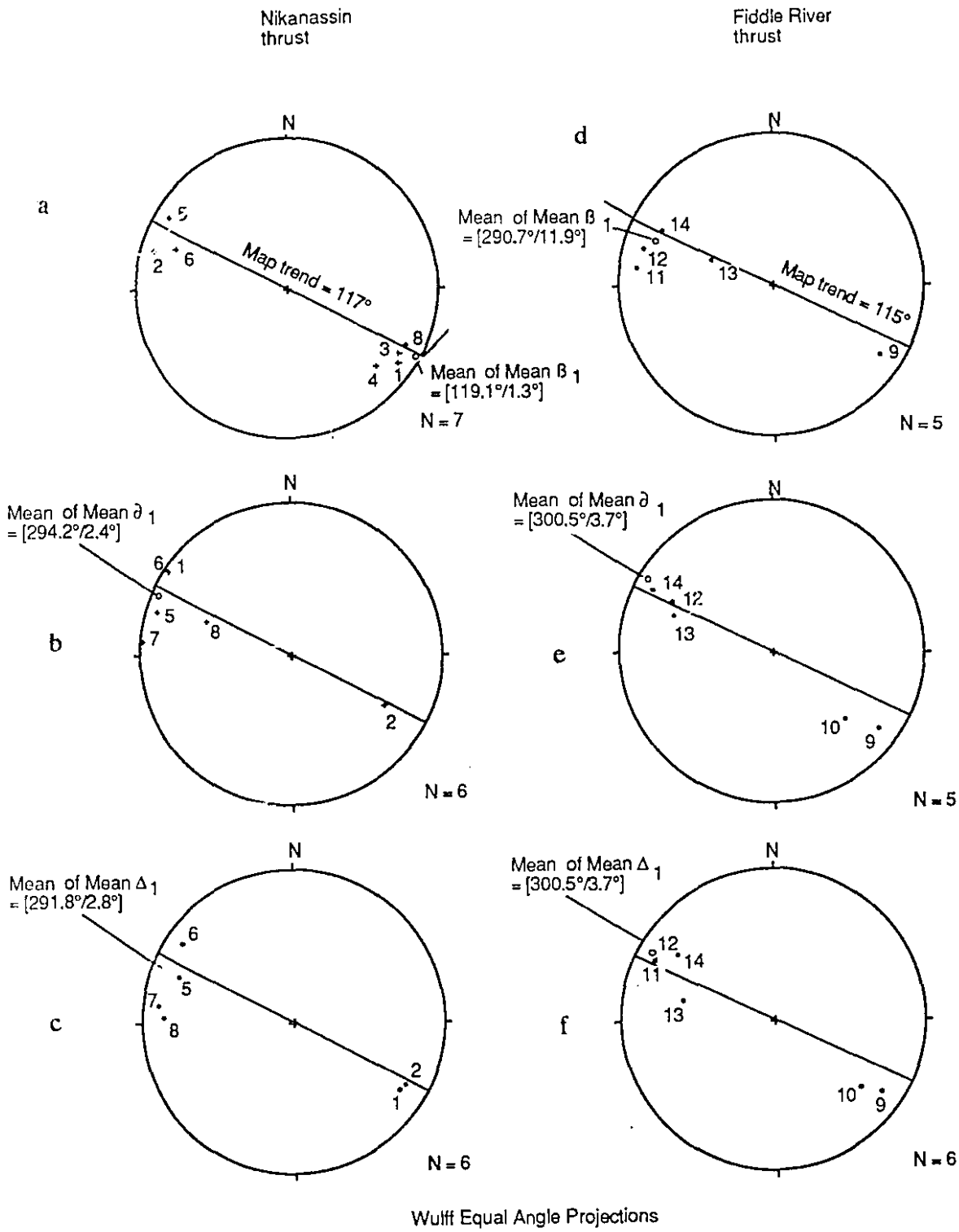

Figure 4. 12: Synoptic stereographic diagrams of all $ß_1$, Δ_1, ∂_1 axes for the different domains of the Nikanassin (4. 12 (a, b, c) and Fiddle River (4. 12 (d, e, f) thrust sheets -- $ß_1$: pole to the best-fit great-circle to S_0 (bedding) poles; ∂_1 : pole to the best-fit great-circle to S_1 (cleavage) poles; Δ_1 : Mean lineation vector of the L^0_1 intersection lineations. Domains are labeled with arabic numbers rather than the roman numbers used elsewhere in this thesis.

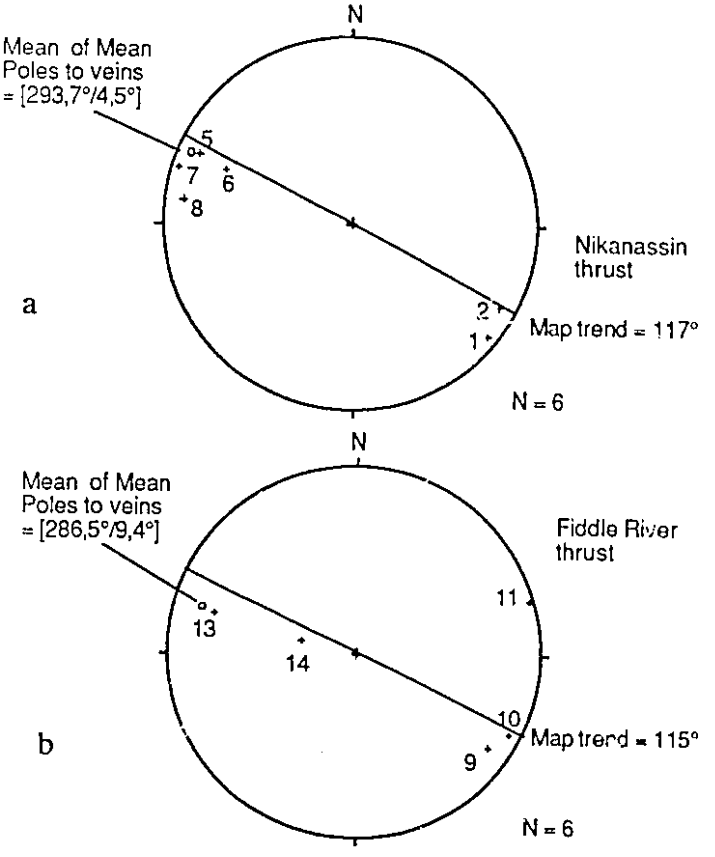

Figure 4. 13: Synoptic sterographic diagrams of all poles to mean veins for the domains of the Nikanassin (4. 13(a)) and Fiddle River (4. 13 (b)) thrust sheets.

Figure 4. 14 (a)-(g): Plots of orientation of calculated structural axes (β_1, ∂_1, Δ_1) and poles to the mean vein sets for each domain of the Nikanassin and Fiddle River thrusts, versus distance (d_j of the domain from a common point of origin situated at the northwestern tip of the Nikanassin-Fiddle thrust fault. (a) trend of β_1 axes against distance; (b): trend of ∂_1 axes against distance; (c): trend of Δ_1 axes against distance; (d): trend of pole to mean vein set per domain against distance; (e): plunge of β_1 axes against distance; (f): all axes against distance, Nikanassin thrust sheet; (g): all axes against distance, Fiddle River thrust sheet. See text for interpretation.

Figure 4.14 a

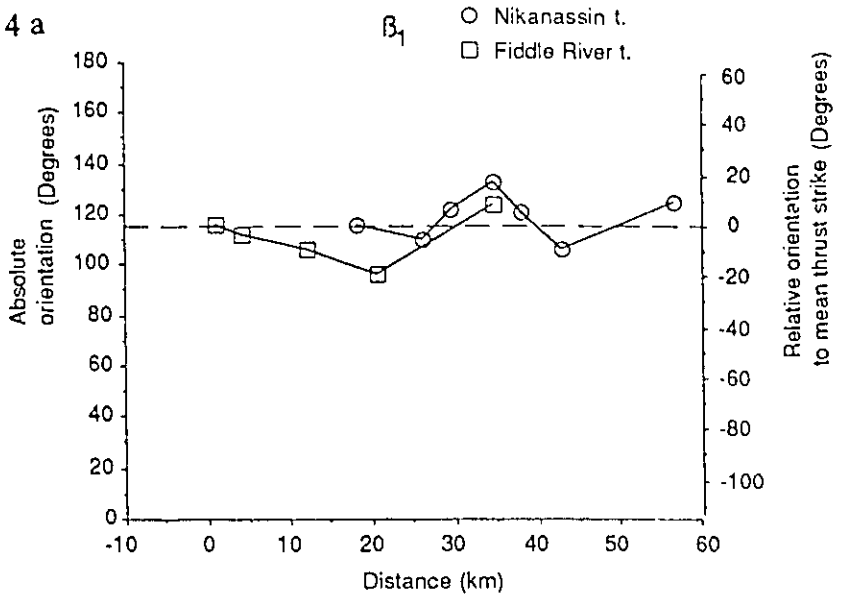

b

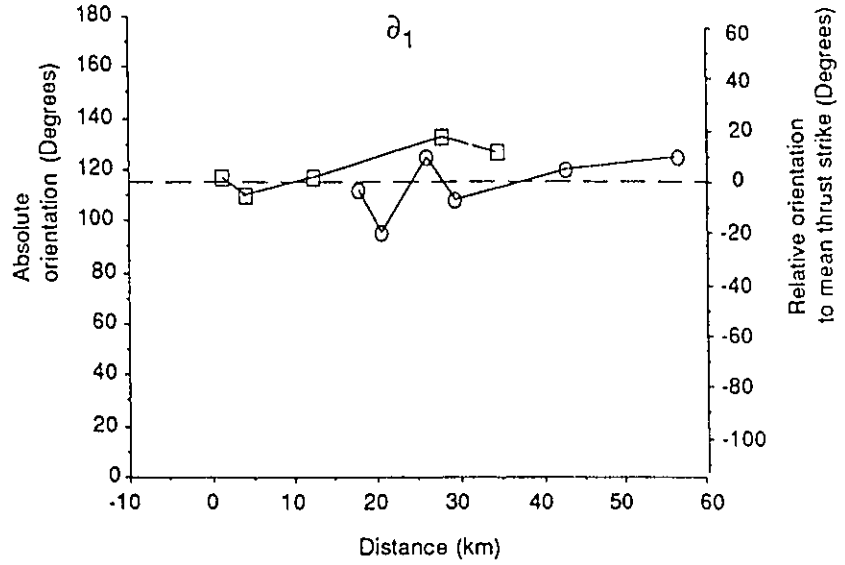

c

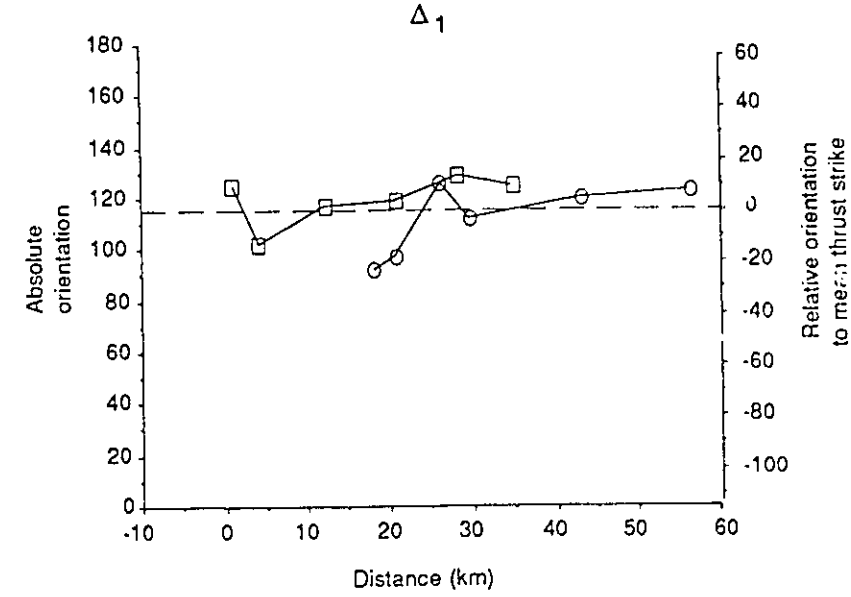

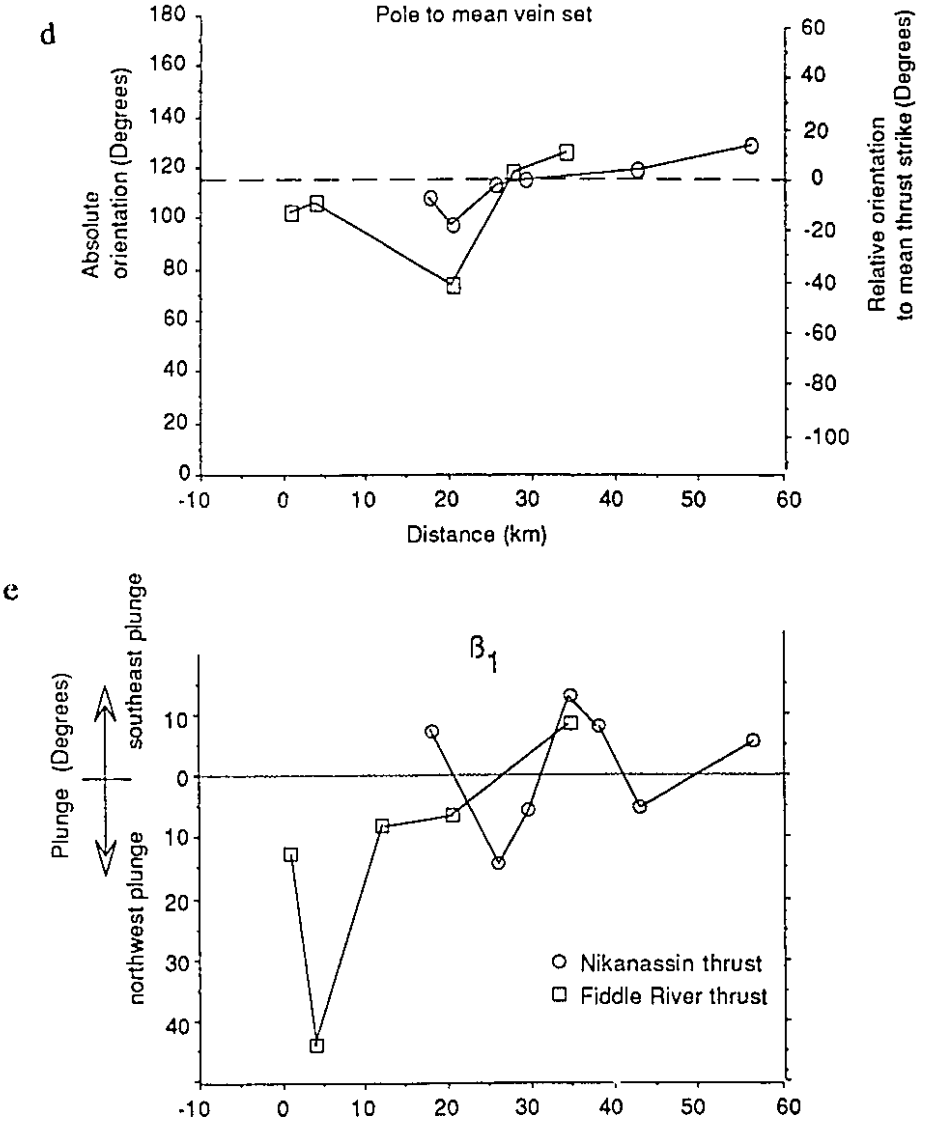

Figure 4.14(d-e)

f

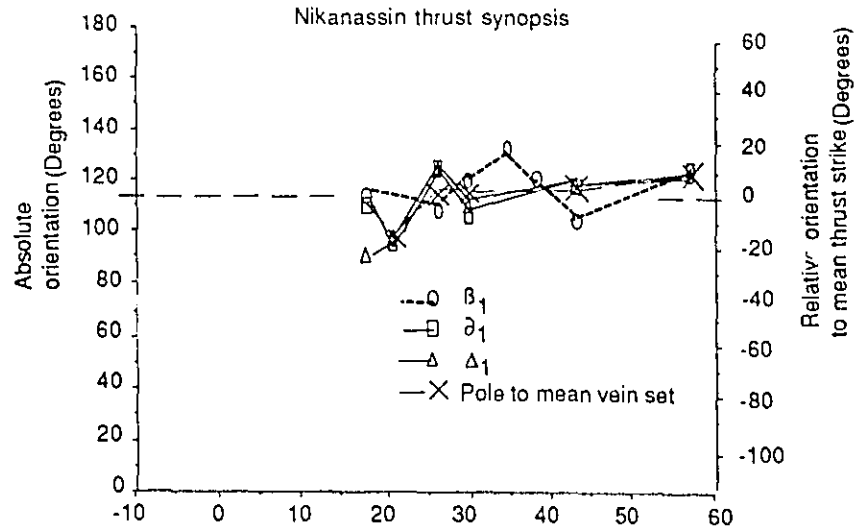

g

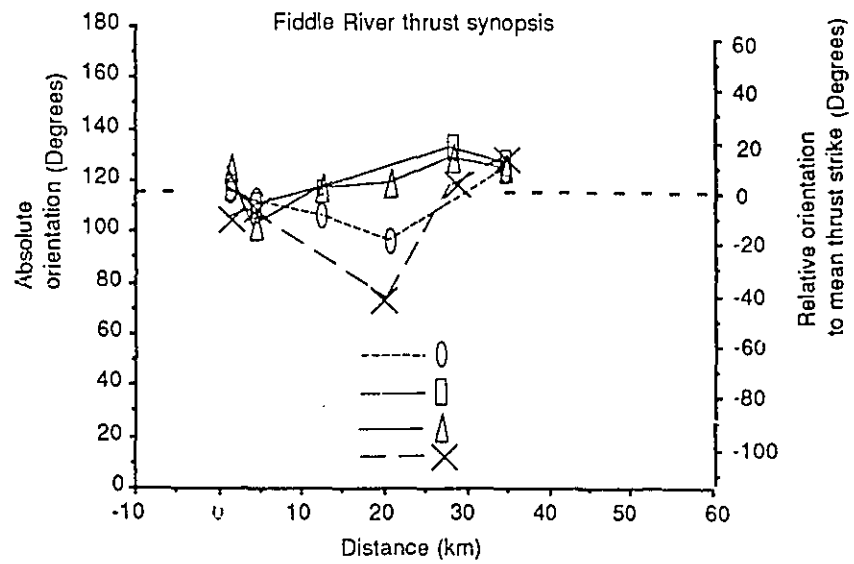

Figure 4.14(f-g)

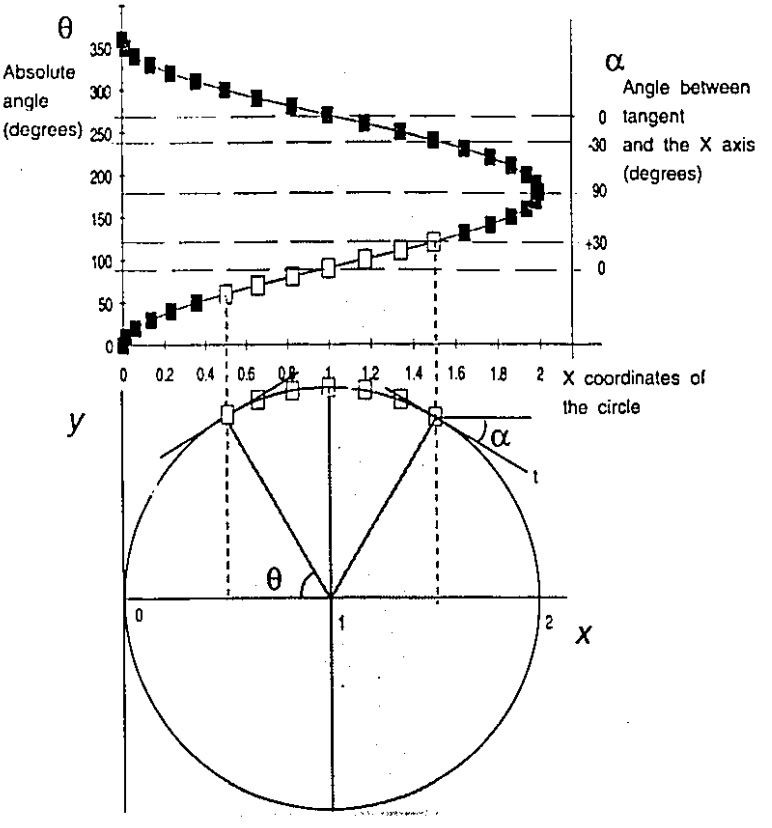

Figure 4. 15 - Variation of x coordinates for a circle within a cartesian reference frame. The lower plot shows a circle with unit radius, with points (white squares) situated along the arc of the circle that has tangents (t) that make a low angle (α) with the x axis (in the shaded area). On the upper graph, the coordinates of these points relative to the x axis plotted against angle from the x axis (θ or α) as a straight line. A positive slope (line of white squares in the shaded area) indicate an inward curvature, a negative slope, an outward curvature. The slope of this curve is proportional to the degree of curvature. Compare with graphs of figure 4. 14 (a)-(g).